2009

Biochemical Analysis of the Protein-Protein Interactions Involved in Karyopherin-Mediated Transport Across the Nuclear Pore Complex

Jaclyn Tetenbaum-Novatt

BIOCHEMICAL ANALYSIS OF THE PROTEIN-PROTEIN INTERACTIONS INVOLVED IN KARYOPHERIN-MEDIATED TRANSPORT ACROSS THE NUCLEAR PORE COMPLEX

A Thesis Presented to the Faculty of

The Rockefeller University

in Partial Fulfillment of the Requirements for

the degree of Doctor of Philosophy

by

Jaclyn Tetenbaum-Novatt

June 2009

BIOCHEMICAL ANALYSIS OF THE PROTEIN-PROTEIN INTERACTIONS INVOLVED IN KARYOPHERIN-MEDIATED TRANSPORT ACROSS THE NUCLEAR PORE COMPLEX

Jaclyn Tetenbaum-Novatt
The Rockefeller University 2009

Nucleocytoplasmic transport occurs through the nuclear pore complex (NPC), which in yeast is a highly symmetric ~50 MDa complex consisting of approximately 30 different proteins. Small molecules can freely exchange through the NPC, but macromolecules larger than ~40 kDa such as proteins, mRNAs, and ribosomal subunits must be aided across by shuttle proteins (karyopherins, or Kaps). Kap-mediated transport involves FG-nups, a family of NPC proteins. While much has been learned about the mechanism of nucleocytoplasmic transport, many details are still unknown; perhaps among the most important missing details is the binding kinetics of almost all the transport-relevant interactions, due to significant technical challenges. The aim of this work is to analyze the protein-protein interactions involved in Kap-mediated transport across the NPC, using biochemical, biophysical, and cell biological approaches. Yeast karyopherins, model cargoes, and full-length FG-nups are enriched from bacteria, and their affinities are studied quantitatively. The presence of competitor proteins and changes in bait protein distribution are seen to effect apparent affinity of these interactions. The relevance of the *in vitro* Kap/NLS-cargo binding measurements is confirmed with a nucleocytoplasmic import assay that allows quantitative measurements of import to be made within

single living cells. Trends observed *in vitro* for Kap/FG-nup interactions were consistent with *ex vivo* observations of interactions of transport factors with *Xenopus* oocyte NPCs and also with *in vitro* measurements of transport through a synthetic NPC-based filter. This work has suggested a role for factors such as non-specific competition in determining the kinetics and selectivity of transport.

This thesis is dedicated to my grandparents, Sol Drabkin, Alyce Drabkin, and Marion Tetenbaum.

Grandpa Si - From our earliest visits to the Museum of Natural History, to your stories of Timmy the Silverback at the Bronx Zoo, you have encouraged me to love nature and explore the beautiful world around me. You have shown me the courage to dive right in to the unknown – even if piranhas are already swimming there.

Grandma Alyce - You have always guided me to explore every question in detail, and to look under the surface and between the lines of every issue. You taught me that it's ok to wear lipstick, and encouraged me to strive for intelligence and beauty at the same time.

Grandma Marion – Your endless love of teaching and learning, in the classroom and at home, continues to inspire me. In your quiet way, you would push me to do better than my best.

You are all a part of me, and for that I am forever grateful.

Acknowledgments

I am deeply indebted to so many people who helped me reach this milestone. First and foremost, I must thank my adviser, Mike Rout. He has been patient and encouraging through this project, and taught me the importance of a walk in the park when you're faced with a seemingly insurmountable obstacle. I am grateful to all members of the Rout lab, both past and present. Roxana Mironska and Anna-Sophia McKenney have both been invaluable to me over the past few years. They were much more than extra pairs of hands – they were additional minds and contributed to this project in every way imaginable. For their support, both in the lab and out, I am very grateful. I have learned so much from Tijana Jovanovic-Talisman. I especially thank her for her omelets, her help with the HPLC, and for shortening my Kap preps from 26 hours to 8. I thank Benjamin Timney for helping me with the microscope and for his patience with my numerous questions. I am grateful to Rosemary Williams and Beth Anne Hatton for all of their behind-the-scenes support. I thank Zachary Quinkert for his help with Native Mass Spectrometry. I am especially grateful to Loren Hough, Tijana Jovanovic-Talisman, Benjamin Timney, Julia Farr and Mike Rout for their critical readings of this thesis and Johanna Napetschnig for her help with Pymol.

I thank my thesis committee: Tom Muir, Sandy Simon, Seth Darst, and Fred Cross. Our discussions were always lively, enjoyable, helpful and productive. I thank David Goldfarb for traveling so far to serve as my external committee

member. I am grateful to Brian Chait, Reiner Peters, Georges Belfort, Jessica Wright and Jennifer Ottesen for stimulating discussions and frequent advice.

I thank Rockefeller University and HHMI for funding. I am grateful to everyone in the Rockefeller Dean's Office, past and present, for your constant support - Sid Strickland, Emily Harms, Marta Delgado, Kristen Cullen, Cristian Rosario, Michelle Sherman, Sue-Ann Chong, and Jean Devlin.

My parents, Barbara and Larry Tetenbaum, have been an endless source of love and inspiration throughout my life. They have always encouraged me to learn and explore. I am very grateful to them for the many opportunities they have given me, and for always being there for me. I thank Matthew and Samara Tetenbaum for their constant support and encouragement, and for always being there when I needed them. I thank my second family – Joan, Ken, and Jennifer Novatt – for their love, acceptance and patience. I thank my friends – Karen Wei, Loren Hough, Jody Franke, Amy Tyszkiewicz, Evelyn Lewis-Enright, Rachel Sperling, Rachel Mantione, Sara Kahn Troster, Alana Rosenstein, and Scott Bleiweis. I think I owe them any remaining sanity I have.

Finally, I am extremely grateful to my husband, Shawn Novatt. I cannot put in words how much his love and support mean to me. When he says "I'm proud of you," I feel like I can fly.

Table of Contents

List of Figures

List of Tables

Chapter One: Introduction

Eukaryotic cells contain their nucleic acid synthesis and processing machineries in a membrane-bound nucleus. The segregation protects the genetic material and allows for tighter regulation of gene expression, but it also presents a problem – histone proteins, transcription factors, ribosomal subunits, RNA complexes, and other select macromolecules must be able to cross the nuclear envelope (Dworetzky and Feldherr 1988). Nuclear pore complexes (NPCs) are the only known means of transport between the nucleus and cytoplasm, and as such, NPCs define the contents of the nucleus. These NPCs form *de novo* as the nuclear envelope (NE) expands during interphase (Winey, Yarar et al. 1997; D'Angelo, Anderson et al. 2006), and in upper eukaryotes they must re-assemble after NE breakdown during each round of cell division (Harel, Chan et al. 2003; Walther, Askjaer et al. 2003). Transport through NPCs enables the regulation of gene expression, cell division, signal transduction, and other cellular processes (reviewed in (Nigg 1997)). Defects in nucleocytoplasmic transport have been detected in many different types of cancer cells (reviewed in (Kau, Way et al. 2004)). Thus, understanding how nucleocytoplasmic transport works may enable the design of therapeutic agents. There is also a technological motive to try and understand the mechanism of transport across the NPC. In the NPC, millions of years of evolution have resulted in a very effective and robust filter – it allows a variety of specific proteins and complexes

to pass while blocking others of similar size and charge. It can prevent relatively small proteins from entering while allowing selective transport of complexes as large as 39 nm in diameter (Pante and Kann 2002). The NPC is also very efficient, with hundreds of specific transport events per pore, per second (Ribbeck and Gorlich 2001). Our ultimate goal is to determine how the NPC works in order to mimic that technology. As we learn the mechanisms behind the NPC's selective filter, we are working to exploit that and ultimately create a selective filter to our specifications.

The *S. cerevisiae* NPC as a model

The structure of the NPC **(Figure 1-1)** (Hinshaw 1992; Akey 1993; Yang, Rout et al. 1998; Kiseleva 2003; Stoffler 2003; Beck 2004; Alber, Dokudovskaya et al. 2007; D'Angelo and Hetzer 2008) and the mechanism of transport through the NPC (Silver 1989; White 1989; Macara 2001; Feldherr, Akin et al. 2002) are both highly conserved among evolutionary divergent species, meaning studies in model organisms can be relevant to all eukaryotes. Our lab uses the budding yeast (*Saccharomyces cerevisiae*) NPC as a model to try to understand nucleocytoplasmic transport. *S. cerevisiae* is an excellent model system for the study of nucleocytoplasmic transport for the following reasons: 1) The sequence of the yeast genome is known, making it easier to identify and manipulate nuclear

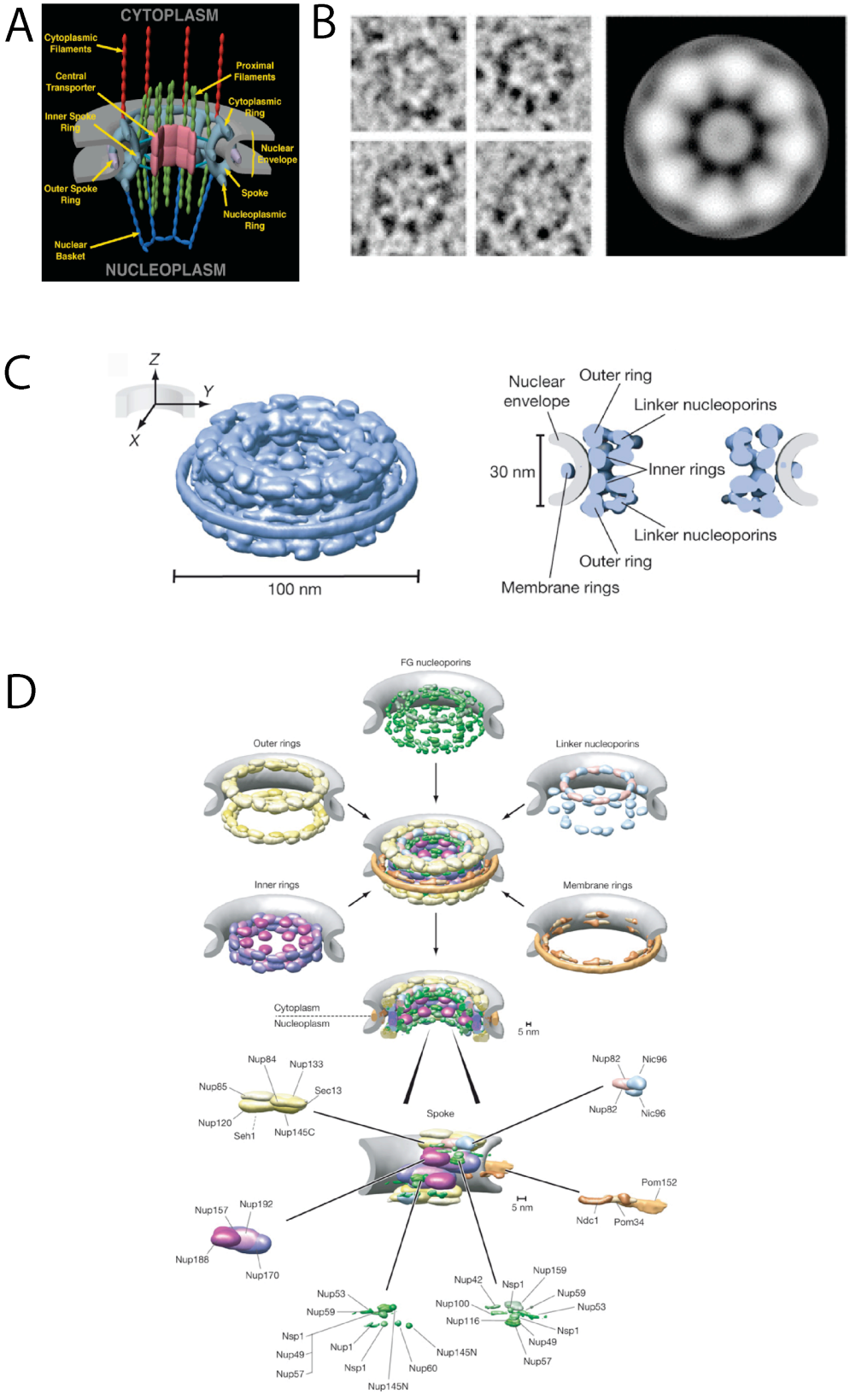

Figure 1-1: Legend on following page.

Figure 1-1: Structure of the nuclear pore complex. A) Schematic of the nuclear pore complex (modified from (Rout and Aitchison 2001)) B) Cryo-electron microscopy images of native, thick-ice embedded Xenopus NPCs reveal donut-shaped, hollow rings most likely representing the distal ring of the nuclear basket. Correlation averages of over 100 pores (larger image) reveal a donut-shaped ring in the center of the pore. This ring was identified as the "central plug" (Stoffler 2003) C) The structured nucleoporin domains of the S. cerevisiae NPC, represented by a density contour (blue) such that the volume of the contour corresponds approximately to the combined volume of the 456 nucleoporins comprising the NPC. Left: view from a point approximately 30° from the equatorial plane of the NPC. Right: a slice along the central Z-axis in which the nuclear envelope is also shown (in grey). Major features of the NPC are indicated (Alber, Dokudovskaya et al. 2007). D) Localization volumes (Alber, Dokudovskaya et al. 2007) of individual nucleoporins, classified into five distinct substructures on the basis of their location and functional properties: the outer rings (yellow), inner rings (purple), membrane rings (brown), linker nucleoporins (blue and pink), and the structured domains of the FG-nups (green). The pore membrane is shown in grey (Alber, Dokudovskaya et al. 2007).

pore complex proteins and transport factors ((Clayton, White et al. 1997) and references therin), 2) *S. cerevisiae* undergoes closed mitosis, so the NPCs and nuclear envelope remain intact throughout all stages of the cell cycle (Byers 1981), 3) The NPC of *S. cerevisiae,* belonging to one of the simplest eukaryotes, lacks many of the complex elaborations present in vertebrate model organisms (Yang, Rout et al. 1998; Rout, Aitchison et al. 2000), and 4) there are many established genetic, molecular biological, biochemical, and cell biological techniques to study complex cellular phenomena in *S. cerevisiae.*

Structure of the NPC

Electron microscopy has shown the NPC to be a roughly cylindrical complex with eight-fold rotational symmetry in the plane of the nuclear envelope (for examples, see (Akey 1993) and (Stoffler 2003), **Figure 1-1 B**). The yeast NPC is a ~50 MDa complex, consisting of approximately 30 proteins with 8, 16, or 32 copies of each protein per pore (Rout, Aitchison et al. 2000). The vertebrate NPC is larger, at approximately 125 MDa, but still consists of only ~30 unique proteins (Cronshaw, Krutchinsky et al. 2002). The proteins that make up the NPC are called nucleoporins, or nups, and they fall into three general categories: nups that span the nuclear membrane, non-membrane proteins that contain multiple repeats of a Phe-Gly motif (FG-nups), and non-membrane proteins that do not contain FG repeats (Alber, Dokudovskaya et al. 2007). The

structure of the NPC partially determines the selectivity of nucleocytoplasmic transport. Small molecules such as water and ions can freely diffuse through the NPC, but proteins and RNA complexes larger than the passive diffusion limit of ~40 kDa require shuttle proteins to help them cross the NPC.

Facilitated transport through the NPC

Karyopherins or Kaps, also known as importins and exportins, are a family of shuttle proteins that transport cargo across the NPC (Dworetzky and Feldherr 1988; Adam and Gerace 1991; Adam and Adam 1994; Gorlich, Prehn et al. 1994; Gorlich, Vogel et al. 1995; Macara 2001; Leslie, Grill et al. 2002; Rout, Aitchison et al. 2003; Mosammaparast and Pemberton 2004; McLane, Pulliam et al. 2008). These Kaps recognize their proteinaceous cargo via nuclear localization signals (NLS) (Goldfarb, Gariepy et al. 1986; Moore and Blobel 1992; Aitchison, Blobel et al. 1996; Lee and Aitchison 1999; Leslie, Zhang et al. 2004; Lee, Cansizoglu et al. 2006; Lange, Mills et al. 2007; Lange, Mills et al. 2008; Suel, Gu et al. 2008) or nuclear export signals (NES) (Wen, Harootunian et al. 1994; Richards, Lounsbury et al. 1996; Ossareh-Nazari, Bachelerie et al. 1997; Scheifele, Ryan et al. 2005; Kosugi, Hasebe et al. 2008; Scott, Cairo et al. 2009) and help them through the NPC to their appropriate destination. Other mechanisms of assisted nucleocytoplasmic transport exist as well. The yeast protein Los1 (Hellmuth, Lau et al. 1998; Sarkar and Hopper 1998) and its

vertebrate homolog exportin-t (Arts, Fornerod et al. 1998; Kutay, Lipowsky et al. 1998) are involved in tRNA export. This karyopherin β-like protein binds selectively to end-mature tRNA (Arts, Fornerod et al. 1998; Kutay, Lipowsky et al. 1998), helping to ensure that tRNAs are not allowed to leave the nucleus prematurely (Lund and Dahlberg 1998; Macara 2001). Another type of shuttle protein is NTF2 (Moore and Blobel 1994; Paschal and Gerace 1995), which mediates the nuclear import of Ran (Ribbeck, Lipowsky et al. 1998; Smith, Brownawell et al. 1998). NTF2 thus helps maintain the RanGTP gradient across the nuclear envelope that is crucial in determining the directionality of nucleocytoplasmic transport (discussed below).

Karyopherin-mediated transport

Transport through the NPC is bidirectional, with shuttle proteins moving both cargo proteins and RNAs in the appropriate direction between the nucleus and the cytoplasm (Dworetzky and Feldherr 1988; Middeler, Zerf et al. 1997; Kapon, Topchik et al. 2008). Some karyopherins work alone (such as Kap121), directly bridging the interaction between cargo molecules and the nuclear pore complex (Aitchison, Blobel et al. 1996; Seedorf 1997; Lee and Aitchison 1999; Leslie, Zhang et al. 2004; Hodel, Harreman et al. 2006; Lee, Cansizoglu et al. 2006; Lange, Mills et al. 2008). Other karyopherins require one or more adapter proteins. For example, the yeast Kap95 requires Kap60, an “NLS receptor.”

Kap60 binds to the cargo molecule, while Kap95 bridges the interaction between the Kap60-cargo complex and the NPC (Gorlich, Vogel et al. 1995). This is homologous to Karyopherin β and Karyopherin α in mammalian cells (Adam and Adam 1994; Enenkel 1995; Riddick and Macara 2007). Although there is some redundancy, these different transport receptor proteins specifically carry their own unique set of protein or RNA cargoes through the NPC (Michaud and Goldfarb 1991; Michaud and Goldfarb 1992; Timney, Tetenbaum-Novatt et al. 2006). Recent work has shown that Kap-mediated transport through the NPC can be fit to a straightforward pump-leak model, where import rates *in vivo* are simply dependent upon the concentrations of karyopherin and cargo (Timney, Tetenbaum-Novatt et al. 2006). Import by vertebrate Importin α/β (Kap95/Kap60 in yeast) has also been modeled as a series of coupled ordinary differential equations, leading to experimentally testable predictions about the effects of altering the concentration of certain components of the pathway (Riddick and Macara 2005). This model considers the Importinα-Importinβ binding step as a two-step reversible reaction (Catimel, Teh et al. 2001) and the nucleotide exchange catalyzed by RCC1 (RanGEF – explained below) as a four-step reversible reaction (Klebe, Prinz et al. 1995). This mathematical simulation predicted that increasing the concentrations of Importin α and Ran would increase the initial rate of import, as expected. Unexpected, however, was the prediction that increasing the concentrations of Importin β and RCC1 would *decrease* the initial import rate. All of these predictions were validated

experimentally, and the unexpected decrease in import rate was explained by an increase in futile shuttling of empty Importin β through the NPC (Riddick and Macara 2005). This group also used computer simulations to suggest that the use of an adapter protein such as Importin α (Kap60) allows the system to be much more robust, able to control cargo accumulation in the nucleus over a wider range of Kap concentrations than an adapter-free system would allow (Riddick and Macara 2007).

Directionality of transport

The directionality of nucleocytoplasmic transport is governed by a gradient of the GTPase Ran across the nuclear membrane (Izaurralde, Kutay et al. 1997) **(see Figure 1-2)**. RCC1, the yeast Ran guanidine exchange factor (RanGEF), stimulates the release of guanine nucleotides from Ran by stabilizing the nucleotide-free state (Klebe, Prinz et al. 1995). Chromatin-bound RCC1 is a constitutively nuclear protein (Ohtsubo, Okazaki et al. 1989), and this localization of the RanGEF ultimately results in a higher RanGTP concentration in the nucleus. The yeast Ran GTPase activating protein (RanGAP) shuttles between the nucleus and cytoplasm (Feng, Benko et al. 1999), but Ran binding protein 1 (RanBP1) is mainly cytoplasmic. RanGAP activity is normally blocked by karyopherins (Floer and Blobel 1996; Gorlich, Pante et al. 1996), but in the

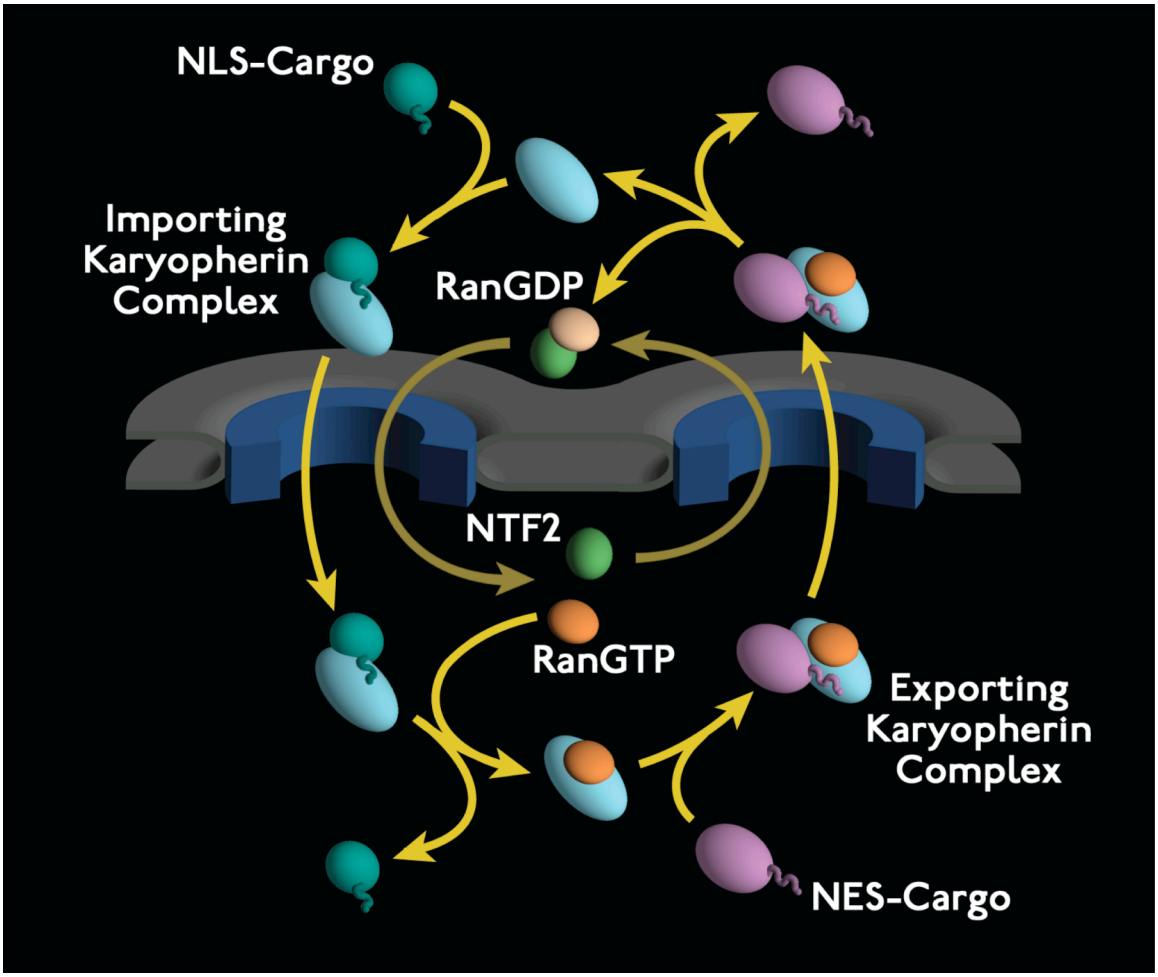

Figure 1-2: Schematic of the Ran cycle that dictates directionality of nucleocytoplasmic transport. An import-bound Kap binds to its NLS-bearing cargo in the cytoplasm and the Kap-cargo complex crosses the NPC. On the nucleoplasmic side, RanGTP binds to the Kap, causing a conformational change which releases the cargo. An export Kap binds its NES-cargo in a trimer with RanGTP. The resulting Kap-cargo-RanGTP complexes pass through the NPC. On the cytoplasmic side, RanGAP stimulates RanGTP hydrolysis, resulting in the release of cargo. RanGDP is then recycled to the nucleoplasm by NTF2 where it is reloaded with GTP by the chromatin-bound RanGEF.

presence of cytoplasmic protein RanBP1, the ability of RanGAP to stimulate RanGTPase activity increases 10-fold (Bischoff, Krebber et al. 1995). Thus, cytoplasmic Ran has a much higher GTPase activity than nuclear Ran. When combined with the nuclear RanGEF activity, this leads to a strong RanGTP gradient across the nuclear envelope (NE), with a high concentration of RanGTP in the nucleus and low levels of RanGTP in the cytoplasm. Karyopherins can form a complex with RanGTP (concentrated in the nucleus) and this has been seen to trigger the disassembly of import carriers from their cargo and promote the assembly of exportin-cargo complexes (Floer, Blobel et al. 1997). Conversely, release of Ran upon GTP hydrolysis in the cytoplasm results in the assembly of import Kap-cargo complexes and the disassembly of export Kap-cargo complexes (reviewed in (Macara 2001)). RanGTP also dissociates the import karyopherin Kapβ (homolog of yeast Kap95) from the NPC (Rexach and Blobel 1995). Nuclear Transport Factor 2 (NTF2) carries the empty Ran back into the nucleus, where it is regenerated into RanGTP (Ribbeck, Lipowsky et al. 1998; Smith, Brownawell et al. 1998). Thus the RanGTP gradient across the nuclear membrane determines the *directionality* of the soluble phase of nucleocytoplasmic transport, distinguishing between nucleoplasm and cytoplasm by promoting different complexes to form on the nucleoplasmic and cytoplasmic sides of the nuclear envelope. The actual translocation step across the pore is energy independent (Kose, Imamoto et al. 1997; Nakielny and Dreyfuss 1998) –

in fact, if the direction of the Ran gradient is reversed, the direction of transport is inverted (Nachury and Weis 1999).

FG-nups

Although much is known about the soluble phase of nucleocytoplasmic transport, the actual mechanism of translocation through the NPC remains largely unknown. Early EM studies indicated the presence of a "central transporter," or a "central plug," which was thought to be the conduit for transport (Akey and Goldfarb 1989; Akey 1990). While this "central plug" is now believed to be cargo complexes caught in transit (Beck 2004), this early work identified the steps of nucleocytoplasmic transport that have been the basis for all future models: peripheral binding to the NPC leading to a docking step over the center of the pore followed by a translocation step (Richardson, Mills et al. 1988; Akey and Goldfarb 1989). Many karyopherin binding sites have been found along the filamentous structures of the NPC, mostly on the FG-repeat regions of FG-nups (Moroianu 1995; Radu, Moore et al. 1995), reviewed in (Doye and Hurt 1997; Fabre and Hurt 1997) (**Figure 1-3)**. Considering the eight-fold symmetry of the NPC, it is estimated that there are at least 130 of these FG-domains in each NPC, combining for a total of ~3,500 FG repeats (Strawn, Shen et al. 2004). X-ray crystallography and computer modeling have demonstrated little more than that karyopherins interact with FG-nups via hydrophobic interactions with the

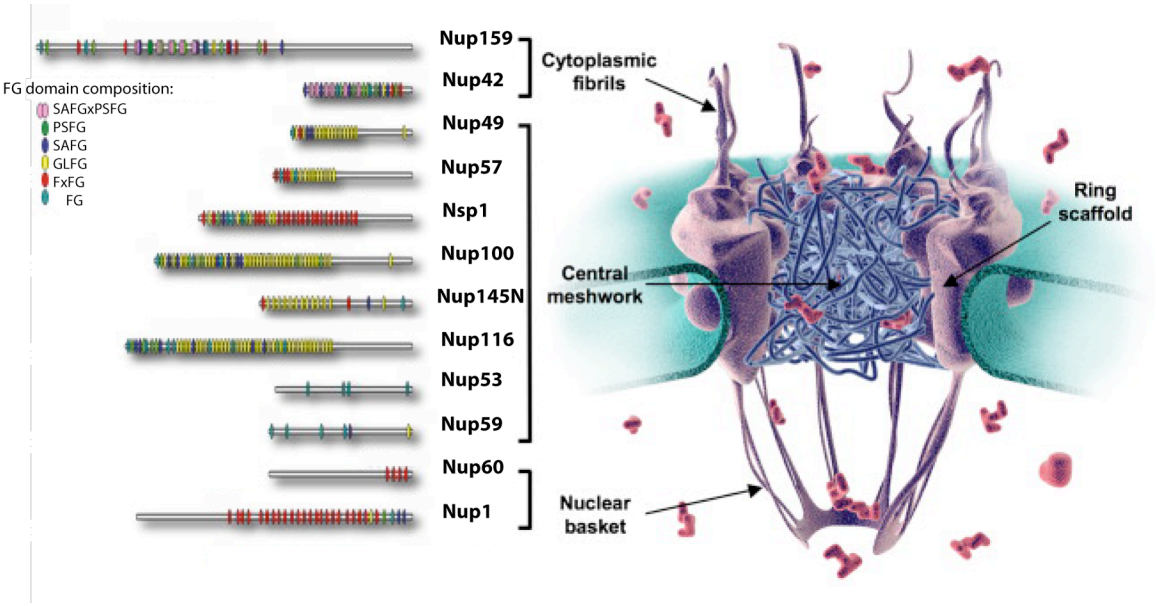

Figure 1-3: Schematic showing one interpretation of the disposition of FG-nups and their localization within the NPC. *S. cerevisiae* FG-nups are shown on the left with vertical tick marks corresponding to individual FG motifs. A cross-section of the NPC is shown on the right, with its ring scaffold, its cytoplasmic fibers, a putative meshwork of FG-domain filaments in its center, and the nuclear basket structure (Figure modified from (Patel, Belmont et al. 2007)).

phenylalanine rings (Bayliss, Corbett et al. 2000; Bayliss, Kent et al. 2000; Bayliss, Littlewood et al. 2000; Bayliss, Leung et al. 2002; Bayliss, Littlewood et al. 2002; Isgro and Schulten 2005; Isgro and Schulten 2007; Isgro and Schulten 2007). When compared to the yeast proteome, the FG-nups are enriched in charged and polar amino acids and depleted in hydrophobic amino acids. This amino acid composition is predicted to lead to disorder in protein secondary structure (Uversky, Gillespie et al. 2000; Dunker, Lawson et al. 2001; Denning, Patel et al. 2003; Denning 2007). Sucrose gradient sedimentation and gel filtration chromatography indicate that monomeric FG-nups exhibit large hydrodynamic dimensions (54-75 Å), and that these dimensions do not change significantly under denaturing conditions (Denning, Patel et al. 2003). FG-nups have been shown to be very sensitive to proteolysis by proteinase K, both as purified proteins and *in situ* in isolated nuclei (Denning, Patel et al. 2003). CD- and FTIR spectra of FG-nups suggest a lack of α helical or β sheet structure with significant contributions from unfolded regions (Denning, Patel et al. 2003). Atomic force microscopy indicates that FG-domains are natively unfolded and flexible (Lim, Huang et al. 2006; Lim, Fahrenkrog et al. 2007). Together this provides strong evidence that FG-nups are natively unfolded, both *in vivo* and *in vitro*. It has been suggested that natively unfolded domains in general are characterized by the ability to bind specifically to a diverse family of proteins, (Kriwacki 1996) perhaps providing some insight as to how the NPC can selectively transport the many karyopherins and other select macromolecules.

Recent work has found some malleable “structure” due to intra-molecular interactions within these unfolded regions, which could indicate both intra- and inter-molecular interactions occur in the FG-repeat-rich environment of the NPC (Krishnan, Lau et al. 2007).

These natively unfolded FG-nups must be incorporated into the NPC. As crystal structures are known for just over 5% of the nucleoporin amino acid residues (for examples, see (Bayliss, Littlewood et al. 2000; Bayliss, Littlewood et al. 2002; Berke, Boehmer et al. 2004; Hsia, Stavropoulos et al. 2007; Melcak, Hoelz et al. 2007; Boehmer, Jeudy et al. 2008; Brohawn, Leksa et al. 2008; Debler, Ma et al. 2008; Schrader, Stelter et al. 2008), bioinformatics was used to assign folds to different domains of all nucleoporins (Devos, Dokudovskaya et al. 2004; Devos, Dokudovskaya et al. 2006; Dokudovskaya, Williams et al. 2006). Several FG-nups are thought to be anchored to the NPC via a terminal coiled-coil domain, while others are predicted to contain an RRM motif or a β-sandwich motif. Still others are predicted to consist primarily of large regions that are natively unfolded (Bailer, Siniossoglou et al. 1998; Devos, Dokudovskaya et al. 2006). At least one sub-complex containing three of the FG-nups (Nsp1, Nup49, and Nup57) is thought to be anchored to the NPC via the interactions of between the GLFG domains of Nup49 and 57 and the coiled-coil domain of Nsp1 with the structural nucleoporin Nic96 (Grandi, Schlaich et al. 1995; Alber, Dokudovskaya et al. 2007; Alber, Dokudovskaya et al. 2007; Schrader, Stelter et al. 2008).

Nsp1, Nup159, and Nup116 are thought to be anchored to the structural protein Nup82 via their C-terminal domains (Grandi, Emig et al. 1995; Belgareh, Snay-Hodge et al. 1998; Hurwitz, Strambio-de-Castillia et al. 1998; Bailer, Balduf et al. 2000; Alber, Dokudovskaya et al. 2007; Alber, Dokudovskaya et al. 2007).

Models of the transport mechanism

The movement of Kap-cargo complex through the NPC is thought to be mediated by a series of docking and release steps between the Kaps and the numerous FG-nups (Rout and Wente 1994; Radu, Blobel et al. 1995; Radu, Moore et al. 1995; Wozniak, Rout et al. 1998). While most FG-nups are symmetrically localized in the NPC, a few are exclusively nucleoplasmic or cytoplasmic and others are biased toward one side or the other (Fahrenkrog, Hurt et al. 1998; Marelli, Aitchison et al. 1998; Strahm, Fahrenkrog et al. 1999; Fahrenkrog, Aris et al. 2000; Ho, Shen et al. 2000; Rout, Aitchison et al. 2000; Solsbacher, Maurer et al. 2000; Griffis, Xu et al. 2003; Krull, Thyberg et al. 2004; Alber, Dokudovskaya et al. 2007). The biased locations of these FG-nups may help in targeting Kaps to the correct side of the NPC (Ben-Efraim and Gerace 2001) and in enabling directional transport to occur more efficiently (Zilman, Di Talia et al. 2007). However, FG-nup localization can not be the only means of directing nucleocytoplasmic transport, as cells with the FG domains of all asymmetric FG-nups simultaneously deleted are still viable and these minimal

NPCs still support transport (Strawn, Shen et al. 2004; Zeitler and Weis 2004). In contrast, certain combinations of symmetric FG regions are essential for cell survival (Strawn, Shen et al. 2004). It has also been shown that GLFG domains, but not FxFG domains, are required for cell viability (Strawn, Shen et al. 2004).

While FG-nups are known to be involved in Kap-mediated transport, exactly how they function remains controversial. Several models for the FG-nup barrier have been proposed. A molecule freely diffusing in the cytosol has a very high entropy because it has a very large space in which to move around. When such a molecule enters the confined space of the NPC (further confined by the space occupied by the unfolded regions of the FG nups), the molecule's ability to move, and thus is entropy, is significantly decreased. Transported molecules must compensate for this decrease in entropy in order to cross the NPC (Rout, Aitchison et al. 2000; Rout, Aitchison et al. 2003; Zilman, Di Talia et al. 2007). The Brownian affinity gate model suggests that the natively unfolded FG-nups form a polymer brush, an entropic barrier that prevents non-interacting molecules from passing through the pore. However, for karyopherins and other select molecules that can bind the FG-nups, the enthalpy of binding would counteract the entropic penalty of entering the pore, leading to a decrease in the energy barrier posed by the NPC (Rout, Aitchison et al. 2000; Rout, Aitchison et al. 2003) **(Figure 1-4)**. To support this model, FG-nups have been shown to have polymer brush-like behavior when tethered to a surface (Lim, Huang et al. 2006).

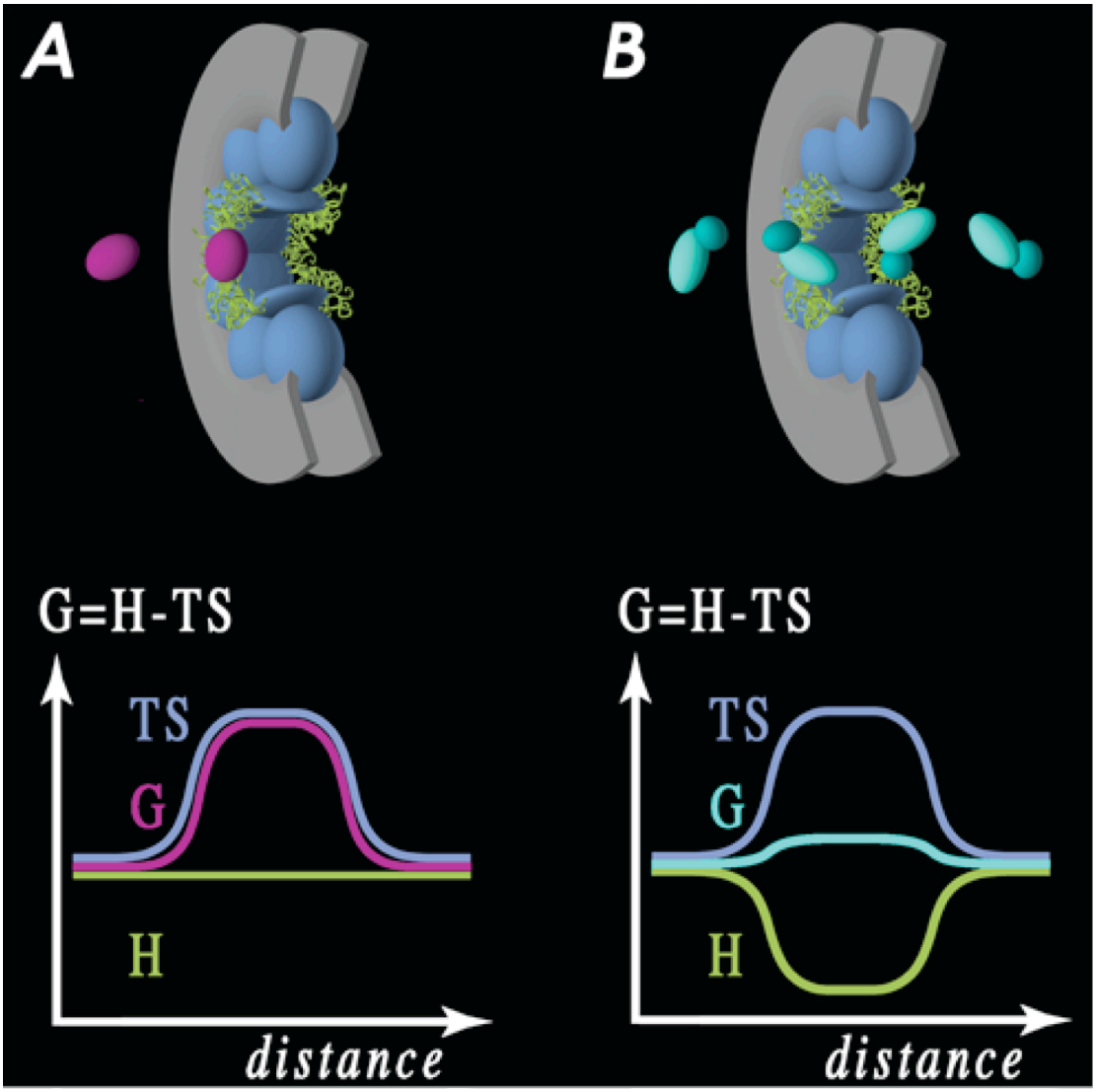

Figure 1-4: Energetics of macromolecular diffusion across the NPC. Illustrations (top) show (A), a macromolecule incapable of binding the NPC (purple), and (B), a similarly-sized karyopherin-cargo complex (light and dark turquoise) able to bind FG-nups (green). Graphs (bottom) showing the energetics of the same processes; TS is the entropic cost for diffusion, H is the enthalpic term for binding, and G the resultant free energy of the process, plotted on the vertical axis. (Figure modified from (Rout, Aitchison et al. 2003))

This entropic brush has been seen to collapse in the presence of hydrophobic solvents such as hexanediol. (Lim, Huang et al. 2006) and in the presence of an interacting karyopherin (Lim, Fahrenkrog et al. 2007). This karyopherin-induced FG-nup collapse is seen *in vitro* as well as *in vivo*, and is reversible upon binding of RanGTP (Lim, Fahrenkrog et al. 2007). These observations led to an amended model in which Kap-cargo complexes cross through the NPC via a series of stochastic binding-collapsing and unbinding-extending processes. In this model, the polymer brush formed from the non-Kap-bound FG-nups that remain in their extended state maintains the entropic permeability barrier (Lim, Fahrenkrog et al. 2007). Induced "structuring" of unfolded protein domains upon binding to a structured partner has been observed in other areas of biology including protein-RNA interactions, transcriptional control and cell cycle regulation (reviewed in (Wright and Dyson 1999; Fuxreiter, Tompa et al. 2008)).

The selective phase model (Ribbeck and Gorlich 2001; Frey and Gorlich 2007) proposes that the phenylalanines of the FG repeats cross-link with each other via hydrophobic interactions to form a gel-like barrier. In this model, proteins to be transported are able to intersperse themselves within this hydrophobic gel, while inert proteins are faced with an impenetrable barricade. To support this model, interactions between FG repeats are disrupted by the addition of hydrophobic solvents (Ribbeck and Gorlich 2002; Shulga and Goldfarb 2003). In addition, the FG domain of yeast nucleoporin Nsp1 has been

seen to form a hydrogel when at very high concentrations *in vitro* (Frey, Richter et al. 2006), and when the FG interactions are saturated, this hydrogel allows selective passage of karyophilic proteins (Frey and Gorlich 2007). It has also been seen that the FG-repeat regions of FG-nups containing GLFG-repeats are cohesive, binding via weak (Kd ~μM) hydrophobic interactions (Patel, Belmont et al. 2007). These nup-nup interactions were shown to rely on the hydrophobic phenylalanines and leucines of the GLFG repeats, and cohesive nups have very few charged residues in the linker regions connecting these GLFG repeats (Patel, Belmont et al. 2007). This cohesion was needed to maintain the passive permeability barrier of the NPC *in vivo* (Patel, Belmont et al. 2007). However, it should be noted that nups containing FxFG repeats, including Nsp1, were found to be non-cohesive in the more physiological conditions used in this study (Patel, Belmont et al. 2007). The finding of cohesive GLFG nups, localized towards the center of the NPC, and non-cohesive FxFG nups, localized towards the NPC periphery, led Patel and co-authors to propose a dual-gate mechanism. They suggest that a selective phase hydrophobic meshwork at the NPC center formed by the interactions between cohesive GLFG nups exists along with a Brownian motion gate composed of the non-cohesive FxFG nups (Patel, Belmont et al. 2007).

An affinity gradient model has also been proposed (Ben-Efraim and Gerace 2001), where karyopherins move through the NPC from nups with low affinity to nups exhibiting higher affinity for Kap complexes. An affinity gradient may help increase the efficiency of transport (Zilman, Di Talia et al. 2007), but it cannot be the only mechanism of transport selectivity because all of the asymmetric FG-nups can be deleted without stopping transport through the NPCs (Strawn, Shen et al. 2004; Zeitler and Weis 2004).

Another model has been proposed in which the FG repeats line the walls of the channel through the nuclear pore complex, and karyopherin-cargo complexes then explore the FG-surface via a two-dimensional random walk rather than a three-dimensional diffusion through space. This model, termed "reduction of dimensionality," can coexist with the virtual gating and affinity models discussed above (Peters 2005). A similar model describes the FG-nups as a layer of "oily spaghetti" which hinders non-binding proteins, but allows carrier proteins to diffuse easily (Macara 2001).

Studies have shown that structural (non-FG) nups such as Nup188 and Nup170 also contribute to the gating ability of NPCs (Shulga, Mosammaparast et al. 2000). Aliphatic alcohols have been seen to not only affect the permeability barrier of NPCs, but to lead to the reversible dissociation of select structural and FG-nups from NPCs in Nup170Δ cells (Shulga and Goldfarb 2003). This has led

to a model in which structural nups and FG-nups work together to create “hinges” to restrict passage through a gated pore (Shulga and Goldfarb 2003).

Although these models vary in the details of the permeability barrier, they all agree that karyopherins are able to cross the pore because of their selective binding to the FG-nups. The FG-nups are part of an entropic barrier blocking entry into the pore, and this barrier is overcome by selective binding. This general principle is referred to as “virtual gating” (Rout, Aitchison et al. 2000). While there is certainly redundancy in the process of karyopherin-mediated transport (one karyopherin may bind many FG-nups, and one FG-nup may bind many karyopherins), it has been shown that different karyopherins may have strong preferences for particular FG repeat classes (Allen 2001). It has also been shown that deletion of certain FG domains greatly affects the function of some karyopherins while others are unimpaired (Strawn, Shen et al. 2004; Terry and Wente 2007). This may indicate that there are separate, though overlapping, pathways across the NPC, and each Kap has a choice of more- or less-favored pathways (Marelli, Aitchison et al. 1998; Strawn, Shen et al. 2004).

The stoichiometry of Kap/FG-nup interactions is not yet known. Crystal structures and computer simulations of Kaps complexed with FG-repeat peptides indicate that multiple phenylalanines insert into multiple hydrophobic pockets on the surface of the kaps (Bayliss, Littlewood et al. 2000; Bayliss, Littlewood et al.

2002; Isgro and Schulten 2005; Liu and Stewart 2005), but it is not known if these sites are occupied *in vivo* by multiple phenylalanines from the same FG-nup, or by single phenylalanines from multiple FG-nups. If multiple phenylalanines from the same FG-nup bind a single karyopherin, the synergistic binding of multiple weak hydrophobic interactions would result in a very strong avidity between the Kap and the FG-nup. Multi-valency increases the apparent strength of an interaction by lowering the off-rate – the multiple connections would all need to release at the same time in order to terminate the interaction. This effect is different than the binding observed for an interaction where the binding partners are in high concentration. If the multiple phenylalanines on the Kap come from different FG-nups, the interaction is mediated by only one connection point per FG-nup, and the off-rate will not change as more Kap binding sites are occupied. It is also unclear if Kap/FG-nup binding is cooperative.

Goals of this work

While a lot is known about the soluble phase of nucleocytoplasmic transport, and the FG-nups have been identified as the components of the NPC responsible for permeability and selectivity, exactly how Kaps, cargo molecules, and the FG-nups work together to create this robust yet selective barrier is unknown. The Kap-NLS recognition mechanism must be selective enough so that Kaps carry only their designated cargoes through the NPC, but the

recognition must be robust enough to allow a single karyopherin to recognize a family of NLSs that vary in structure and sequence (Lee, Cansizoglu et al. 2006; Suel, Gu et al. 2008). The FG-nups must form a barrier that can allow select macromolecules through that have a wide variety in size and charge, while blocking transport of other macromolecules of similar size and charge. In this work, we used biochemical and cell biological techniques to quantitatively examine the interactions between karyopherins, cargo molecules, and FG-nups under a variety of conditions to better understand the protein-protein interactions involved in karyopherin-mediated transport across the NPC. We used enriched recombinant proteins and *in vitro* binding assays to measure the strength of interaction between Kaps and NLSs and between Kaps and FG-nups. We measured the strengths of Kap/NLS interactions in order to try and understand how different Kaps recognize and transport their own specific set of cargoes, and to identify the basis of redundancy in the system. We then measured the affinities between Kaps and FG-nups with the goal to identity the specific set of FG-nups that each karyopherin interacts with on its way across the NPC. We expected to see different subsets of FG-nups exhibiting significantly tighter affinity for different Kaps. Once identified, these sets of "favored" FG-nups combined with the predicted location of these FG-nups in the NPC (Alber, Dokudovskaya et al. 2007) would allow us to identity the exact path that each karyopherin takes as it transverses the NPC.

Our results led us to examine Kap/NLS and Kap/FG-nup interactions in a variety of environments. Most *in vitro* measurements of protein-protein interactions are performed using enriched proteins in dilute solutions. However, the addition of non-specifically interacting material to the surrounding buffer has have been shown to influence reaction rates and steady-state equilibria (Zimmerman and Trach 1991; Zimmerman and Minton 1993; Garner and Burg 1994; Minton 2006; Minton 2006). In a living cell there is an abundance of proteins, nucleic acids, and lipid material that are not specifically involved in the interaction of interest. Therefore we examined Kap/NLS and Kap/FG-nup interactions in the presence of bacterial lysate. As bacteria do not have nuclei, they should have no endogenous karyopherins, FG-nups, or NLS-cargoes to specifically compete with the reactions of interest. These experiments were performed to see how these proteins interact in an environment that more closely resembles what the NPC experiences *in vivo*.

Through this work, we aim to provide some insight as to how Kap/NLS and Kap/FG-nup interactions have been fine-tuned to create an efficient sorting mechanism in the highly crowded environment of the living cell.

Chapter Two: Obtaining the starting materials – Karyopherins, cargoes, and FG-nups

In order to study protein-protein interactions, one must first obtain enriched samples of the proteins in question. Our initial plan was to purify Kaps expressed in yeast under their endogenous promoters as Protein A-tagged fusions. However, our assays required much more protein than endogenous expression, or even over-expression, in yeast can provide (36 liters of yeast culture produced only 200 μg of enriched Kap. We find this yield is typical for proteins expressed in yeast). For this reason we decided to switch to recombinant protein expression in *E. coli*. In all cases, problems with protein production were encountered, which have hampered other attempts to study these proteins (see below). We have therefore introduced modifications to general protocols that have allowed us to produce sufficient amounts of full-length proteins for such studies, and these modifications are described in this chapter.

Expression and purification of karyopherins

There are 13 homologues of importin β and one homolog of importin α in the yeast *Saccharomyces cerevisiae* (Pennisi 1998). One of the best-studied import pathways is that of the lysine-rich "classical" NLS. Kap60 (Srp1p, the

importin α homolog) binds the lysine-rich NLS sequence of its cargo molecule, and this Kap60/cargo complex forms a hetero-trimer with Kap95 (one of the importin β homologs). This Kap95/Kap60/cargo hetero-trimer then crosses the NPC via interactions between Kap95 and the FG-nups (Adam and Adam 1994; Gorlich, Prehn et al. 1994; Moroianu 1995; Radu, Moore et al. 1995). As this is a well-characterized import pathway, we wanted to examine the relevant interactions of Kap95. We also wanted to examine at least one other yeast karyopherin, as Kap95 is unique in its need for the adapter protein Kap60. Kap123 and Kap121 (Pse1p) are related proteins, homologues of importin β3, and partially redundant in their function (Rout, Blobel et al. 1997). Kap121 is essential while Kap123 is not, meaning that *in vivo* work can be done on cells lacking Kap123. Kap121 has been shown to partially rescue import of Kap123 cargoes in ΔKap123 cells (Timney, Tetenbaum-Novatt et al. 2006). Kap104 is the yeast homolog of karyopherin β2, and transports a distinct set of cargoes from Kaps 121 and 123 (Aitchison, Blobel et al. 1996; Lee and Aitchison 1999). Plasmids encoding GST-tagged versions of the yeast karyopherins Kap95 and Kap121 were a kind gift from J. Aitchison and D. Leslie (Leslie, Zhang et al. 2004). Kap123 was transferred from the yeast plasmid BT028 into a bacterial GST vector. (Timney, Tetenbaum-Novatt et al. 2006) (See **Table 2-1** for a list of Kap plasmids in this study). A detailed purification protocol is in the Materials and Methods chapter, but a brief summary follows here. For all Kaps, plasmids were transformed into BL21DE3 RIL *E. coli* cells, and protein expression was

Table 2-1: Karyopherin and cargo plasmids used in this study

Descriptive Name	Formal Name	Construction	Source
RPL25NLS-GFP-His	pJN001	RPL25NLS-GFP amplified from pBT001, with AseI and SalI sites engineered into upstream and downstream PCR primers respectively; fragment inserted into NdeI-SalI of pET21b (Novagen).	(Timney, Tetenbaum-Novatt et al. 2006)
Rpl25NLS-GFP-His (K21A K22A)	pJN002	Mutated rpl25NLS-GFP amplified from pBT009, with AseI and SalI sites engineered into upstream and downstream PCR primers respectively; fragment inserted into NdeI-SalI of pET21b (Novagen).	(Timney, Tetenbaum-Novatt et al. 2006)
PHO4NLS-YFP-His	pJN003	PHO4-NLS-YFP amplified from pBT031 in NdeI-SalI of pET21b (Novagen).	(Timney, Tetenbaum-Novatt et al. 2006)
NAB2NLS-GFP-His	pJN004	NAB2NLS-GFP amplified from pBT032, with AseI and SalI sites engineered into upstream and downstream PCR primers respectively; fragment inserted into NdeI-SalI of pET21b (Novagen).	(Timney, Tetenbaum-Novatt et al. 2006)
GST-GFP	GST-GFP	GFP ORF in SalI-NotI of pGEX-4T3 (GE Healthcare)	J. Rosenblum
GFP-HIS	pJN006	GFP ORF in NdeI-SalI of pET21b (Novagen)	This study
GST-KAP104	GST-KAP104	KAP104 in BamHI of pGEX-2TK (GE Healthcare)	(Lee and Aitchison 1999)
GST-KAP121	GST-KAP121	KAP121 in BamHI-XhoI of pGEX-4T1 (GE Healthcare)	(Marelli, Aitchison et al. 1998)
GST-KAP123	pJN005	KAP123-HA from pBT028 in SalI of pGEX-4T3 (GE Healthcare)	(Timney, Tetenbaum-Novatt et al. 2006)

induced with 1 mM IPTG when OD_{600} (optical density at 600 nm) reached 0.8. Cells were harvested after shaking at 30 ºC for ~16 hours, lysed in TBT buffer (recipe in Materials amd Methods chapter), and the GST-Kap was enriched using glutathione Sepharose fast flow (GE Healthcare). Protein was eluted in reduced glutathione (Sigma Aldrich). This GST-tagged karyopherin was shown to be functional because it still recognized its cognate NLS and Nup binding partners (see following chapters). The GST was linked to the karyopherin via a thrombin cleavage site, and when removal of the GST was required, the recombinant proteins were cleaved with biotinylated thrombin (Novagen). The thrombin was then removed with avidin-Sepharose (Novagen), and the cleaved GST was removed with glutathione Sepharose 4B (GE Healthcare) leaving protease- and GST-free karyoherin (**Figure 2-1 A)**.

Karyopherins often expressed full-length, but they were found to be aggregated by gel filtration chromatography and by native PAGE analysis. Centrifugation for 2 hours at 112,000 x g_{av} at 4ºC in a TLA55 rotor (Beckman) removed the aggregates, resulting in largely monomeric protein (**Figure 2-1 B and C**).

Kap123 is the most abundant karyopherin in yeast, and the kinetics of its import have been well characterized *in vivo* (Timney, Tetenbaum-Novatt et al. 2006). Therefore, Kap123 would be the quintessential karyopherin to study

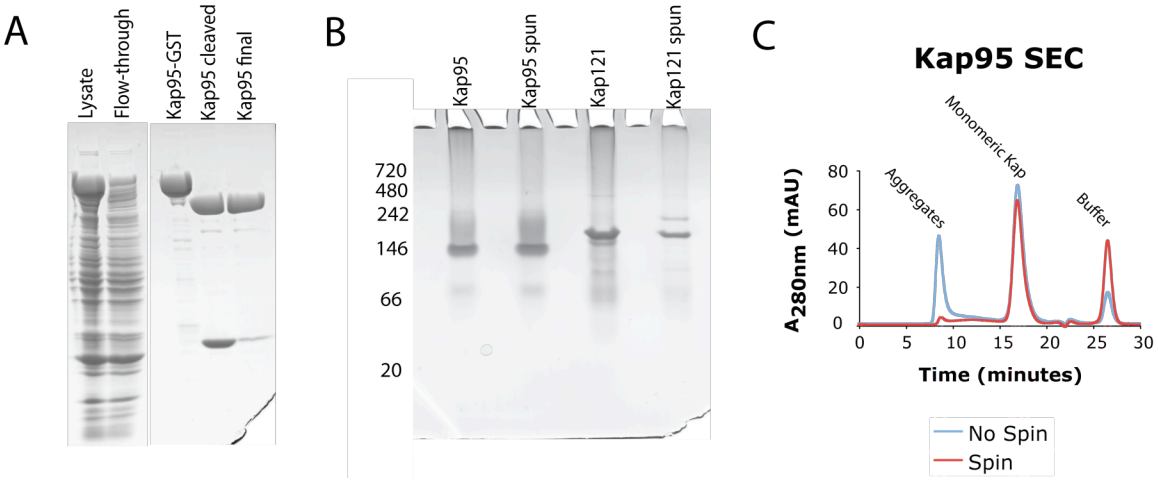

Figure 2-1: Obtaining enriched and monomeric karyopherin from bacteria. A) Coomassie blue stained SDS-PAGE gel of Kap95-GST purification and thrombin cleavage. Lysate before and after incubation with glutathione Sepharose is shown in lanes 1-2. Enriched Kap95-GST before and after thrombin cleavage to remove the GST is shown in lanes 3-4. An additional incubation with glutathione Sepharose was used to remove the cleaved-off GST. The final product is shown. B) Native gel of Kap95 and Kap121 before and after a 2 hour spin at 112,000 x g. The spin is seen to remove aggregates. MW standards are indicated. C) Size exclusion chromatography of Kap95 before and after a 2 hour spin at 112,000 x g. Again, this spin is seen to remove aggregates, resulting in monomeric Kap.

biochemically. Unfortunately, we were unable to obtain enough full-length Kap123 for our studies. Full-length protein could be enriched from yeast, but we would only get several hundred μg of enriched Kap from 36 litres of yeast culture. When we tried to express this protein in bacteria, a second band at ~70kD was always seen. Mass spectrometric analysis of a trypsin digest of this "contaminating" gel band indicated that the contaminant was in fact full-length Kap123 itself – the protein cleaved into two equal pieces that run together on SDS PAGE (**Figure 2-2 A and B)**. This cleavage product has been published previously, where the cleavage product reacted with anti-GST antibodies, and was thus identified as part of Kap123-GST (Isoyama, Murayama et al. 2001). After thrombin cleavage was used to remove the GST from Kap123, one of the halves is now 26 kDa smaller than the other, and the two bands separate. Size exclusion chromatography was able to enrich for full-length Kap to some extent (**Figure 2-2 C**), but the yield was much too low for our needs. Other separation techniques such as differential ammonium sulfate precipitation or ultra-centrifugation were unable to separate the cleaved from full-length protein.

Since we could not separate the cleavage product from full-length Kap after purification, we next aimed to prevent the cleavage from occurring in the first place. Amino acid sequencing allowed us to identify the cleavage site, and we attempted to use site-directed mutagenesis to change the amino acids at and around the cleavage site to remove any potential cryptic protease site. However,

this was unsuccessful in preventing the cleavage. Adding protease inhibitors to the growth media, changing cell strains, and co-expressing with chaperone proteins all failed to prevent the cleavage. Therefore, although Kap123 is a very well characterized karyopherin *in vivo*, we will use it sparingly in this biochemical study, knowing that the protein is partially cleaved.

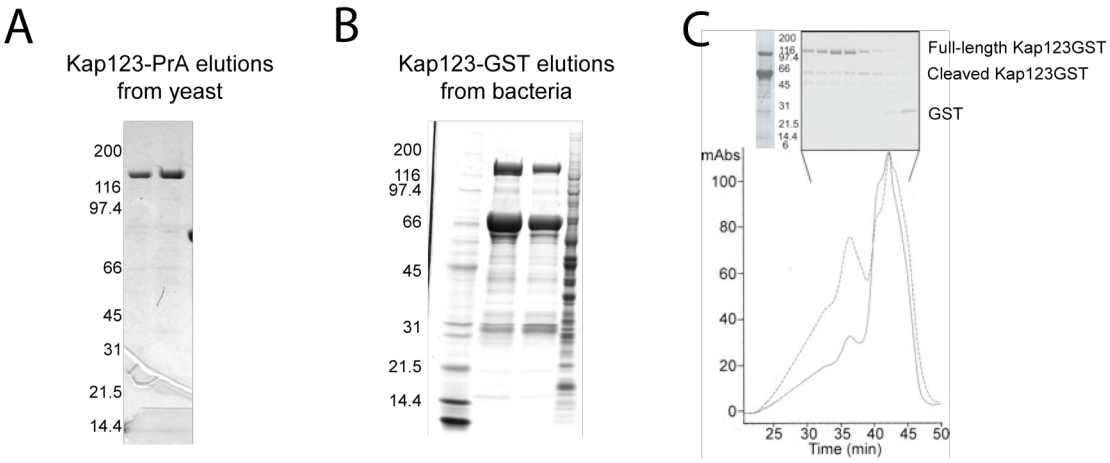

Figure 2-2: Expression of Kap123 in bacteria results in a combination of cleaved and full-length Kap123. We are unable to prevent the cleavage nor to adequately separate cleaved protein from full-length. However, this inability to separate cleaved from full-length protein, plus the observation that the cleaved protein still recognizes its cargo (chapter 3) leads us to believe that, despite the nick, the secondary structure of the protein is still intact, and the protein is at least partially functional. A) Full-length Kap123-PrA expressed under the endogenous promoter and enriched from yeast. No cleavage is observed. B) Kap123-GST expressed and enriched from bacteria. The protein is seen to cleave in half, as evidenced by the two bands - one at ~150kD and one at ~75kD. C) Attempt to separate cleaved from uncleaved Kap123 by size exclusion chromatography. The left-most lane shows the starting material, and the lanes to the right are elutions from size exclusion chromatography. Enrichment of full-length protein was somewhat successful, but we were unable to get the yield high enough for our needs.

Expression and purification of sample cargo molecules

Karyopherins recognize their cargo molecules via nuclear localization sequences, or NLSs (Dingwall and Laskey 1986; Goldfarb, Gariepy et al. 1986; Moore and Blobel 1992), and it has been shown that the short NLS peptide is sufficient to target normally non-imported proteins to the nucleus (for an example, see (Goldfarb, Gariepy et al. 1986)). A particularly useful construct to study import consists of an NLS sequence fused to Green Fluorescent Protein (GFP). This construct allows import to be monitored in real time in living cells using fluorescent microscopy (Shulga, Roberts et al. 1996). For his PhD work, Benjamin Timney further developed this nuclear import assay to quantitatively measure import kinetics of different karyopherin/NLS-cargo combinations (Timney, Tetenbaum-Novatt et al. 2006). Using fluorescent constructs of karyopherins and NLS-conjugates, Timney monitored karyopherin and cargo concentrations and how they related to import rate in living yeast. To accompany these *in vivo* measurements, my goal was to measure the strength of interactions between karyopherins and their NLS-cargoes *in vitro*. To this end, I transferred the DNA encoding for the NLS-GFP and NLS-YFP constructs into plasmids for expression in bacteria (see **Tables 2-1 and 2-2** for the NLS sequences and plasmid construction). The initial plan of using thrombin to remove a GST tag from the enriched protein was unsuccessful because the flexible NLS domain was non-specifically cleaved off by the thrombin. I therefore re-cloned the fluorescent NLS constructs into pET vectors to purify them with a His_6-tag. This

allowed us to do the entire lysis and purification in the presence of protease inhibitors. The unfolded NLS domain was so protease sensitive that we found 0.1 mM EDTA was required in addition to protease inhibitors to prevent the exposed NLS domain from being cleaved off (**Figure 2-3**).

Table 2-2: NLS-GFP fusion proteins

Name	Function of protein	NLS sequence	Karyopherin	Reference
Rpl25p	Ribosomal protein	MAPSAKATAAKKAVVKGT NGKKALKVRTSATFRLPK TLKLARAPK (aa 1-45)	Kap123p	(Schaap, van't Riet et al. 1991)
Rpl25p mutant	Ribosomal protein	MAPSAKATAAKKAVVKGT NGAAALKVRTSATFRLPK TLKLARAPK (aa 1-45)	Kap123p	(Schaap, van't Riet et al. 1991; Timney, Tetenbaum-Novatt et al. 2006)
Pho4p	Phosphate regulation	ANKVTKNKSNSSPYLNKR RGKPGPDSATSLFELPDS VIPTPKPKPKPKQYPK VILP (aa 141-196)	Kap121p/Kap123p	(Kaffman, Rank et al. 1998; Timney, Tetenbaum-Novatt et al. 2006)
Nab2p	mRNA binding	DNSQRFTQRGGGAVGKN RRGGRGGNRGGRNNNST RFNPLAKALGMAGESN (aa 201-250)	Kap104p	(Lee and Aitchison 1999)

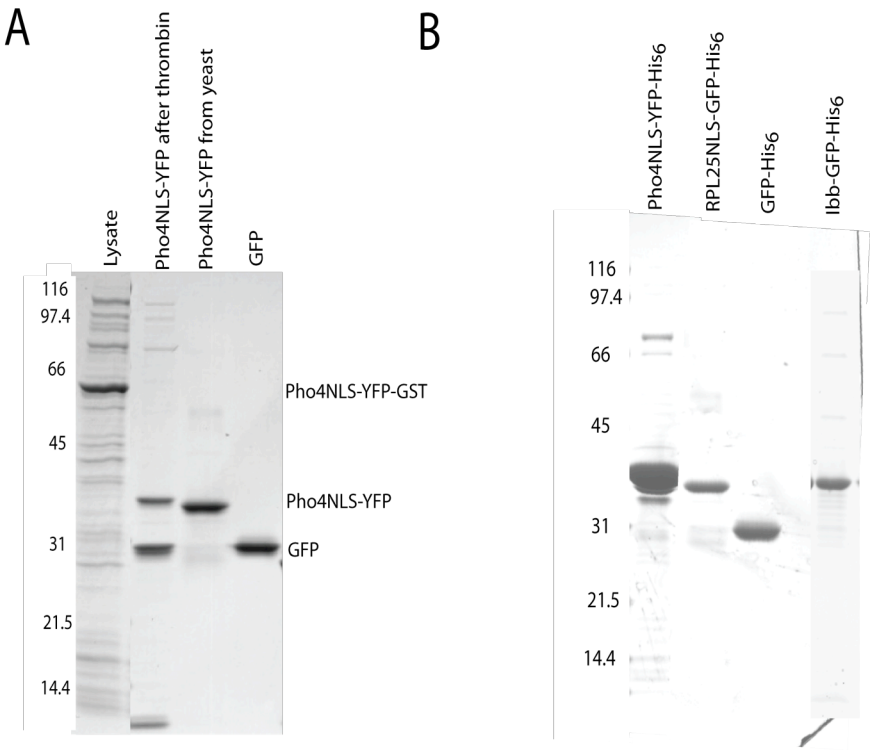

Figure 2-3: Expression and purification of NLS-GFP constructs. A) SDS Page gel showing the enrichment and cleavage of PhoNLSYFP-GST. Note that treatment with thrombin to remove the GST also removes some of the unfolded protease-sensitive NLS domain, resulting in a mixture of YFP +/- Pho4NLS. Note that the Pho4-GFP elution from bacteria is slightly heavier than from yeast because of the extra amino acids from the thrombin cleavage site. B) Elutions of His6-tagged NLS constructs. Eliminating the need for thrombin cleavage enables the entire purification procedure to be done in the presence of protease inhibitors, resulting in a product that is mostly in tact.

Expression and purification of FG-nups

FG-nups are natively unfolded (Denning, Patel et al. 2003), and thus highly sensitive to proteases. For this reason, most work studying FG-nups using recombinant proteins is done with fragments of FG-nups rather than the full-length protein (for examples, see (Bayliss, Littlewood et al. 2000; Allen, Patel et al. 2002; Bayliss, Leung et al. 2002; Bayliss, Littlewood et al. 2002; Denning, Patel et al. 2003; Pyhtila and Rexach 2003)). However, it has been shown that non-FG regions of the FG-nups can be involved in karyopherin interactions (Pyhtila and Rexach 2003). For this reason, we aimed to express and purify full-length constructs of as many of the FG-nups as possible. As these proteins are natively unfolded, they are often insoluble or in inclusion bodies when expressed in *E. coli*. 8 M urea was found to successfully solubilize the FG-nups, and as they are already natively unfolded, the denaturing conditions were not a concern. 6-amino-n-caproic acid, a lysine analog, was found to decrease the amount of proteolysis that occurred during the purification process.

The DNA sequence of full-length nups were amplified by PCR from yeast genomic DNA or from other plasmids, and inserted into the pET family of vectors (**Table 2-3)**. Unlike GST, the His_6 tag does not need to be structured and will function in 8 M urea. Expression times and temperatures were optimized for each FG-nup to produce the most protein with the least breakdown (**Table 2-4**).

Table 2-3: FG-Nup plasmids used in this study

Descriptive Name	Vector	Cloning Site	His-Tag	Source
Nsp1- N tag	pET15b	NdeI/BamHI	N-terminal	Svetlana Dokudovskaya
Nsp1-C tag	pET21b	NdeI/XhoI	C-terminal	This study
Nup1	pET28a	NdeI/EcoRI	N-terminal	This study
Nup42	pET28b	NcoI/XhoI	C-terminal	Svetlana Dokudovskaya
Nup49	pET28b	NcoI/XhoI	C-terminal	Svetlana Dokudovskaya
Nup53	pET15b	NdeI/BamHI	N-terminal	Svetlana Dokudovskaya
Nup57	pET28b	NcoI/XhoI	C-terminal	Svetlana Dokudovskaya
Nup59	pET15b	NdeI/XhoI	N-terminal	PCRd from Nup59 in pGEX-3x from Patrick Lusk (Univ Alberta)
Nup60	pET28b	NdeI/XhoI	N-terminal	This study
Nup100 – N tag	pET28b	NdeI/XhoI	N-terminal	Subcloned from pSW151 (Susan Wente)
Nup100 – C tag	pET21b	NdeI/XhoI	C-terminal	This study
Nup145N	pET21a	EcoRI/NotI	C-terminal	This study

Table 2-4: Protein expression conditions

Protein Name	Induction time (hours)	Induction temp (°C)
Nup1 (+ Kap95)	4	22
Nsp1	10	30
Nsp1 (+ Kap95)	4	30
Nup42	2	37
Nup49	4	30
Nup53	4	30
Nup53 (+ Kap95)	4	30
Nup57	1	37
Nup59	4	30
Nup59 (+ Kap95)	4	30
Nup60	2	30
Nup100	1	30
Nup100 (+ Kap95)	4	30
Nup145N	2	37
Nsp1FG-cys	3.5	30
Nup100FG-cys	2	37
RL25NLS-GFP	4	30
Pho4NLS-GFP	4	30
Nab2NLS-GFP	4	30
IBB-GFP	4	30
RL25NLS-GFP (mutant)	4	30
NTF2-GST (WT and W7A)	12	30
NTF2-YFP-His	12	23
GST-Kaps	16	30

Although there were degradation products, many of the FG-nups did express efficiently as full-length proteins after these protocol modifications (**Figure 2-4**). Post-translational modifications have not been reported for yeast FG-nups, therefore the behavior of recombinant proteins should be indicative of the behavior of endogenous proteins.

Full-length FG-nup expression was improved further in some cases upon co-expression with Kap95. In those cases, Kap95 and the FG-nup were cloned into plasmids with different antibiotic resistance markers and co-transformed into BL21DE3 RIL cells. Co-expression with Kap enabled us to obtain full-length Nup1, which had been previously described as unable to be expressed in *E. coli* (Gilchrist, Mykytka et al. 2002) (**Figure 2-5**). As FG-nups are thought to wrap around Kaps when bound (Bayliss, Littlewood et al. 2000; Bayliss, Littlewood et al. 2002), we propose that binding to Kap95 in the bacteria protects the normally unstructured FG domains from proteolysis. In most cases, we were able to obtain approximately 5 mg FG-nup per liter of bacterial culture. We were unable to obtain full-length versions of Nup116 and Nup159, even when co-expressed with Kap95, so they were not used in this study.

Despite our best efforts to obtain full-length protein, many of the FG-nups did purify with cleavage products and other contaminants (**Figure 2-4).** Enrichment of full-length FG-nups was improved up to 4-fold by binding to

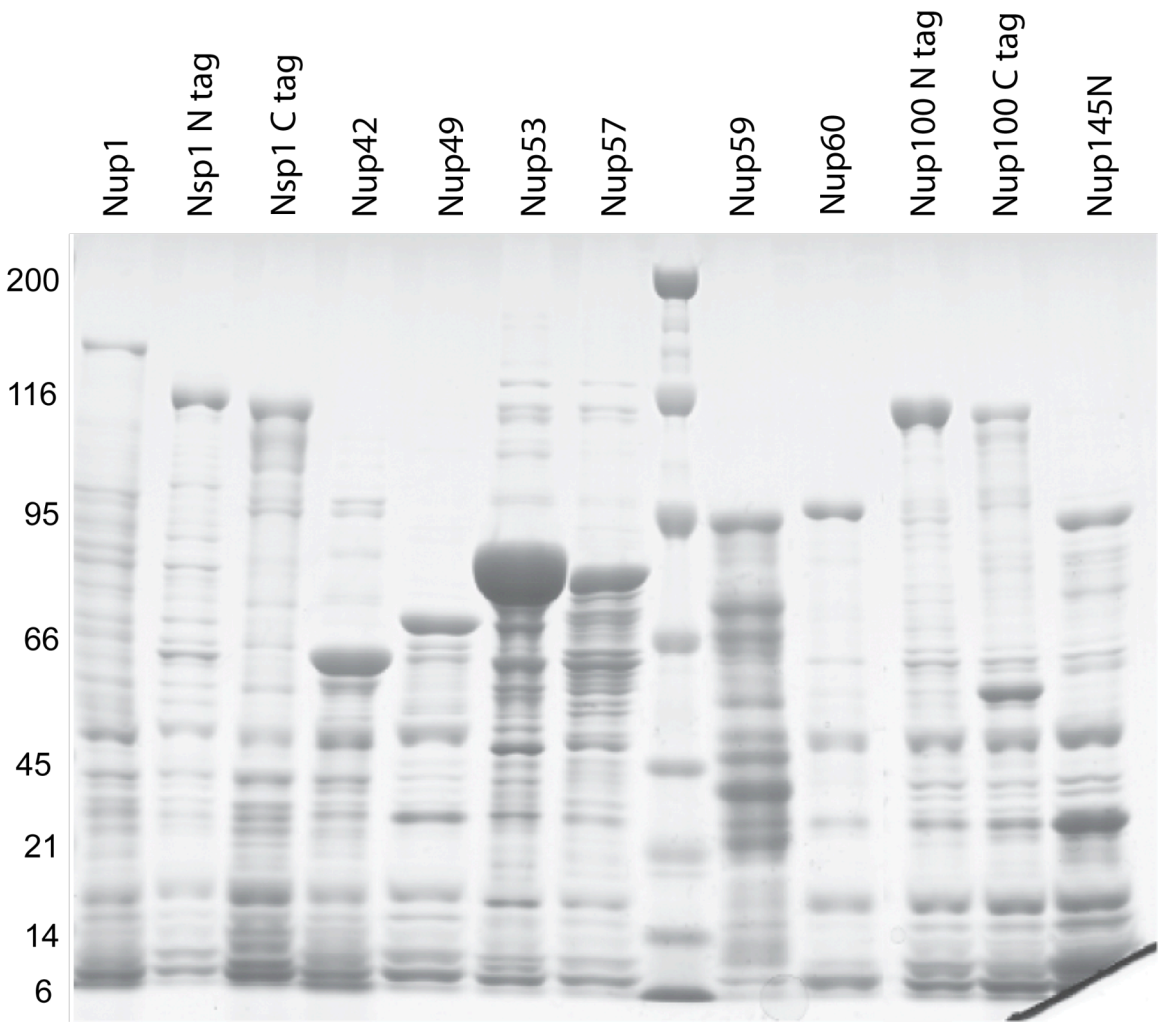

Figure 2-4: Enriched his-tagged FG-nups as eluted off of TALON Sepharose. Molecular weight standards are indicated on the left side. Expected molecular weights of the full-length FG-nups are: Nup1 (116 kDa), Nsp1 (87.5 kDa), Nup42 (44 kDa), Nup49 (50 kDa), Nup53 (53 kDa), Nup57 (57 kDa), Nup59 (59 kDa), Nup60 (61 kDa), Nup100 (101 kDa), Nup145N (66 kDa)

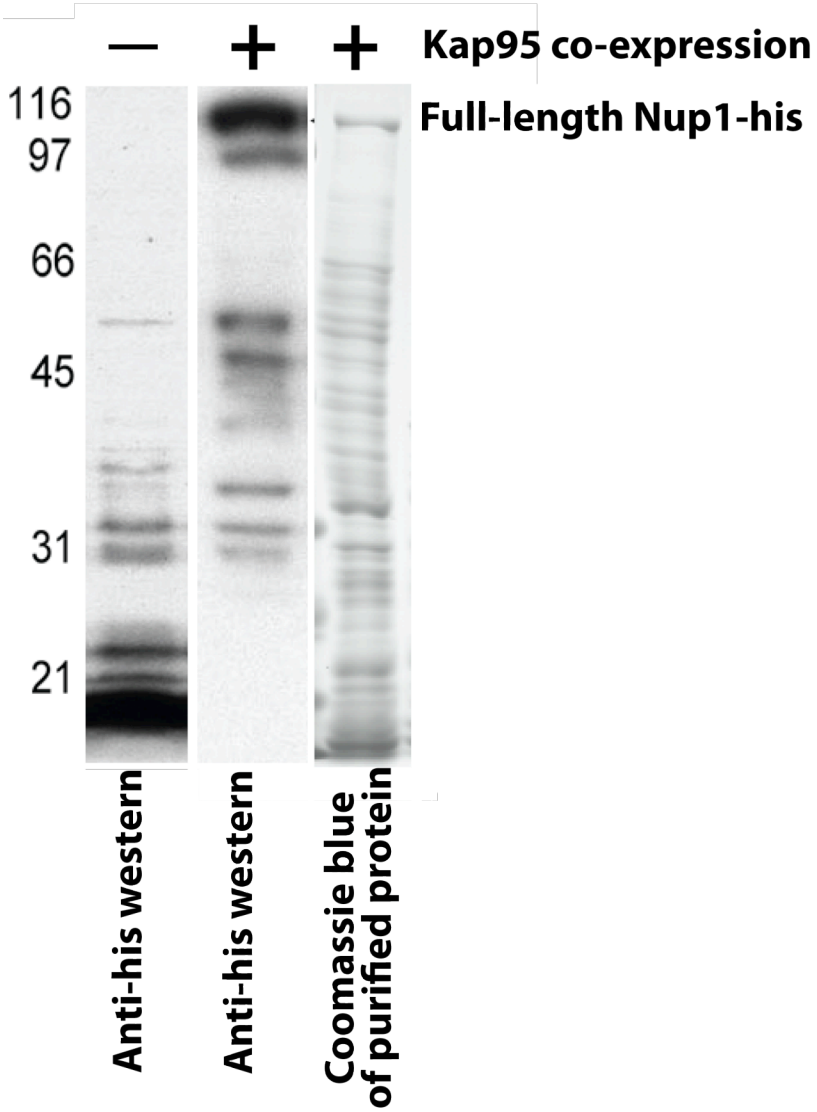

Figure 2-5: Obtaining full-length Nup1 from bacteria. Nup 1 has been previously described as "unable to be expressed in E coli. " (Gilchrist and Rexach 2003) We found that for Nup1 and other FG-nups, co-expression with Kap95 results in a higher yield and less breakdown. Both proteins were expressed from IPTG-induced plasmids that were co-transformed into the same cells. We conclude that binding to Kap95 while in the bacteria prevents the proteases from accessing the normally unfolded FG-nups. As the cells are lysed in 8 M urea, we are confident that the Kap is completely denatured and washed away from the nup during the enrichment process.

Dynabeads TALON® during our binding assays (see **Table 2-5, Figure 2-6,** and Chapter 4 for a description of the binding assays). When absolutely pure full-length protein was needed, electrophoretic purification was used (similar to the method reported in (Wang, Wei et al. 2003)). Because the FG-nups are natively unfolded (Denning, Patel et al. 2003), they still retain their Kap-binding ability after being boiled in SDS and run on a PAGE gel. Therefore, we ran tens of μg of His-enriched FG-nup on an SDS-PAGE gel, cut out the band containing full-length protein, and then used an electric current to elute the pure, full-length protein from the gel band. A schematic of the purification setup is shown in **Figure 2-7**.

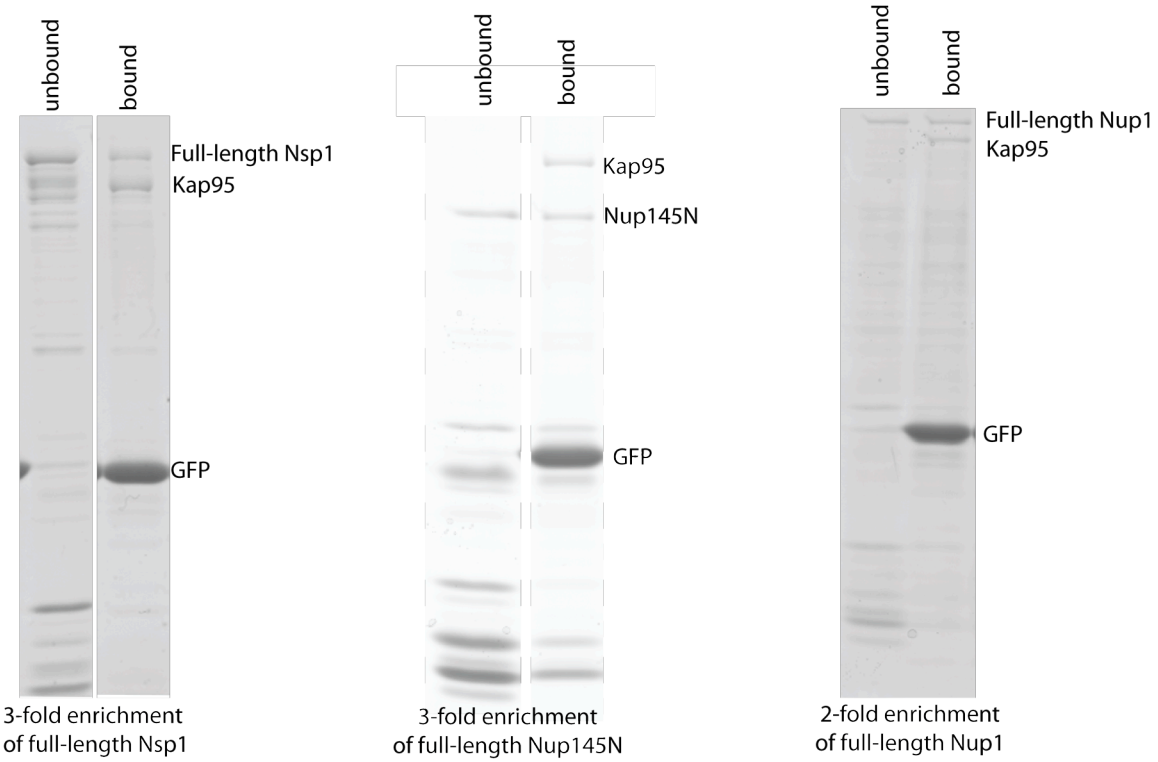

Figure 2-6: Enrichment of full-length FG-nups upon binding to Dynabeads TALON. After the initial enrichment using TALON Sepharose, his-tagged FG-nups are mixed with his-tagged GFP and bound to Dynabeads TALON for the karyopherin binding assays. This second round of TALON is seen to increase the fraction of full-length protein in some cases (see also **Table 2-5**).

Table 2-5: Enrichment upon binding to Dynabeads

FG-nup	Fold enrichment from stock to data point
Nsp1	3
Nup1	2
Nup42	1.2
Nup49	4
Nup53	1
Nup57	1
Nup59	2.5
Nup60	1.6
Nup100	1.5
Nup145N	3

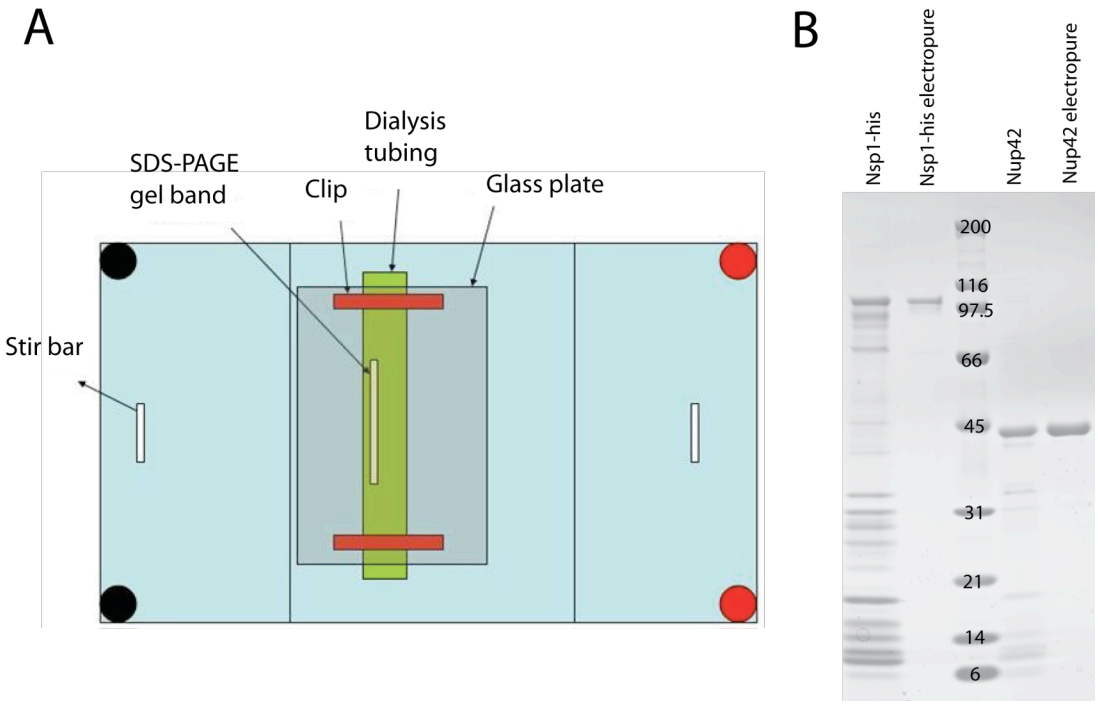

Figure 2-7: Electropurification. A) Schematic of the setup used to electrolytically purify FG-nups. The technique is described in the text of Chapter 2, and more thoroughly in Chapter 8, Materials and Methods. B) SDS-PAGE gel showing enriched FG-nups before and after electropurification. Bands are visualized with Coomassie Blue.

Conclusion

My thesis work is a biochemical analysis of the protein-protein interactions involved in nucleocytoplasmic transport. Our method of detection, Coomassie staining of SDS-PAGE gels, is less sensitive than other methods, such as radioactive labeling (for example, (Pyhtila and Rexach 2003)). Therefore, our experiments required many microgram to milligram quantities of protein. Obtaining large amounts of full-length protein is a challenge faced by many biochemists, and is often addressed by expressing and purifying small, well-behaved portions of protein for further study. This is true for studies of FG-nups (Bayliss, Littlewood et al. 2000; Allen, Patel et al. 2002; Bayliss, Leung et al. 2002; Bayliss, Littlewood et al. 2002; Denning, Patel et al. 2003; Pyhtila and Rexach 2003) and structural nups (Berke, Boehmer et al. 2004; Melcak, Hoelz et al. 2007; Schrader, Stelter et al. 2008). For our purposes, however, it was important to obtain full-length proteins, as different fragments of FG-nups exhibit different binding behaviors (Pyhtila and Rexach 2003). Obtaining large enough quantities of full-length proteins was a challenging aspect of this work. In many cases, full-length protein could be enriched from yeast, however the yields were orders of magnitude lower than were required for our experiments. Obtaining full-length and soluble versions of these protease-sensitive proteins from *E. coli* required trying a variety of tags, expression strains, growth and purification conditions. Co-expression of FG-nups with Kap95 was found in many cases to

improve the amount of full-length FG-Nup obtained. The addition of 6-amino-n-caproic acid, a lysine analog, helped prevent proteases from attacking the lysine-rich domains. 0.1mM EDTA was found to prevent metal-activated proteases from digesting off the flexible NLS domains from our GFP-NLS constructs. Doing as much of the FG-nup purification as possible at room temperature as opposed to 4ºC helped maintain protein solubility. All of these protocol modifications will be useful in future studies with these and other protease-sensitive proteins.

Chapter Three: Interactions between karyopherins and cargo molecules

Karyopherins bind to their cargo molecules via nuclear localization sequences (NLSs) or nuclear export sequences (NESs) (Mosammaparast and Pemberton 2004). The first NLSs to be identified were short, highly basic, lysine-rich domains that are recognized by Kap60 (importin α in mammals) (Goldfarb, Gariepy et al. 1986; Adam and Gerace 1991; Adam and Adam 1994; Gorlich, Prehn et al. 1994; Lange, Mills et al. 2007). The Kap60-cargo complex then joins with Kap95 (importin β in mammals) in the cytoplasm, and this hetero-trimer crosses through the nuclear pore complex. The import Kap-cargo complex then disassembles in the RanGTP-rich environment of the nucleus (Izaurralde, Kutay et al. 1997). Many other types of NLSs have since been found. Some arginine-rich NLSs bind to importin β without the need for the importin α adapter (Palmeri and Malim 1999). Other NLSs are transported by one of the other importin β homologs in yeast. These Kaps don't use adapters, but bind directly to their cognate NLSs (Aitchison, Blobel et al. 1996; Lee and Aitchison 1999; Leslie, Zhang et al. 2004; Hodel, Harreman et al. 2006; Lee, Cansizoglu et al. 2006; Lange, Mills et al. 2008). The criteria that define a peptide as being the NLS for a particular Kap are poorly defined, but may consist of one or two patches of lysine- or arginine-rich sequence (termed monopartite or bipartite NLSs) (Makkerh, Dingwall et al. 1996; Macara 2001; Hodel, Harreman et al. 2006; Bradley, Bowl et al. 2007; Hatayama, Tomizawa et al. 2008). While different

karyopherins recognize different NLSs, there is some overlap and redundancy. Certain Kaps can recognize more than one type of NLS, and the same cargo is sometimes transported by multiple Kaps. For example, Kap121 has been found to recognize and transport cargo proteins with both lysine-rich and arginine-rich (rg) NLSs, and the import of some of these rgNLS-proteins can be carried out by Kap104 when Kap121 is compromised (Leslie, Zhang et al. 2004). However, other importin β homologues such as Kap123 and Kap108 do not transport these rgNLS-proteins (Leslie, Zhang et al. 2004). It is not fully understood how karyopherin-mediated import can be so redundant and robust, yet so specific. For his thesis work, Benjamin Timney sought to address this question by examining the *in vivo* import kinetics of a model yeast karyopherin, Kap123, and it's ribosomal import cargo, Rpl25.

My investigations into the *in vitro* interactions between particular NLS-bearing cargoes and their Kaps were part of this much larger work. Kap123 is the most abundant karyopherin in yeast (Timney, Tetenbaum-Novatt et al. 2006), that binds and imports a number of ribosomal proteins (Rout, Blobel et al. 1997). In spite of its abundance and the importance of its ribosomal cargo, Kap123 is not essential (Rout, Blobel et al. 1997; Schlenstedt, Smirnova et al. 1997; Seedorf 1997). This led us to examine the kinetics of its import and the nature of its redundancy with Kap121, a less abundant member of the importin β family (Timney, Tetenbaum-Novatt et al. 2006) that is partially homologous to Kap123

and also imports ribosomal proteins (Rout, Blobel et al. 1997). Ben Timney developed an assay to quantitatively measure import kinetics in living cells (Timney, Tetenbaum-Novatt et al. 2006), based on a previously published method (Shulga, Roberts et al. 1996). He fused known NLSs to GFP (green fluorescent protein) or YFP (yellow fluorescent protein), creating fluorescent import substrates that could be visually monitored in real time (Shulga, Roberts et al. 1996; Timney, Tetenbaum-Novatt et al. 2006). He observed that although Kap123 was responsible for the majority of the import of its known ribosomal cargoes, Kap121 provided a backup import pathway. Indeed, when Kap121 was over-expressed in Δkap123 cells to similar levels as endogenous Kap123, Rpl25NLS-GFP was imported at equivalent rates (Timney, Tetenbaum-Novatt et al. 2006). To further dissect the nature of this redundancy, we needed to measure the relative affinity between these two Kaps and their common cargo.

Obtaining karyopherins and NLS-cargo molecules

In order to measure the affinity between these Kaps and the Rpl25NLS, I cloned the same Rpl25NLS-GFP construct that was used in the *in vivo* import assays into bacterial plasmids in order to express and purify this NLS-GFP as a His_6-tagged protein (see **Table 2-1** for plasmids in this study). Thus, we performed *in vivo* and *in vitro* assays using the same constructs, allowing us to directly compare results from both types of experiments. Karyopherins were

expressed as GST-tagged proteins in *E. coli* and enriched using glutathione Sepharose (Leslie, Zhang et al. 2004).

As noted in Chapter Two, we were unable to obtain pure, full-length Kap123. Some of the protein has been partially proteolysed, resulting in a "nicked" Kap123. Cleavage of recombinant Kap123 has been seen before (Isoyama, Murayama et al. 2001). However, we suggest that the cleaved Kap has proper secondary structure and is functional, as the full-length and cleaved proteins do not fully separate upon gel filtration and both the full-length and cleaved Kap bind to NLSs (**Figure 3-1**). Therefore, we measured the affinity of this partially cleaved Kap123 to Rpl25NLS-GFP, assuming that the nick was not influencing the function of the protein.

Method Development

We needed to develop a method to reliably measure the equilibrium dissociation constants (K_ds) between enriched Kaps and the NLS-GFP constructs. We first adopted the method of Delphin et al (Delphin, Guan et al. 1997), where NLS-GFP is bound to the bottom of a microtiter plate that is then probed with Kap. This method proved to be unreliable in our hands because the amount of NLS adhered to each well varied greatly between and within assays,

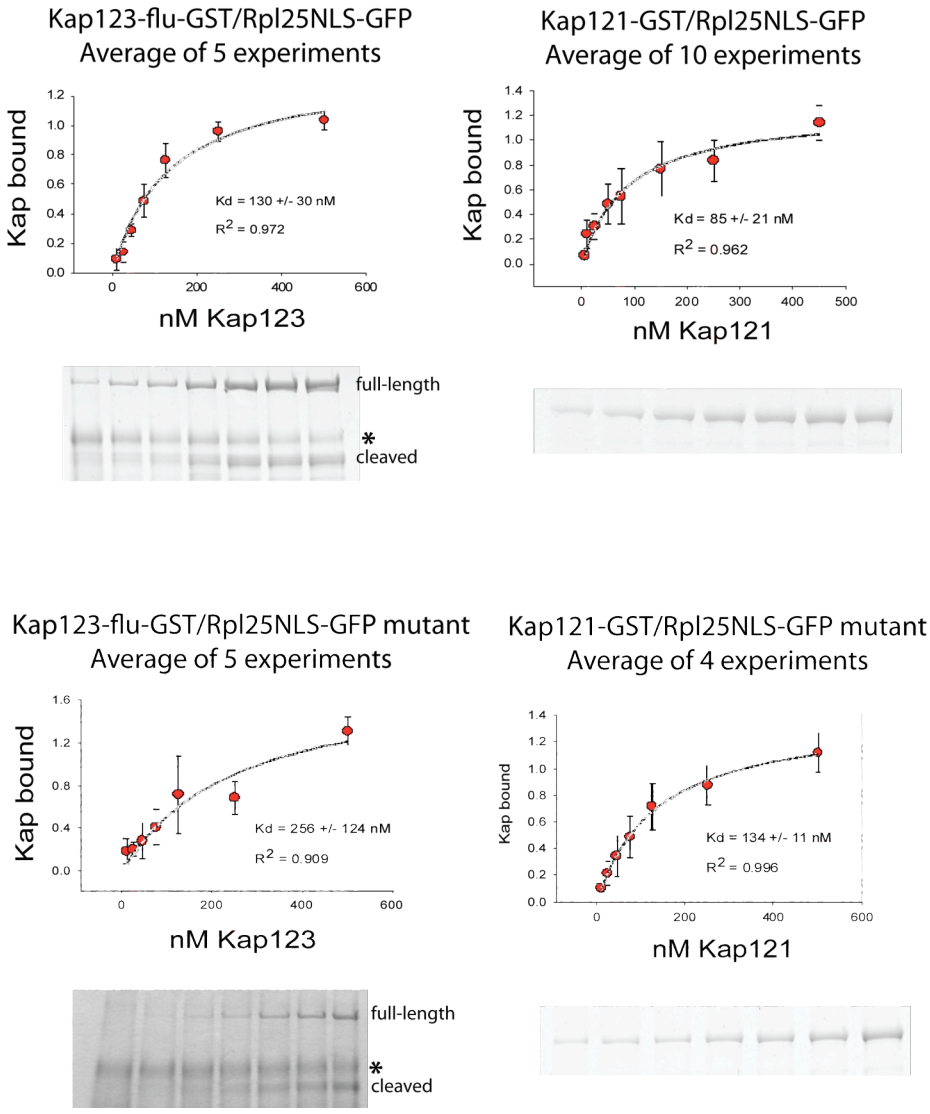

Figure 3-1: Example results of Kap 123 and Kap121 binding measurements over wild type and mutant Rpl25NLS-GFP. Increasing concentrations of Kap in 2.5% milk were incubated with a constant amount of GFP-NLS immobilized on anti-GFP Sepharose. Bound proteins were eluted with SDS and run on a gel. Coomassie stained bands were quantified, and the intensity of the Kap band was plotted versus the concentration of Kap. Each experiment was normalized, and the data was averaged across multiple repetitions. Plotted are the mean bound-Kap band intensities at each Kap concentration. Error bars indicate standard deviation. The band in the Kap123 gels indicated with a * is a milk protein.

and furthermore Kap was seen to bind non-specifically to the surface of plates where no NLS was bound (**Figure 3-2 A**).

We therefore explored different methods to immobilize our NLS-GFP bait proteins. We used TALON Sepharose (Clontech) resin to anchor our GFP-NLS constructs via their His_6 tag, and this resin-bound protein was probed with varying concentrations of Kap. A workable quantity of TALON Sepharose, if saturated with NLS-GFP-His, would require >1 liter of Kap solution maintain molar excess of Kap over NLS-GFP in each binding assay. We could not use sub-saturating amounts of NLS-GFP on the resin because we observed that Kap would exhibit some non-specific binding to empty TALON Sepharose. This strong interaction between a Kap and IMAC (metal ion affinity chromatography) resin was seen previously during the identification of importin α (homolog of Kap60) from Xenopus laevis (Gorlich, Prehn et al. 1994).

We therefore searched to find an inert protein with which to dilute NLS-GFP on the surface of the resin and thus block Kaps from sticking non-specifically to the TALON resin. Bovine serum albumin (BSA) is often used as a blocking agent to prevent non-specific interactions (Bayliss, Littlewood et al. 2002; Gilchrist, Mykytka et al. 2002; Gilchrist and Rexach 2003; Pyhtila and Rexach 2003), so we thought to dilute NLS-GFP-saturated TALON Sepharose in BSA-conjugated Sepharose. This would result in a workable amount of resin

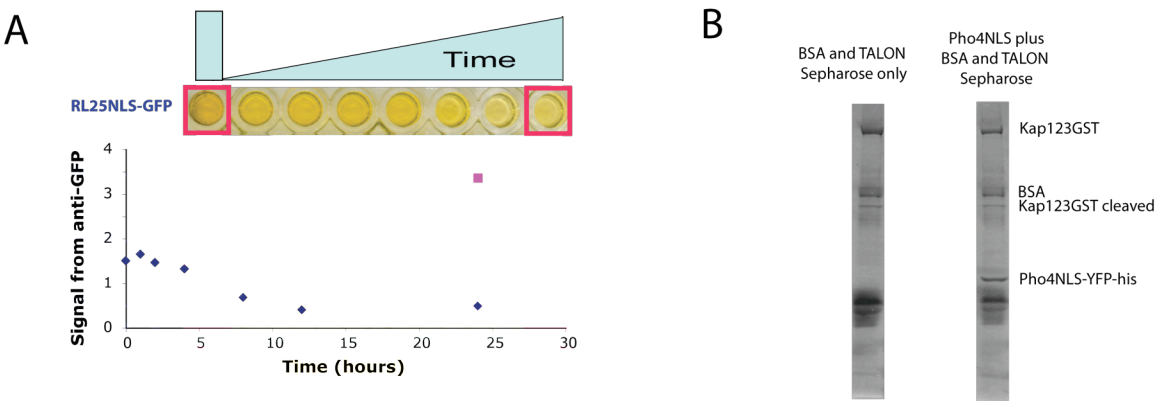

Figure 3-2: Towards the development of a reliable assay to measure Kap/Cargo affinities. A) Inconsistent amounts of NLS-GFP bound to a microtiter plate. Equivalent amounts of the indicated NLS-GFP were applied to the surface of each well and incubated for varying lengths of time. Anti-GFP signal was used to determine the amount of NLS-GFP remaining bound in each well. A plot showing the change in anti-GFP signal with incubation time is shown. Of note - the two wells marked with red squares are both 24 hour time points, and were treated exactly the same. B) Kap binds non-specifically to BSA and TALON Sepharose. 135nM Kap123GST were incubated with BSA-conjugated Sepharose mixed with TALON Sepharose with and without Pho4NLS-YFP-His bound to the TALON Sepharose. Bound proteins were eluted in SDS, run on a gel, and visualized with Coomassie blue. Kap123 is seen to bind nearly as well (if not better) to the Sepharose where no NLS is present.

with a smaller amount of NLS-GFP, enabling us to have molar excess of Kap over NLS while still keeping our assays at a reasonable volume. However, we found that Kaps bound non-specifically to BSA (**Figure 3-2 B)**. In hindsight, this was not necessarily surprising, as the surface of BSA contains many hydrophobic patches that could bind non-specifically to the hydrophobic patches on the Kaps (Gelamo and Tabak 2000; Alvarez, Pazos et al. 2001). We then decided to take advantage of the GFP moiety on our NLS constructs. CNBr Sepharose was coated with anti-GFP antibody, and this ant-GFP resin was used to immobilize GFP-NLS. The binding capacity of this resin for GFP-NLS is much smaller than that of TALON Sepharose, so dilution of the resin was not required. A resin binding assay in which GFP-NLS was bound to anti-GFP-conjugated Sepharose thus proved to be the best way to measure affinities between Kaps and their cargo.

Results from Sepharose-based binding assay

Polyclonal rabbit anti-GFP antibodies were conjugated to CNBr Sepharose 4B (Pharmacia). This anti-GFP resin was then saturated with enriched NLS-GFP-His_6. NLS-GFP-resin was then incubated overnight with mixing at 4ºC in various concentrations of recombinant karyopherin in TBT (see *Materials and Methods* for buffer recipes and more detailed protocols) plus 2.5% milk. Volumes were adjusted so that Kap was always in at least 3-fold molar excess over NLS.

The NLS-GFP-resin with bound Kap was then transferred to mini-centrifugation columns (BioRad). Resin was collected on the filters of the columns, washed quickly, and the bound proteins were eluted from the resin with ammonium hydroxide. Elutions were dried and the pellets re-suspended in SDS-PAGE loading buffer. The bound proteins were run on an SDS-PAGE gel and stained with Coomassie Blue R-250 (MP Biomedicals). Gel images were digitized and band intensities were quantified by densitometry using OpenLab image analysis software (Improvision) or ImageJ (NIH). Kap band intensity (Kap bound) was plotted as a function of Kap concentration, and the resulting curves were fit using equation 1 in SigmaPlot (Systat Software, Inc). Kap_{bound} is the Kap band intensity from the Coomassie stained gel, B_{max} is the band intensity at saturation, nM Kap is the concentration of Kap, and K_d is the calculated dissociation constant. This equation assumes no cooperativity between Kap/NLS binding events. A schematic of this method is shown in **Figure 3-3**.

$$Kap_{bound} = \frac{B_{max}(\text{nM Kap})}{K_d + \text{nM Kap}} \qquad (1)$$

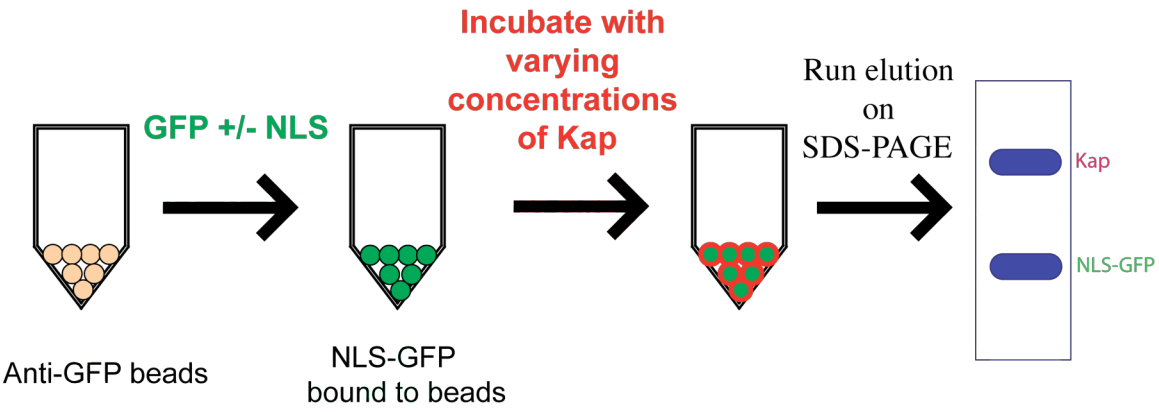

Figure 3-3: Schematic of resin binding assay. NLS-GFP constructs were immobilized on anti-GFP-conjugated Sepharose. The NLS-GFP resin was then incubated with increasing concentrations of Kap, always ensuring that Kap is in at least three-fold molar excess over NLS. Unbound proteins were washed away, and bound proteins were eluted in SDS, run on a gel, and visualized by Coomassie Blue. Images were digitized and analyzed as discussed in the text.

Controls

To validate this method, we measured the affinity between Protein A (PrA) from *Staphylococcus aureus* and rabbit IgG. The published K_d for this interaction is 16 nM (Karlsson, Jendeberg et al. 1995). We used the same anti-GFP resin as for the Kap/NLS binding assays, where the Fc domain of the rabbit anti-GFP (IgG) acted as "bait" for its interaction with PrA. This anti-GFP resin was incubated with various concentrations of recombinant PrA (Pierce). These assays were processed and analyzed the same way as the Kap/NLS assays were described above. We measured the K_d between PrA and rabbit IgG to be 22 +/- 8 nM (**Figure 3-4, bottom**), which is consistent with the published K_d.

It was important to determine if Kaps interacted with the NLS-GFP constructs via the NLS as expected, or non-specifically via the GFP domain. To test for this possibility, the same binding assay was performed using GFP-his_6 (with no NLS domain) as bait for Kap binding. Minimal to no Kap was observed to bind to GFP-his with no NLS (**Figure 3-5**). Therefore, we concluded that the Kap was interacting with the GFP-NLS via the NLS domain, and did not interact with GFP alone.

Most experiments were performed using GST-tagged karyopherin. To ensure that the observed binding was not due to non-specific interactions with

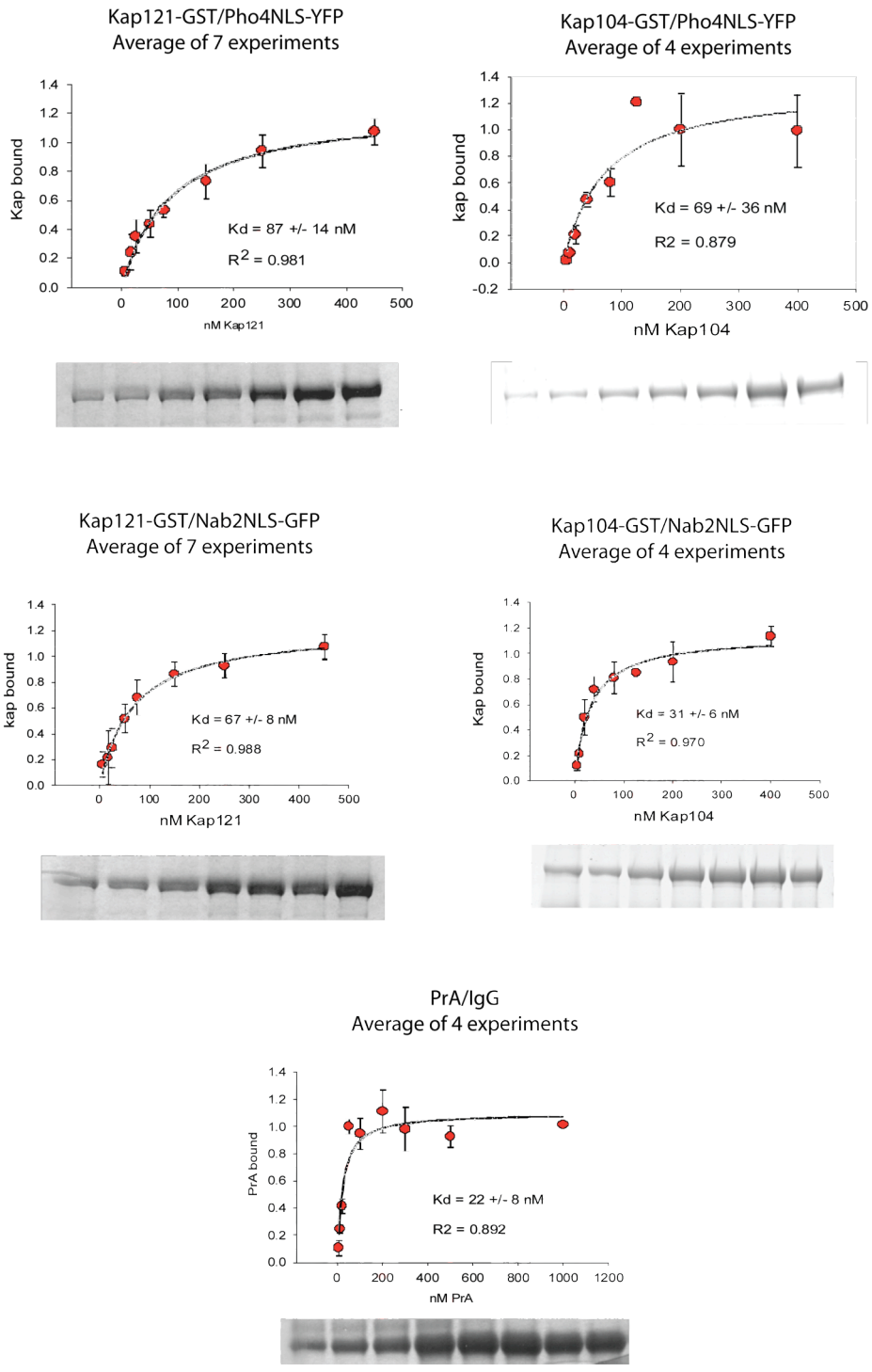

Figure 3-4: Example results of Kap/NLS binding measurements. Experiments were performed and analyzed as described for Figure 3-1. The PrA/IgG control is shown on the bottom.

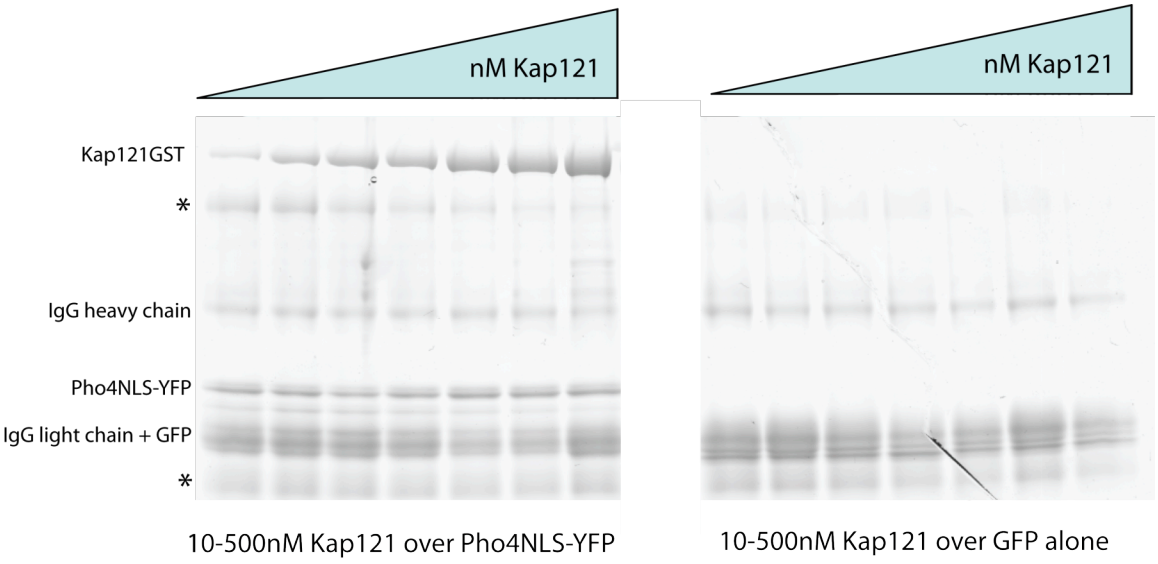

Figure 3-5: Kap121 interacts with the NLS-GFP constructs via the NLS. The Kap does not bind non-specifically to the GFP region. Bands marked with an * are milk proteins. The experiment shown here tested the binding of fluorescent-labeled Kap121 to GFP +/- NLS to ensure that labeling did not affect binding specificity or apparent affinity. Similar results were seen with unlabeled Kap.

the GST, we measured affinities between Kap and NLS where the GST was removed from the Kap with thrombin. Apparent affinity was not significantly changed by removal of the GST (Timney, Tetenbaum-Novatt et al. 2006). This may indicate that even though GST dimerizes, only one member of the Kap-GST dimer is sterically able to interact with the immobilized NLS.

Results

Apparent affinities were measured between Rpl25NLS-GFP-his constructs and Kap121 and Kap123. Binding curves of Kap121 and Kap123 bound to Rpl25NLS-GFP as a function of Kap concentration are shown in **Figure 3-1**, and the results are summarized in **Table 3-1**. These K_ds differ slightly from those published in (Timney, Tetenbaum-Novatt et al. 2006) because we have since improved the method used to fit our data. The Kap/NLS curves were re-analyzed using Equation 1 listed above using SigmaPlot (Systat Software, Inc) in order to be consistent with our analysis of the Kap/FG-nup interactions (discussed in Chapter 4). Generally, the improved analysis resulted in slightly different apparent affinities, and these changes did not affect our conclusions.

Both Kap123 and Kap121 were measured to interact with Rpl25NLS-GFP with apparent affinities of approximately 100 nM K_d, within the error of the measurement (**Figure 3-1** and **Table 3-1**). These nearly indistinguishable

Table 3-1: Kap/NLS affinities as measured in this study

Kap	Mean Kap concentration in vivo (nM)	Cargo	K_d (nM)	Std Error (nM)	R^2	N
Kap104	600	Nab2NLS	31	6	0.970	4
Kap104		Rpl25NLS	30	9	0.937	4
Kap104		Pho4NLS	69	36	0.937	4
Kap121	1000	Nab2NLS	67	8	0.988	7
Kap121		Rpl25NLS	85	21	0.962	10
Kap121		Pho4NLS	87	14	0.981	7
Kap121		rpl25NLS (K21A K22A)	134	11	0.996	4
Kap123	5300	Nab2NLS	175	44	0.973	2
Kap123		Rpl25NLS	130	30	0.972	5
Kap123		Pho4NLS	Poor binding			2
Kap123		rpl25NLS (K21A K22A)	260	120	0.909	5

affinities might explain the *in vivo* observations that Rpl25NLS-GFP is imported equally by Kap121 and Kap123 when they are expressed at equal concentrations (Timney, Tetenbaum-Novatt et al. 2006). One possible reason for the difference in import rate between cargoes of Kap121 and Kap123 in wild type cells is the difference in intracellular concentrations of the karyopherins. In order to see if this is a general trend, we looked at the import rates of two other model cargoes, which are often used as reporters for different import pathways: Nab2NLS and Pho4NLS.

Nab2 is an essential mRNA binding protein that is normally transported into the nucleus by Kap104 (Aitchison, Blobel et al. 1996; Lee and Aitchison 1999). It is recognized by an arginine-glycince-rich rgNLS (Lee and Aitchison 1999). Pho4 is a transcription factor that is normally cytoplasmic, but localizes to the nucleus when yeast are starved for phosphate (O'Neill, Kaffman et al. 1996). Under low phosphate conditions, Kap121 recognizes the NLS of Pho4 and transports the transcription factor into the nucleus (Kaffman, Rank et al. 1998). When phosphate is plentiful, the NLS of Pho4 is phosphorylated (O'Neill, Kaffman et al. 1996), which prevents its interaction with Kap121, and thus the Pho4 protein remains cytoplasmic (Kaffman, Rank et al. 1998).

The arginine-glycine-rich Nab2NLS, primarily a cargo of Kap104 (Lee and Aitchison 1999), exhibited significant binding to all karyopherins tested, with apparent K_ds ranging from 31-175 nM (**Table 3-1)**. The nuclear localization of Nab2NLS-GFP is largely disrupted at the restrictive temperature in Kap104ts cells (Lee and Aitchison 1999), indicating that the majority of Nab2 import is carried out by Kap104. Indeed, the tightest binding affinity we measured for Nab2NLS was for Kap104 (31 +/- 6 nM), which is very close to another published measurement of this interaction by isothermal titration calorimetry (37 +/- 20 nM) (Suel, Gu et al. 2008). It has been suggested that Nab2 may use some alternative method to gain entry to the nucleus in the absence of Kap104, (Marfatia, Crafton et al. 2003; Suntharalingam, Alcazar-Roman et al. 2004),

although that method has not been defined. These binding data suggest that Kap121 or Kap123 might assist in the import of Nab2NLS, although this cannot be certain, since the distribution of Nab2NLS-GFP in vivo is not affected in either kap121ts cells (Leslie, Zhang et al. 2004) or Δkap123 cells (Timney, personal communication). Thus, *in vitro* binding is necessary, but not sufficient to identify bona fide Kap-cargo interactions. However, affinities measured *in vitro* can help us understand more about the mechanism of selectivity in Kap-mediated transport as discussed below and in Chapters 4 and 5.

The Pho4NLS is normally imported into the nucleus by Kap121. The interaction between Kap121 and Pho4NLS-GFP was measured to have a K_d of 87+/-14 nM (**Table 3-1**). Kap123 does not appear to transport Pho4 to a significant extent, as Pho4 remains cytoplasmic at the restrictive temperature in Kap121ts cells (Kaffman, Rank et al. 1998) and Pho4NLS-GFP distribution is not affected in kap123Δ cells (Timney, personal communication). Consistent with this, we found that Kap123 shows no significant binding to the Pho4NLS (**Table 3-1)**. In addition to being consistent with our own *in vivo* measurements, our *in vitro* K_d results also agree with Kap104/Nab2NLS K_ds as measured by isothermal titration calorimetry (Lee, Cansizoglu et al. 2006; Suel, Gu et al. 2008) and are within the range of K_d measurements reported for other Kap/NLS pairs (**Table 3-1** and **Table 3-2**).

Kap/Cargo affinity may be related to transport rate

These experiments have shown that binding affinity *in vitro* can help explain import behavior *in vivo.* To specifically test whether changing the affinity of a cargo for its karyopherin would alter its import rate, we created a mutant Rpl25NLS-GFP construct where lysines 21 and 22 of the Rpl25NLS were changed to alanines. This was expected to lower the affinity of Kap for the mutant NLS. Indeed, Timney found that this mutant NLS was imported into the nucleus nearly ~3.5 times less rapidly than the wild type NLS *in vivo* (Timney, Tetenbaum-Novatt et al. 2006). Furthermore, we measured a clear decrease in apparent affinity of the mutant NLS to Kap121 and Kap123 *in vitro* (Timney, Tetenbaum-Novatt et al. 2006) (**Figure 3-1** and **Table 3-1)**. This indicated that simply changing the affinity of a protein to its karyopherin will alter its import rate *in vivo*, and illustrates the importance of quantifying these interactions in order to fully understand the kinetics of nuclear import.

Table 3-2: Kap/NLS affinities from the literature

Karyopherin	NLS-Cargo	Apparent K_d (nM)	Method	Reference	Apparent Kd from this study (nM)
Kap104	Hrp1p NLS (AA 506-532)	32 +/- 16	ITC	(Suel, Gu et al. 2008)	N.D.
Kap104	Nab2 NLS (AA 214-241)	37 +/- 20	ITC	(Suel, Gu et al. 2008)	31 +/- 6
Kap104	M9 NLS (AA 257-305)	42 +/- 2	ITC	(Lee, Cansizoglu et al. 2006)	N.D.
Kap104	hnRNP M NLS (AA 41-70)	10 +/- 1.7	ITC	(Cansizoglu, Lee et al. 2007)	N.D.
Importin α/β	SV40 large T antigen NLS	35	BIAcore	(Catimel, Teh et al. 2001)	N.D.
Importin α/β	Nucleoplasmin NLS	48	BIAcore	(Catimel, Teh et al. 2001)	N.D.
Kap95/ Kap60	Cbp80NLS (AA 1-30)	< 0.149 +/- 0.021	Sepharose binding assay	(Gilchrist, Mykytka et al. 2002)	N.D.
Importin β	Importin α	14	BIAcore	(Catimel, Teh et al. 2001)	N.D.
Kap95	Kap60	< 0.153 +/- 0.021	Sepharose binding assay	(Gilchrist, Mykytka et al. 2002)	N.D.
Kap60	Cbp80NLS (AA 1-30)	2.8 +/- 0.3	Sepharose binding assay	(Gilchrist, Mykytka et al. 2002)	N.D.
Importin α ΔIBB	MycNLS	6 +/- 3	Fluoresence anisotropy	(Hodel, Corbett et al. 2001; Hodel, Harreman et al. 2006)	N.D.
Importin α ΔIBB	SV40 large T antigen NLS	9 +/- 4	Fluoresence anisotropy	(Hodel, Corbett et al. 2001; Hodel, Harreman et al. 2006)	N.D.

Results in the context of living cells

This correlation between K_d and import rate of wild type and mutant cargoes, while intuitive, is actually unexpected if considered in the context of the intracellular concentrations of Kaps and cargoes. The dissociation constants between Kaps and NLSs were measured in the range of tens to hundreds of nM. However, the endogenous concentrations of karyopherins in living yeast range from 600 nM (Kap104) to 5300 nM (Kap123) (Timney, Tetenbaum-Novatt et al. 2006)). Further, in our *in vivo* experiments, the NLS-GFP cargo molecules were present in yeast at 10,000-100,000 nM. At these concentrations, with these dissociation constants, it would be presumed that essentially all Kap molecules would be complexed with cargo molecules *in vivo*. It would also suggest that a change in K_d from ~130 to ~260 nM between WT and mutant Rpl25NLS-GFP should not effect import rate *in vivo* – Kap123 should be completely complexed with either NLS in an environment of ~5 μM Kap123 and 10-100 μM NLS. However, *in vivo* transport rate measurements decreased ~3.5-fold decrease in import rate between wild type and mutant (K21A K22A) Rpl25NLS-GFP. (Timney, Tetenbaum-Novatt et al. 2006)

A related apparent inconsistency was the observation that increasing NLS-GFP concentrations well above presumed endogenous cargo levels did not saturate Kap-mediated transport. There was a linear relationship between cargo

concentration and import rate beyond ~100 μM NLS-GFP (Timney, Tetenbaum-Novatt et al. 2006). It should be noted that karyopherins were not over-expressed in these cells, so the observed import rate continued to increase after the concentration of NLS-GFP exceeded the ~5 μM concentration of karyopherin of Kap123 in these cells by more than 20-fold.

The simplest explanation that could account for these apparent discrepancies is *in vivo* competition for the NLS-Kap interaction. In living yeast, our engineered NLS-GFP cargoes are competing for Kap binding sites with the many endogenous, unlabeled cargoes, thus reducing the ability of our NLS-GFP to saturate the Kap. Specific competition for Kap binding has been reported previously. An engineered NLS-like peptide with ~100 pM affinity for Kapβ2 (human homolog of yeast Kap104) was seen to be a specific inhibitor for import of endogenous cargoes of Kapβ2 that have affinities for Kapβ2 $\geq$10 nM (Cansizoglu, Lee et al. 2007).

A single Kap may have hundreds of different endogenous cargoes. However, due to the enormous concentration of NLS-GFP in the assayed cells, Timney estimated that the total amount of competing natural cargoes in the cytoplasm needed to reproduce the linear import relationships we observed in our import assays would be ~6 mg/mL for each Kap (Timney, Tetenbaum-Novatt et al. 2006). Considering that there are 13 β karyopherins in yeast, that would

require ~80mg/mL of specifically imported cargo proteins in the cytoplasm. This is physiologically unreasonable, as the total concentration of proteins in the cytoplasm is only on the order of ~100mg/mL (Zimmerman and Trach 1991; Zimmerman and Minton 1993). Thus, we postulated that binding between Kaps and NLSs is indeed competitive, but that the competition for binding is with non-specific cytosolic proteins. This idea of non-specific binding is not unreasonable, considering that Kaps and NLSs are seen to be generally sticky. For example, Nab2 was seen to bind significantly to Kap123, even though Kap123 does not import Nab2 *in vivo* (Leslie, Zhang et al. 2004). This will be discussed further in Chapter Five of this thesis.

Potential relationship between Kap concentration and affinity to NLS

As shown in **Table 3-1** and **Figure 3-6**, there is a possible trend where more abundant karyopherins have weaker affinities for their cargo molecules. This inverse relationship between Kap-NLS interaction strength and Kap concentration could play a role in determining how Kaps bind specifically to their diverse set of cargoes. More abundant karyopherins might clog the system if their affinities for cargo were too tight, while less abundant karyopherins would never bind to their cargos if their affinities were too weak. This inverse relationship was predicated by Anton Zilman in a mathematical model of

nucleocytoplasmic transport (Zilman, Di Talia et al. 2007) and will be discussed further in later chapters as it also applies to Kap/FG-nup interactions.

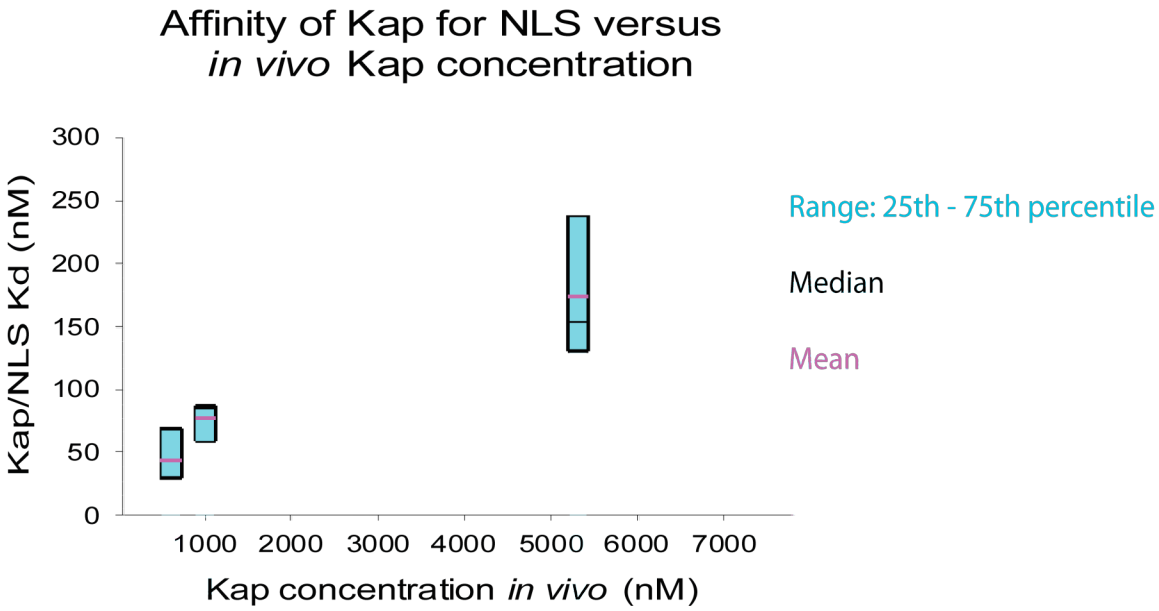

Figure 3-6: There is a possible trend that the more abundant Kaps in vivo have weaker apparent affinities for their cargo. The range, median, and mean of all the apparent affinity measurements are illustrated.

Chapter Four: Kap/FG-nup Interactions

The nuclear pore complex (NPC) is the selective gateway between the nucleus and cytoplasm, allowing small molecules and a specific subset of macromolecules and macromolecular complexes to pass through (reviewed in (Macara 2001; Weis 2002; Suntharalingam and Wente 2003; Pemberton and Paschal 2005; Tran and Wente 2006) among others). This selectively permeable barrier is thought to be formed by a family of nuclear pore complex proteins called FG-nups that are rich in phenylalanine-glycine (FG) repeats (Rexach and Blobel 1995; Strawn, Shen et al. 2004). There are several types of FG repeats present in these FG-nups, including FxFG, GLFG, FxF, SAFGxPSFG, and simply FG (Rout and Wente 1994; Bayliss, Littlewood et al. 2002; Strawn, Shen et al. 2004; Patel, Belmont et al. 2007).

The exact structure and mechanism of the FG-nup permeability barrier remains controversial, and several models have been proposed. These models suggest that the FG-nups either create an affinity gradient across the NPC (Ben-Efraim and Gerace 2001; Pyhtila and Rexach 2003), a gel linked by hydrophobic interactions (Ribbeck and Gorlich 2001; Ribbeck and Gorlich 2002; Frey, Richter et al. 2006; Frey and Gorlich 2007), an entropic brush via Brownian motion of the unfolded domains (Rout and Aitchison 2000; Rout, Aitchison et al. 2003; Lim, Huang et al. 2006; Lim, Fahrenkrog et al. 2007), or a combination of these (Patel,

Belmont et al. 2007; Patel and Rexach 2008). It has also been proposed that the FG-nups simply form a two-dimensional surface along which binding molecules can slide (Peters 2005). While these models disagree in the details of the structure of the FG-nup barrier (as discussed in Chapter One), they are all based on the idea that the barrier formed by the FG-nups prevents large molecules from entering the nucleus, and this barrier is somehow overcome when transported molecules bind to the FG-nups. This concept of a barrier that does not open and close, but instead is overcome by selective binding, is termed virtual gating (Rout, Aitchison et al. 2000).

One family of proteins that cross the NPC by binding to FG-nups is the karyopherins (Dworetzky and Feldherr 1988; Adam and Gerace 1991; Adam and Adam 1994; Gorlich, Prehn et al. 1994; Gorlich, Vogel et al. 1995; Macara 2001; Leslie, Grill et al. 2002; Rout, Aitchison et al. 2003; Mosammaparast and Pemberton 2004; McLane, Pulliam et al. 2008). Karyopherins serve as shuttle proteins, carrying their cargoes into and out of the nucleus as appropriate (Goldfarb, Gariepy et al. 1986; Moore and Blobel 1992; Wen, Harootunian et al. 1994; Aitchison, Blobel et al. 1996; Richards, Lounsbury et al. 1996; Ossareh-Nazari, Bachelerie et al. 1997; Lee and Aitchison 1999; Leslie, Zhang et al. 2004; Scheifele, Ryan et al. 2005; Lee, Cansizoglu et al. 2006; Lange, Mills et al. 2007; Kosugi, Hasebe et al. 2008; Lange, Mills et al. 2008; Suel, Gu et al. 2008; Scott, Cairo et al. 2009). The interactions between karyopherins and NLS-cargo

molecules were examined in Chapter Three. This work aims to further our understanding of karyopherin-mediated transport by quantifying the interactions between karyopherins and the FG-nups.

Members of the karyopherin β family (Kaps) are large (~100kD) proteins made up primarily of HEAT repeats, pairs of anti-parallel alpha helices (Chook and Blobel 1999; Cingolani, Petosa et al. 1999; Bayliss, Littlewood et al. 2000; Bayliss, Littlewood et al. 2002; Lee, Matsuura et al. 2005; Liu and Stewart 2005; Conti, Muller et al. 2006; Cansizoglu and Chook 2007). Crystal structures of Kaps in complex with FxFG and GLFG repeat peptides indicate that FG-nups bind to Kap by inserting the hydrophobic side chains of the FG-nups' many phenylalanine residues into hydrophobic pockets on the Kap (Bayliss, Littlewood et al. 2000; Bayliss, Littlewood et al. 2002; Liu and Stewart 2005). Computer simulations have supported this, and have also indicated that specificity in Kap/FG-nup interactions is possibly due to the distribution of hydrophobic pockets over the surface of the Kap, which corresponds to the distribution of hydrophobic residues along the length of the FG-nups (Isgro and Schulten 2005; Isgro and Schulten 2007). Recent computer simulations of arrays of FG-domains tethered to a surface suggest that FG-nups form dynamic bundles with many of the hydrophobic phenlylalanines exposed on the surface. This arrangement produces hydrophobic spots in the correct arrangement to interact with transport factors (Miao and Schulten 2009).

Much work has been done to gain an understanding of Kap/FG-nup interactions. However, as discussed in Chapter Two, most of this work has been done using FxFG or GLFG repeat peptides (Bayliss, Littlewood et al. 2000; Bayliss, Littlewood et al. 2002) or using recombinant fragments of FG-nups expressed in bacteria (Ben-Efraim and Gerace 2001; Gilchrist, Mykytka et al. 2002; Gilchrist and Rexach 2003; Pyhtila and Rexach 2003; Lim, Huang et al. 2006; Patel, Belmont et al. 2007; Patel and Rexach 2008; Jovanovic-Talisman, Tetenbaum-Novatt et al. 2009). These fragments consist of ~400-800 amino acids, ranging from 37-69% of the full-length protein (**Table 4-1**). This work has been very informative, indicating that different Kap/FG-nup pairs exhibit a wide range of affinities (Bayliss, Littlewood et al. 2002; Gilchrist, Mykytka et al. 2002; Gilchrist and Rexach 2003), and identifying a potential affinity gradient for import karyopherins from the cytoplasmic to the nucleoplasmic side of the pore (Ben-Efraim and Gerace 2001; Pyhtila and Rexach 2003). However, this work has also shown that the apparent affinity for a Kap interaction with a given FG-nup can vary dramatically if different FG-nup fragments are used **(see Table 4-1)**. For example, a high-affinity binding site for Kap95 has been identified on the extreme C-terminus of Nup1. If these 36 amino acids are not in the Nup1 fragment tested, the apparent affinity for Kap95 decreases >400 fold (Pyhtila and Rexach 2003). We therefore chose to measure the apparent affinities between karyopherins and *full-length* FG-nups to prevent a situation like that observed for

Table 4-1: Kap/FG-nup affinities from the literature (page 1)

Kap	FG-nup (fragment)	Additional molecules present	Non-specific competitor	Apparent K_d (nM)	Method	Reference	Apparent K_d from this study for full-length nup (nM)
Kap95	Nup1 (aa 423-816)	-	30mg/mL BSA	350	Microtiter plate	(Bayliss, Littlewood et al. 2002)	7 +/- 2
Kap95	Nup1 (aa 332-1076)	-	1mg/mL BSA	7.9 +/- 1.7	Sepharose resin	(Pyhtila and Rexach 2003)	7 +/- 2
Kap95	Nup1Δ36 (aa 332-1040)	-	1mg/mL BSA	2500 +/- 700	Sepharose resin	(Pyhtila and Rexach 2003)	7 +/- 2
Kap95	Nup1ΔN (aa 332-1076)	Kap60 + Cbp80 NLS-MBP	1mg/mL BSA	0.40 +/- 0.02	Sepharose resin	(Gilchrist, Mykytka et al. 2002)	7 +/- 2
Kap95	Nup1ΔN (aa 332-1076)	Kap60	1mg/mL BSA	≤ 0.05 +/- 0.01	Sepharose resin	(Gilchrist, Mykytka et al. 2002)	7 +/- 2
Kap95	Nup1 (aa 332-1076)	Kap60	1mg/mL BSA	≤ 0.05	Sepharose resin	(Pyhtila and Rexach 2003)	7 +/- 2
Kap95	Nup1Δ36 (aa 332-1040)	Kap60	1mg/mL BSA	11.2 +/- 1.4	Sepharose resin	(Pyhtila and Rexach 2003)	7 +/- 2
Importin β (vertebrate Kap95)	Nup153-C (Nup1), aa 609-1475)	-	30 mg/mL BSA	9 +/- 2.5	Microtiter Plate	(Ben-Efraim and Gerace 2001)	7 +/- 2
Kap95	Nsp1 (aa 262-603)	-	30 mg/mL BSA	160 +/- 40	Microtiter plate	(Bayliss, Littlewood et al. 2002)	0.7 +/- 0.1

Table 4-1: Kap/FG-nup affinities from the literature (page 2)

Kap	FG-nup (fragment)	Additional molecules present	Non-specific competitor	Apparent K_d (nM)	Method	Reference	Apparent K_d from this study for full-length nup (nM)
p97 (vertebrate Kap95)	p62 (Nsp1), full length	-	30 mg/mL BSA	14	Microtiter plate	(Delphin, Guan et al. 1997)	0.7 +/- 0.1
Importin β (vertebrate Kap95)	p62 (Nsp1), full length	-	30 mg/mL BSA	100 +/- 8	Microtiter plate	(Ben-Efraim and Gerace 2001)	0.7 +/- 0.1
Importin β (vertebrate Kap95)	p62 (Nsp1), full length)	IBB domain	30 mg/mL BSA	105 +/- 6	Microtiter plate	(Ben-Efraim and Gerace 2001)	0.7 +/- 0.1
Kap95	Nup100 (aa 2-610)	-	30 mg/mL BSA	110 +/- 10	Microtiter plate	(Bayliss, Littlewood et al. 2002)	1.1 +/- 0.3
Kap95	Nup100 (aa 1-640)	-	1 mg/mL BSA	223 +/- 38	Sepharose resin	(Pyhtila and Rexach 2003)	1.1 +/- 0.3
Kap95	Nup100 (aa 1-640)	Kap60 + CbpNLS -MBP	1mg/mL BSA	90 +/- 9	Sepahrose resin	(Pyhtila and Rexach 2003)	1.1 +/- 0.3
Kap95	Nup100 (aa 1-640)	Kap60	1 mg/mL BSA	255 +/- 66	Sepharose resin	(Pyhtila and Rexach 2003)	1.1 +/- 0.3
Kap95	Nup42 (full length)	-	1mg/mL BSA	1500 +/- 200	Sepharose resin	(Pyhtila and Rexach 2003)	9 +/- 2
Kap95	Nup116 (161-730)	-	30mg/mL BSA	110 +/- 10	Microtiter plate	(Bayliss, Littlewood et al. 2002)	Not Tested

Table 4-1: Kap/FG-nup affinities from the literature (page 3)

Kap	FG-nup (fragment)	Additional molecules present	Non-specific competitor	Apparent K_d (nM)	Method	Reference	Apparent K_d from this study for full-length nup (nM)
Importin β (vertebrate Kap95)	Nup58 (Nup49)	-	30mg/mL BSA	101 +/- 2	Microtiter plate	(Ben-Efraim and Gerace 2001)	11 +/- 2
Importin β (vertebrate Kap95)	Nup58 (Nup49)	IBB domain	30mg/mL BSA	107 +/- 8	Microtiter plate	(Ben-Efraim and Gerace 2001)	11 +/- 2
Importin β (vertebrate Kap95)	Nup54 (Nup57)	-	30mg/mL BSA	111.5 +/- 6.5	Microtiter plate	(Ben-Efraim and Gerace 2001)	8 +/- 1
Importin β (vertebrate Kap95)	Nup54 (Nup57)	IBB domain	30mg/mL BSA	108.5 +/- 8.5	Microtiter plate	(Ben-Efraim and Gerace 2001)	8 +/- 1

When vertebrate FG-nups were used, the yeast homolog is indicated in parentheses. Homolog identities are taken from (Suntharalingam and Wente 2003).

Nup1, where a high-affinity binding site could be missed. These unfolded and protease-sensitive proteins proved difficult to purify, and the methods used to obtain these proteins are discussed in Chapter Two.

The presence of Kap60 (importin α) and/or NLS-cargo was also shown to influence the apparent affinity between Kap95 (importin β) and FG-nups *in vitro* (Gilchrist, Mykytka et al. 2002; Pyhtila and Rexach 2003) and in permeabilized cells (Kubitscheck, Grunwald et al. 2005). Kap95 and Kap60 both bind independently to certain FG-nups *in vitro* (Gilchrist, Mykytka et al. 2002) and *in silico* (Isgro and Schulten 2005; Isgro and Schulten 2007). Therefore, it is unclear if the increase in apparent affinity (decrease in measured K_d, likely due to a decrease in off rate) is due to a cooperativity effect where both Kap95 and Kap60 are binding simultaneously, or if Kap60 is actually altering the binding properties of Kap95. Of note, the presence of the Importin β binding domain (IBB) of Importin α alone did not influence the apparent affinity of Importin β to a portion of Nsp1 (Bayliss, Littlewood et al. 2002) or other FG-nups (Ben-Efraim and Gerace 2001). The IBB domain of Importin α is only the portion that interacts with Importin β. This might indicate that the increase in apparent affinity of Kap95 for FG-nup when Kap60 is present is due to the simultaneous independent binding of other domains of Kap60 to the FG-nup. To prevent confusion, we have chosen to examine the binding of empty karyopherins to FG-

nups, with no importin α or other cargo molecules present. These interactions are biologically relevant as empty karyopherins do shuttle back and forth across the NPC (Riddick and Macara 2005). While studying the interaction of Kap/cargo complexes with the NPC would be informative, the simplest combination of empty Kap and full-length FG-nups provides a platform to develop our assays and a place to start. Future work will determine the effect of cargo molecules on these interactions.

Directionality of nucleocytoplasmic transport is thought to be dictated by the gradient of RanGTP (Gsp1-GTP in yeast) across the nuclear envelope. (Floer, Blobel et al. 1997; Nachury and Weis 1999; Macara 2001). Consistent with this, the presence of RanGTP analogs has been found to dramatically change the binding behavior between karyopherins, FG-nups and their NLS-cargo (Moroianu, Blobel et al. 1996; Chook and Blobel 1999; Allen 2001; Allen, Patel et al. 2002; Gilchrist and Rexach 2003; Pyhtila and Rexach 2003; Lee, Matsuura et al. 2005). This work focuses on karyopherin interactions relevant to *import,* therefore our experimental conditions mimic a cytoplasmic environment with no RanGTP added.

Method development

The first goal of this part of the project was to find a method to reliably measure Kap/FG-nup interactions. Unlike the GFP-NLS constructs, which we could attach to anti-GFP Sepahrose, the FG-nup constructs we used only had a His_6-tag which binds to the cobalt-based TALON® (Clontech) functionality. As discussed in Chapter Two, the His_6-tag was needed to allow purification of these insoluble proteins under denaturing conditions. Other tags such as GST or MBP are not functional under the denaturing conditions required to solubilize the FG-nups. Therefore we could only use TALON or other IMAC resin to immobilize our His_6-tagged FG-nups. As karyopherin was seen to bind non-specifically to BSA on TALON Sepharose (see Chapter Three), we continued our search for an inert protein with which to dilute the FG-nup on the surface of the resin. It turns out that an appropriate protein was in our hands the whole time. When we measured GFP-NLS interactions with Kap, we confirmed that the interaction was occurring via the NLS domain by ensuring that GFP alone did not bind non-specifically to Kap (Chapter Three, **Figure 3-4**). We therefore cloned eGFP-His_6 (**Table 2-1** for plasmids used in this study) for expression in *E. coli* and used the enriched protein to dilute our FG-nup on the surface of the TALON Sepharose resin. This was successful, as Kap did not bind significantly to GFP-coated Sepharose but it did bind to TALON coated with GFP and FG-nup.

At this time, other members of our lab were working to optimize "pullouts," affinity purification assays to isolate protein complexes from yeast. One protein at a time was genomically tagged with a Protein A (PrA) motif from *Staphylococcus aureus.* This motif binds tightly to the F_c domain of IgG and thus can be used as an affinity tag to pull out proteins and complexes (Strambio-de-Castillia, Tetenbaum-Novatt et al. 2005; Alber, Dokudovskaya et al. 2007; Oeffinger, Wei et al. 2007). IgG-conjugated Dynabeads® (Invitrogen) enabled more rapid harvesting, resulting in faster pullouts with less background than IgG-conjugated Sepharose (Oeffinger et al, personal communication). Unlike Sepharose resin, Dynabeads® are made of plastic and are thus biologically inert. They are spherical and not porous, with a very high surface area to volume ratio. These qualities prevent non-specific binding to the beads. We tried performing our binding assays using Dynabeads® TALON (Invitrogen), and found that the results were cleaner and more reproducible than they were with TALON Sepharose (Clontech) (**Figure 4-1**). We therefore used Dynabeads® TALON to measure the affinities between Kap95 and Kap121 and different FG-nups.

Results and discussion

For Kap/FG-nup binding experiments, His_6-FG-nup and His_6-eGFP were mixed and bound to Dynabeads® TALON. 10-50 pmoles of FG-nup and 830 pmoles of GFP were added per data point. The excess GFP was necessary to

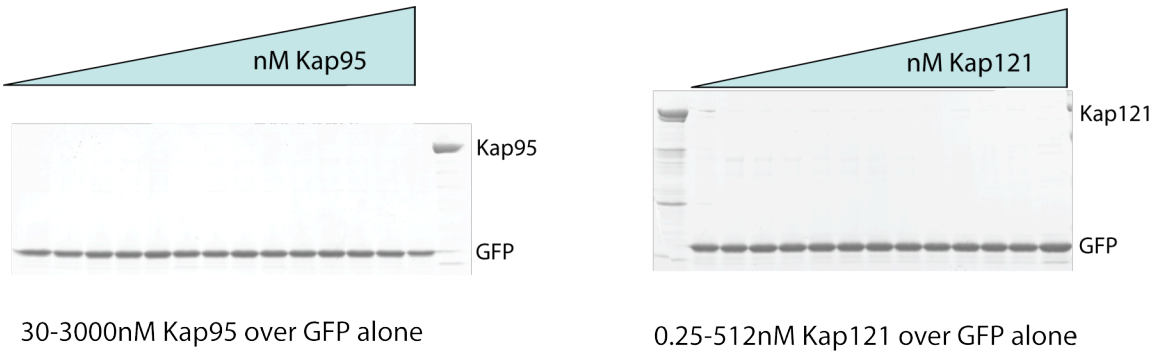

Figure 4-1: Bead binding assay where increasing concentrations of karyopherin were incubated with Dynabeads TALON saturated with eGFP-His6 alone. Neither Kap95 nor Kap121 was seen to bind non-specifically to GFP. Therefore, we are confident that Kap we see bound to Dynabeads coated with GFP and FG-nup is in fact bound specifically to the FG-nup.

fully saturate the TALON surface, preventing any non-specific binding of the Kaps to the Dynabeads. Beads were washed to remove unbound protein and incubated on a rotating wheel overnight at 4 ºC with increasing concentrations of Kap, always ensuring that Kap was in at least three-fold molar excess over FG-nup. Beads were washed to remove unbound protein, and bound protein was eluted by boiling in SDS-PAGE sample buffer. Eluates were run on gels, and protein bands were visualized with Coomassie Brilliant Blue. Gel images were digitized, and bands were quanitified using ImageJ (NIH). More detailed protocols can be found in Chapter Eight, Materials and Methods.

The results from our affinity measurements are presented in **Table 4-2**. Kap and FG-nup band intensities were quantified, and the ratio of band intensities (Kap bound per unit FG-nup) was plotted versus Kap concentration in SigmaPlot (Systat Software, Inc) and fit using equation 1 (Chapter Three). Example gels and plots from Kap95 and Kap121 over the GLFG Nup57 are seen in **Figure 4-2 A and B**. In order to ensure that lane order was not influencing the results, some experiments were done with the lanes loaded in order of increasing concentration while others were done with lanes loaded in a random order. This did not affect the apparent affinity (**Figure 4-3)**. Each Kap/FG-nup pair was measured at least three times, with up to thirteen repeats for a given pair. To combine the data from these multiple repeats, each experiment was normalized to 100% max binding, and the data points were averaged across all experiments. The combined normalized and averaged data from all repeats was plotted and fit using SigmaPlot (Systat Software, Inc). Error bars indicate standard deviation for each point. Summary curves for Kap95 and Kap121 over Nup57 are seen in **Figure 4-2 C**.

Table 4-2: Kap/FG-Nup affinities as measured in this study

				Kap95 (3000nM in vivo)			Kap121 (1000nM in vivo)		
Yeast FG-nup (vertebrate homolog)	**Type of repeat**	**Localization** (Rout, Aitchison et al. 2000)	**# of Fs**	**K_d +/- SE (nM)**	**R^2**	**N**	**K_d +/- SE (nM)**	**R^2**	**N**
Nsp1 (Nup62)	FxFG	Symmetric	62	0.7 +/- 0.1	0.890	9	8 +/- 2	0.804	4
Nup100 (Nup98)	**GLFG**	**Symmetric**	**60**	**1 +/- 0.3**	**0.885**	**4**	**1 +/- 0.2**	**0.821**	**6**
Nup1 (Nup153)	FxFG	Nuclear	70	7 +/- 2	0.774	4	5 +/- 1	0.876	3
Nup57 (Nup54)	**GLFG**	**Symmetric**	**23**	**8 +/- 1**	**0.871**	**8**	**10 +/- 2**	**0.923**	**7**
Nup145N (Nup98)	**GLFG**	**Symmetric**	**35**	**8 +/- 1**	**0.920**	**5**	**2 +/- 1**	**0.722**	**3**
Nup42 (NLP1/ hCG1)	**SAFGx PSFG**	**Cytoplasmic**	**38**	**9 +/- 2**	**0.854**	**5**	**1 +/- 0.4**	**0.766**	**4**
Nup60	FxF	Nuclear	23	13 +/- 3	0.876	7	4 +/- 1	0.806	5
Nup49 (Nup58, Nup45)	**GLFG**	**Symmetric**	**25**	**11 +/- 2**	**0.847**	**13**	**5.4 +/- 1.5**	**0.739**	**7**
Nup59 (Nup35)	FG	Symmetric	23	28 +/- 7	0.916	3	11 +/- 2	0.942	3
Nup53 (Nup35)	FG	Symmetric	23	54 +/- 8	0.928	11	4.5 +/- 1	0.741	9

Bold font = cohesive (Patel, Belmont et al. 2007)

Regular font = non-cohesive (Patel, Belmont et al. 2007)

Vertebrate homologues are from (Suntharalingam and Wente 2003)

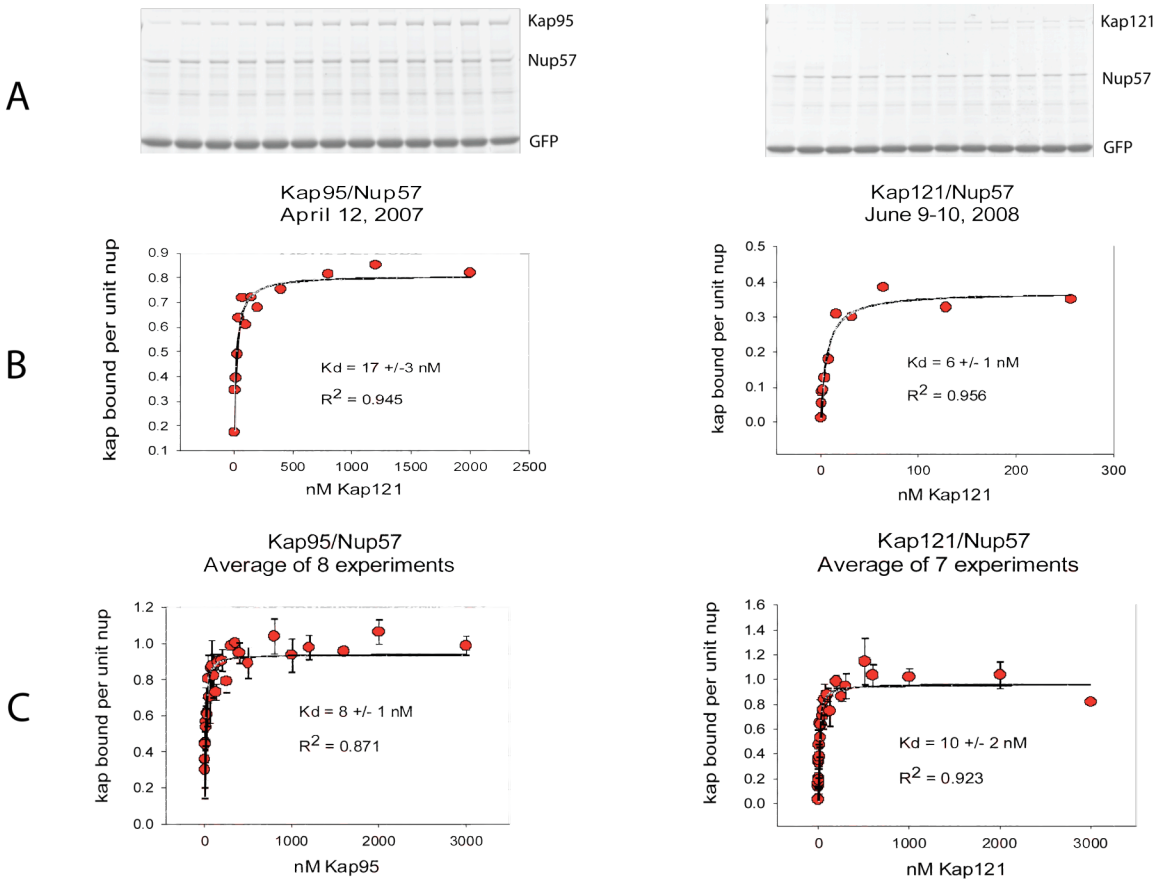

Figure 4-2: Sample results from bead binding assays of Kap95 and Kap121 over Nup57. A) Coomassie Brilliant Blue stained SDS-Page gel of the eluates from the dynabeads. B) Quantitation of the band intensity of the gels shown in A. Curves are fit using equation 1. C) Combined data from many repeats of the binding assay. Data from each individual experiment was normalized and the average of all experiments was plotted. Error bars indicate standard deviation. Combined data was fit using equation 1.

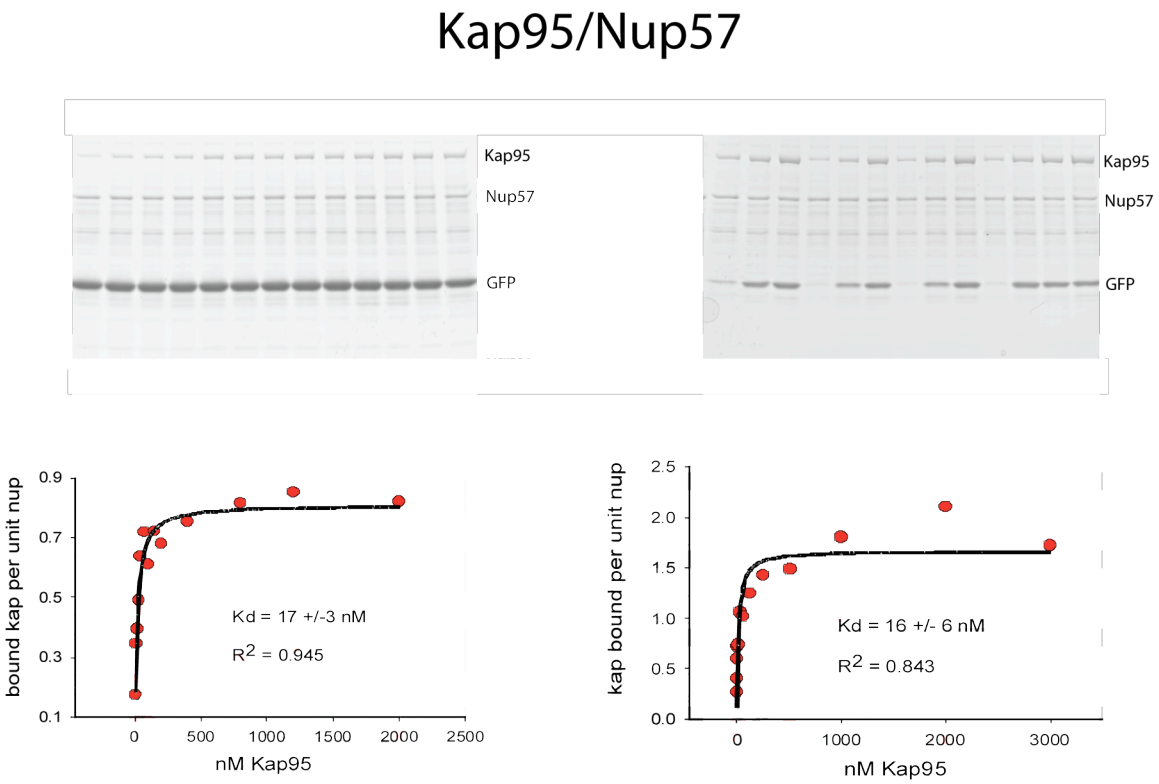

Figure 4-3: Lane order does not influence results. Two individual binding assays of Kap95 over Nup57 are shown. The left gel was loaded in order of increasing concentrations of karyopherin. The right gel was loaded in a mixed fashion. Band intensities were quantified and plots of Kap bound per unit nup versus concentration are shown below each gel. Curves were fit using equation 1.

It is important that all karyopherin used in these experiments be functional (able to bind to FG-nup), because otherwise the concentration of total Kap added will not equal the concentration of *active* Kap and our affinity measurements will not be accurate. Kap functionality was tested by incubating 400 nM Kap over increasing amounts of FG-nup, ranging from molar excess Kap over FG-nup to molar excess FG-nup over Kap. Both the bound protein and unbound fractions were analyzed, and Kap was deemed to be 100% functional if ultimately no detectible Kap remained unbound as FG-nup amount increased. Both Kap95 and Kap121 completely disappeared from the supernatant as FG-nup increased to just above equimolar amounts (**Figure 4-4**), so we can assume that the concentration of Kap measured for each experiment is equal to the concentration of active Kap.

Kap/FG-nup interactions measured in this work gave apparent K_ds ranging from <1 - ~50 nM. Our results are often very different than affinities reported by others ((Delphin, Guan et al. 1997; Bayliss, Littlewood et al. 2002; Gilchrist, Mykytka et al. 2002; Pyhtila and Rexach 2003) and compare **Table 4-1** with **Table 4-2)**. For example, in contrast to previous results (Ben-Efraim and Gerace 2001; Pyhtila and Rexach 2003) (**Table 4-1**) we did not observe a dramatic affinity gradient – all FG-nups exhibited K_ds for import karyopherins in the low nM range and there was no relationship between apparent affinity for Kap and the FG-nups' predicted location in the nuclear pore (**see Table 4-2)**. However, as

Figure 4-4: Functionality of karyopherins. 500μL of 400nM Kap (200pmoles Kap) was incubated with increasing amounts of Dynabeads TALON saturated with FG-nup. After incubating overnight to bind Kap to FG-nup, both the bound and unbound fractions were analyzed. In all cases, no Kap bound to the beads when no FG-nup was present, and there was no Kap remaining in the unbound fraction when there was molar excess FG-nup over Kap. This indicates that the Kap had all bound to the FG-nup and was therefore functional.

asymmetrically located FG-nups are not required for efficient transport (Strawn, Shen et al. 2004; Zeitler and Weis 2004), an affinity gradient is not an essential part of NPC function.

This apparent discrepancy between the affinities reported by different groups could be a consequence of using different FG-nup fragments or full-length proteins. It could also be due to the use of different experimental techniques. Previously published affinity measurements were either done using FG-nup fragments bound to the surface of microtiter plates (Delphin, Guan et al. 1997; Ben-Efraim and Gerace 2001; Bayliss, Littlewood et al. 2002) or FG-nup fragments bound to Sepharose resin in 40 μL Kap solution (Gilchrist, Mykytka et al. 2002; Pyhtila and Rexach 2003). Our experiments were done using magnetic Dynabeads® TALON tumbling in solution volumes between 300 μL – 240 mL. Thus, the volume of Kap solution was large enough to ensure adequate mixing throughout the incubation with karyopherin. As mentioned in Chapter Three, in our hands microtiter plates did not provide reproducible results, and Dynabeads have proven to be more specific than Sepharose resin. We have also observed that karyopherins interact both specifically and non-specifically with many proteins and that their behavior is greatly affected by their surroundings. These effects will be discussed in the following chapters of this thesis.

We also observed a trend towards higher affinity for Kap95 as the number of FG-nup phenylalanines increases ($p < 0.05$) (**Figure 4-5**). The dependence of affinity to Kap95 on the number of phenylalanines has been observed previously (Patel and Rexach 2008), and is consistent with the mechanism proposed for Kap95/FG-nup interaction via insertion of FG-nup phenylalanine side chains into hydrophobic pockets of Kap95/Importin β (Bayliss, Littlewood et al. 2000; Bayliss, Littlewood et al. 2002; Isgro and Schulten 2005). If the interaction were mediated by phenylalanines, more phenylalanines would result in more potential connection points and thus a stronger interaction. There is no significant relationship between affinity for Kap121 and number of phenylalanines ($p > 0.5$), indicating that the interaction between FG-nups and Kap121 may depend on interactions with residues other than phenylalanine to a different extent than interactions with Kap95.

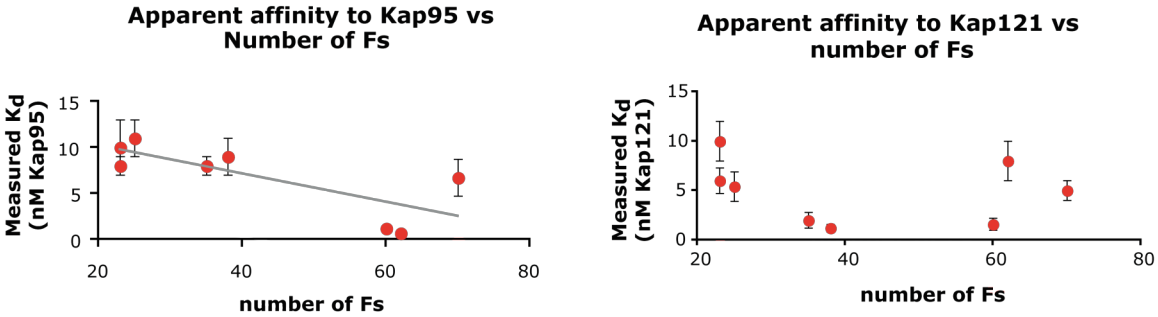

Figure 4-5: Apparent affinities are plotted versus the number of Phenylalanines in each FG-nup. Affinities to Nup53 and Nup59 are not included in these plots.

There is no significant relationship between measured K_d and FG repeat type. Accordingly, there is also no apparent relationship between measured K_d and the observed cohesiveness of FG-nups (Patel, Belmont et al. 2007). The only FG-nups that behave significantly differently than others in our assays are Nup53 and Nup59. These proteins have only four and six FG repeats respectively, which could explain their low affinity for Kap95. This difference in affinity is not observed for Kap121, which further supports the idea that FG-nup interaction with Kap121 is partially phenylalanine-independent. Due to their few FG repeats, Nup53 and Nup59 are not always even classified as FG-nups (Strawn, Shen et al. 2004). However, as they do contain FG repeats, have predicted natively unfolded regions, and are sometimes considered as FG-nups (Patel, Belmont et al. 2007), we have included them in our study with the understanding that they are not *bona fide* FG-nups.

In a mathematical model of nucleocytoplasmic transport, Anton Zilman (Zilman, Di Talia et al. 2007) predicted that in order for efficient transport to occur, the strength of interaction between a transported molecule and FG-nups should be inversely proportional to the concentration of that transported molecule *in vivo*. Kap95 is thought to be three times more abundant than Kap121 in living yeast ((Timney, Tetenbaum-Novatt et al. 2006) and Timney unpublished data), therefore Kap121 would be predicted to have a higher affinity towards FG-nups than Kap95. In **Figure 4-6** we've compared the measured affinities of each FG-

nup to Kap121 versus its affinity to Kap95. As predicted by the calculations, the majority of FG-nups exhibit significantly tighter interactions with Kap121 than they do with Kap95. This potential relationship between abundance and affinity needs to be confirmed by testing other Kaps, but it adds to our understanding of how efficient transport through the NPC is accomplished.

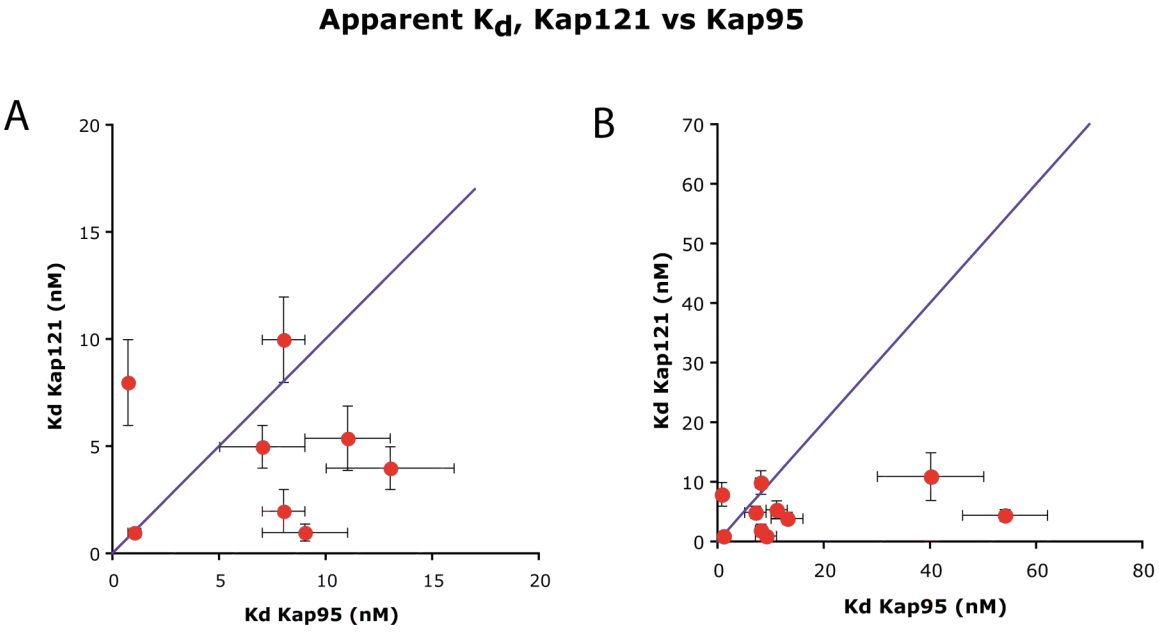

Figure 4-6: Apparent affinities of FG-nups to Kap121 vs Kap95 are plotted. Error bars equal standard error. A) Apparent affinites of all FG-nups except Nup53 and Nup59. B) Apparent affinities of all FG-nups including Nup53 and Nup59. The purple line indicates equal affinities to Kap121 and Kap95.

However, the main conclusion to make from measured Kap/FG-nup is that all *in vitro* affinities as measured are very tight. Many Kap/FG-nup interactions exhibit apparent K_ds *in vitro* of 50 nM or tighter, with several published interactions showing pM K_ds (see **Table 4-1** for affinities measured by others, and **Table 4-2** for affinities from this study). Concentrations of Kap95 and Kap121 in living yeast are thought to be 3000 nM and 1000 nM respectively ((Timney, Tetenbaum-Novatt et al. 2006) and Timney unpublished data), and FG-nup concentrations in the NPC have been calculated to on the order of ~10 μM (10,000 nM) based on the copy number of each FG-nup per pore and the pore volume (Gilchrist, Mykytka et al. 2002). Given these *in vivo* concentrations of Kap and FG-nup, if the measured affinities of Kap/FG-nup interactions are accurate, Kap/FG-nup interactions should be constantly saturated. Although several Kaps are seen to accumulate at the nuclear rim in living cells (Moroianu 1995; Yaseen and Blobel 1997), a completely saturated NPC is not consistent with an effective transport system in which Kaps must shuttle back and forth between the nucleus and cytoplasm. In addition, recent FRAP experiments indicate that the exchange rate of individual Kap molecules at the NPC is very fast (Benjamin Timney, unpublished observation). This apparent inconsistency between high affinity *in vitro* and efficient transport with rapid binding and unbinding *in vivo* was addressed by examining the effect of environment on Kap/FG-nup interactions, and this will be discussed in Chapter Five.

Chapter Five: The effect of environment on Kap/FG-nup interactions

There is an apparent conflict between *in vitro* affinities of interactions involving Kaps and the rapid on-off rates required for their function *in vivo*. Our experiments indicated that Kaps and FG-nups interact *in vitro* with affinities in the low nM range (**Table 4-2)**. Other groups report Kap/FG-nup affinities ranging from pM to low μM affinities (**Table 4-1** (Delphin, Guan et al. 1997; Ben-Efraim and Gerace 2001; Bayliss, Littlewood et al. 2002; Gilchrist, Mykytka et al. 2002; Pyhtila and Rexach 2003)). A reaction is diffusion-limited if the rate of reaction is proportional to the rate at which the reacting partners encounter each other – the rate of transport through the surrounding medium. I believe that the interactions between Kaps and FG-nups are likely diffusion-limited for several reasons. First, transport factors have been measured to cross native NPCs (Ribbeck and Gorlich 2001) and NPC mimics ((Jovanovic-Talisman, Tetenbaum-Novatt et al. 2009), discussed in detail in Chapter Six of this thesis) at rates expected for purely diffusion-controlled reactions. Second, as FG-nups are natively unfolded, their orientation is not as important as it would be for an interaction between two globular proteins, making it likely that almost every encounter between an FG-nup and a transport factor can result in a productive binding interaction. Assuming that the rate of Kap/FG-nup binding was diffusion-limited (with an on rate of 10^7 $M^{-1}s^{-1}$), and considering that K_d is equal to K_{off}/K_{on}, a K_d of ~10 nM would require an off rate of ~0.1 s^{-1}. Such a slow off rate (one interaction every

10 seconds) is not compatible with the millisecond residence times observed for Kaps at the NPC (Yang, Gelles et al. 2004; Kubitscheck, Grunwald et al. 2005). Thus, the apparent affinities as measured *in vitro* are all very tight – too tight for rapid and effective transport. This is especially true given the 0.6-5.3 μM concentrations of karyopherins in cytoplasm (Timney, Tetenbaum-Novatt et al. 2006) and the ~10 μM local concentrations of FG-nups at the NPC (Gilchrist, Mykytka et al. 2002; Alber, Dokudovskaya et al. 2007), which would indicate that Kap/FG-nup interactions would be constantly saturated. This apparent discrepancy led us to try to understand how such tight apparent affinities could result in fast, efficient transport in living cells.

Non-specific competition

Like most measurements of biochemical rates and equilibria, our *in vitro* measurements of Kap/FG-nup interactions were carried out using dilute solutions of enriched proteins. However, this is not the environment in which these interactions occur *in vivo*. The cellular milieu is very crowded. *E. coli*, for example, are thought to contain 300-400 mg of protein and RNA per mL of cytoplasm (Zimmerman and Trach 1991; Garner and Burg 1994). Although the bulk contents of the cytoplasm are often ignored when examining protein-protein interactions *in vitro,* the potential differences between enriched proteins in dilute

solution and endogenous proteins in the crowded cellular environment can and should be taken into account (Minton 2006; Minton 2006).

Elegant calculations have shown that the volume occupied by inert background proteins in solution increases the effective concentration of a protein of interest via an excluded volume effect (reviewed in (Zimmerman and Minton 1993)). As two proteins cannot occupy the same space at the same time, the protein of interest can only occupy that portion of space where it does not overlap with other solute molecules. This decreases the volume available for the select molecule to occupy, and is thus predicted to increase its effective concentration (Zimmerman and Minton 1993; Garner and Burg 1994). This effect is shown schematically in **Figure 5-1** (adapted from **(Zimmerman and Minton 1993)**) and would result in an apparent affinity that is tighter than the affinity measured with no background proteins present.

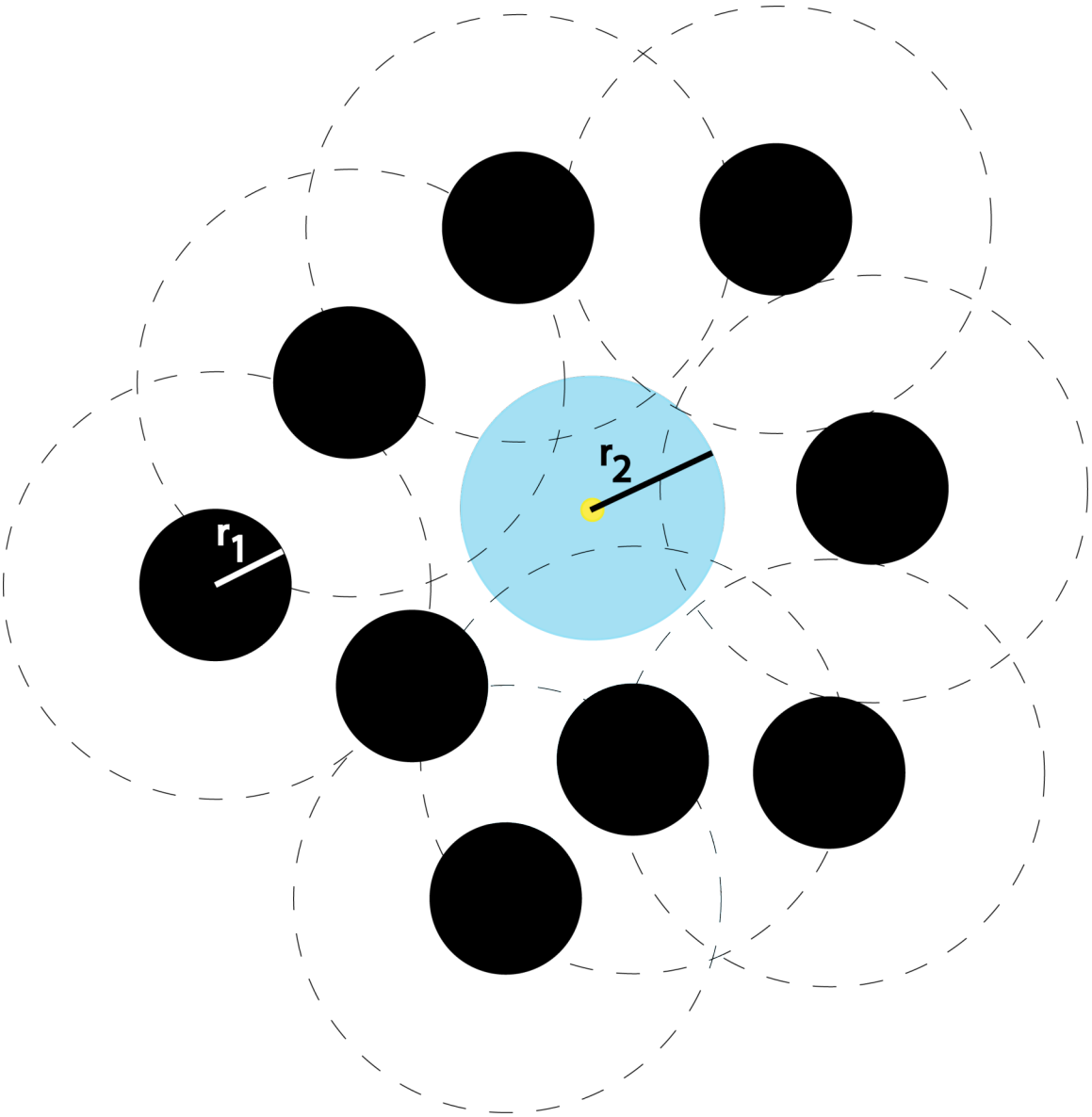

Figure 5-1: Illustration of the volume available to a particle of interest (blue particle) in an environment containing background solute (black) particles. The background particles sit at the center of a sphere (dashed line) that has a radius of r_1+r_2. This spherical region is inaccessible to the center of mass of the blue particle, indicated by the yellow dot (adapted from (Zimmerman and Minton 1993)).

Background proteins are not always inert, however. A common problem in analysis of protein complexes is the prevalence of contaminating proteins (Brunet, Thibault et al. 2003; Tackett, DeGrasse et al. 2005). Methods to increase the stringency of purifications such as increasing salt or detergent have been used to increase specificity of recovered interactions, and labeling methods have been developed to determine which members of an isolated complex are interacting non-specifically (Brunet, Thibault et al. 2003; Marelli, Smith et al. 2004; Cristea, Williams et al. 2005; Tackett, DeGrasse et al. 2005; Oeffinger, Wei et al. 2007). In addition to providing possibly misleading evidence of a interaction that may be non-specific, these co-enriching background proteins could cause a decrease in the apparent affinity of a real, specific interaction. If the protein of interest were occupied in non-specific interactions with proteins in the surrounding media, the effective concentration of that protein available to interact with its specific partner would be less than the total concentration. This would result in an apparent affinity that is weaker than the affinity measured with no competitor proteins present. One might predict interactions involving natively unfolded proteins with an unusually high potential binding surface area to volume ratio, such as the FG-nups, to be particularly vulnerable to this effect.

In order to best represent the bulk proteins present in the cytoplasm, without introducing additional karyopherins, FG-nups, or NLS-cargo, we used lysate from *E. coli*. As *E. coli* are prokaryotes, they contain many of the

components of eukaryotic cytoplasm but do not contain any proteins that function in nucleocytoplasmic transport. The use of *E. coli* lysate as a non-specific competitor has been published by ourselves (Timney, Tetenbaum-Novatt et al. 2006) and others (Schrader, Stelter et al. 2008).

We first monitored Kap/NLS binding in the presence of increasing amounts of bacterial whole cell lysate. We observed that increasing the amount of non-specific competitor protein (*E. coli* lysate) while keeping total Kap concentration constant decreased the amount of Kap that bound to its cargo (**Figure 5-2)** (Timney, Tetenbaum-Novatt et al. 2006). 1 mg/mL lysate caused Kap/cargo binding to decrease by 50%, and 10 mg/mL lysate disrupted Kap/cargo binding by more than 90% (Timney, Tetenbaum-Novatt et al. 2006). Note that this large effect on Kap/cargo interactions was seen in an environment approximately ten-fold less crowded than the cytoplasm (Zimmerman and Minton 1993). We then checked to see if the presence of non-specific competitor protein affected the apparent affinity between Kaps and their cargo as well as affecting total Kap/cargo binding. We observed over a three-fold decrease in apparent affinity of Kap121 to the Pho4NLS when the assay was performed in 7 mg/mL lysate (**Table 5-1**).

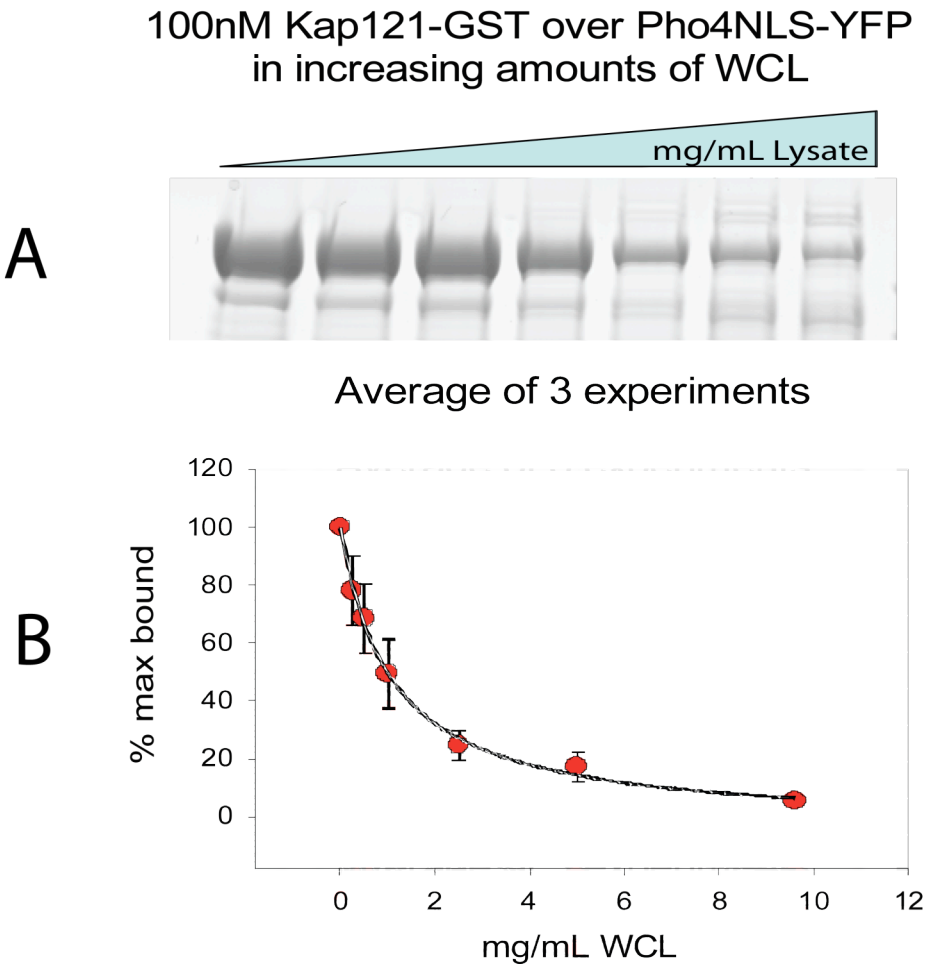

Figure 5-2: The presence of non-specific competitor protein (E. coli lysate) decreased the amount of karyopherin that binds to a given amount of NLS, even though the total concentration of karyopherin remains the same. A) Coomassie stained gel showing one experiment where 100nM Kap121-GST was incubated with beads coated in Pho4NLS-YFP in the presence of increasing amounts of bacterial lysate. B) Quantitation of the average results from three repeat experiments. The fit line is included to guide the eye (Timney, Tetenbaum-Novatt et al. 2006).

Table 5-1: Non-specific competition

			No WCL			0.1mg/mL WCL			
Pair	**Type of FG repeat**	**Localization**	**K_d +/- SE (nM)**	**R^2**	**N**	**K_d +/- SE (nM)**	**R^2**	**N**	**Fold change**
Kap121/ Pho4NLS	-	-	87 +/- 14	0.981	7	307 +/- 66	0.987	2	3.5
Kap95/ Nsp1	FxFG	Symmetric	0.67 +/- 0.14	0.887	4	25 +/- 7	0.839	3	37
Kap95/ Nup100	GLFG	Symmetric	1.1 +/- 0.3	0.885	4	63 +/- 16	0.907	3	57
kap95/ Nup42	SAFGx PSFG	Cytoplasmic	9 +/- 3	0.854	5	164 +/- 30	0.963	5	18
Kap95/ Nup53	FG	Symmetric	53 +/- 8	0.928	10	730 +/- 166	0.964	3	14
Kap121/ Nsp1	FxFG	Symmetric	8 +/- 2	0.804	4	61 +/- 13	0.939	3	8
Kap121/ Nup100	GLFG	Symmetric	1.1 +/- 0.2	0.821	6	106 +/- 11	0.989	3	96
Kap121/ Nup42	SAFGx PSFG	Cytoplasmic	1.2 +/- 0.4	0.766	4	80 +/- 20	0.942	3	67
Kap121/ Nup53	FG	Symmetric	1.5 +/- 0.2	0.877	5	112 +/- 22	0.971	3	75

The Kap121/Pho4 NLS interaction was measured in 7mg/mL WCL.

We then examined the effect that non-specific competitor proteins had on Kap/FG-nup interactions. The apparent affinities between Kap95, Kap121, and several FG-nups were measured in the presence of 0.1 mg/mL (0.01%) bacterial lysate. We chose examples of FxFG (Nsp1), GLFG(Nup100), SAFGxPSFG (Nup42), and FG(Nup53) nups for these experiments to see if the effect was specific to a certain subset of FG-nups. We also chose both symmetric (Nsp1, Nup53, Nup100) and asymmetric (Nup42) nups to see if direct exposure to the cytoplasm *in vivo* would make an FG-nup more susceptible to non-specific competition *in vitro*. It should be noted that the protein concentration in the cytoplasm of living cells is estimated to be on the order of 100 mg/mL (Zimmerman and Minton 1993), therefore our experiments were done in an environment that is nearly 1000-fold less competitive than these proteins experience *in vivo*. Nevertheless, even this small amount of competitor protein had a significant effect on the apparent affinities of all Kap/FG-nup interactions tested (**Table 5-1** and **Figure 5-3).** The apparent affinities between Kaps and FG-nups decreased between one and two orders of magnitude when 0.1mg/mL bacterial lysate was added**.** If this trend were to continue, in the presence of 100 mg/mL cytosol, the apparent affinities between Kaps and FG-nups would be in the mM range. Assuming a diffusion-limited on rate, an interaction with a mM K_d would have an off rate of 10^4 s^{-1}, which is more consistent with the millisecond residence times observed for transported molecules at the NPC (Yang, Gelles et al. 2004; Kubitscheck, Grunwald et al. 2005). It is interesting to note that at low

concentrations of karyopherin, whole cell lysate proteins bind non-specifically to the FG-nup and are seen in the gel (marked by * in **Figure 5-4 A)**. As karyopherin concentration increases, these non-specific binding partners are competed away by the specific binding of the karyopherin. This competition between specifically and non-specifically binding proteins may also help explain the apparent stickiness of the Nab2NLS, as discussed in Chapter Three. Nab2NLS may behave as a "non-specific" binder to all karyopherins tested. It remains to be seen if Nab2NLS-GFP continues to bind to Kap121 or Kap123, which do not appear to transport it *in vivo*, in the presence of their cognate NLSs or other specifically binding proteins.

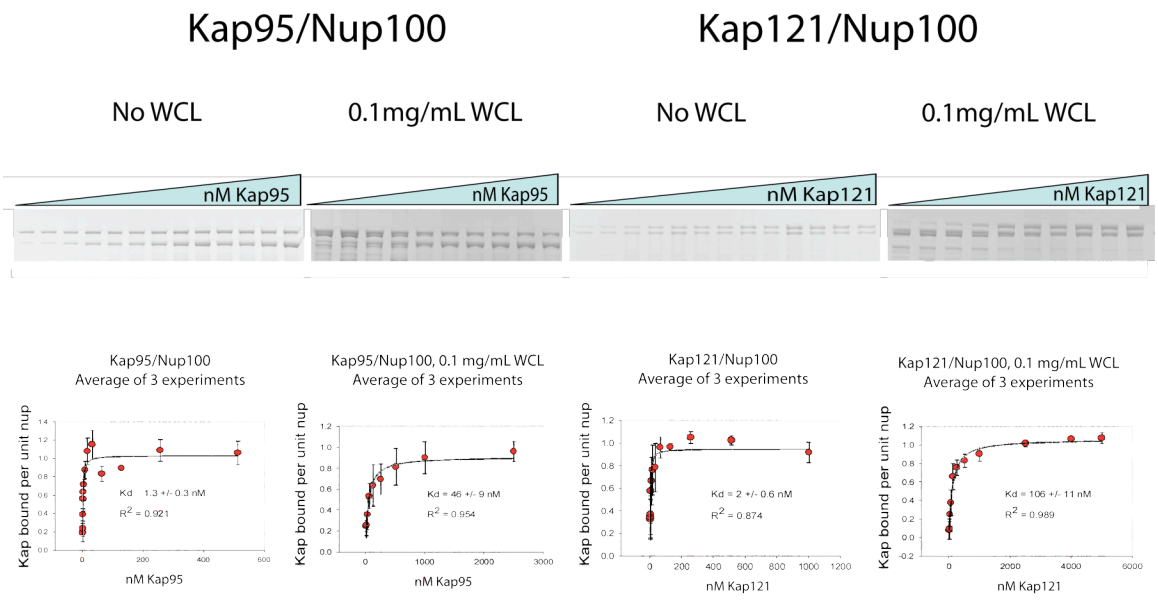

Figure 5-3: The presence of 0.1 mg/mL E. coli lysate causes a significant decrease in the apparent affinity of karyopherin for FG-nup.

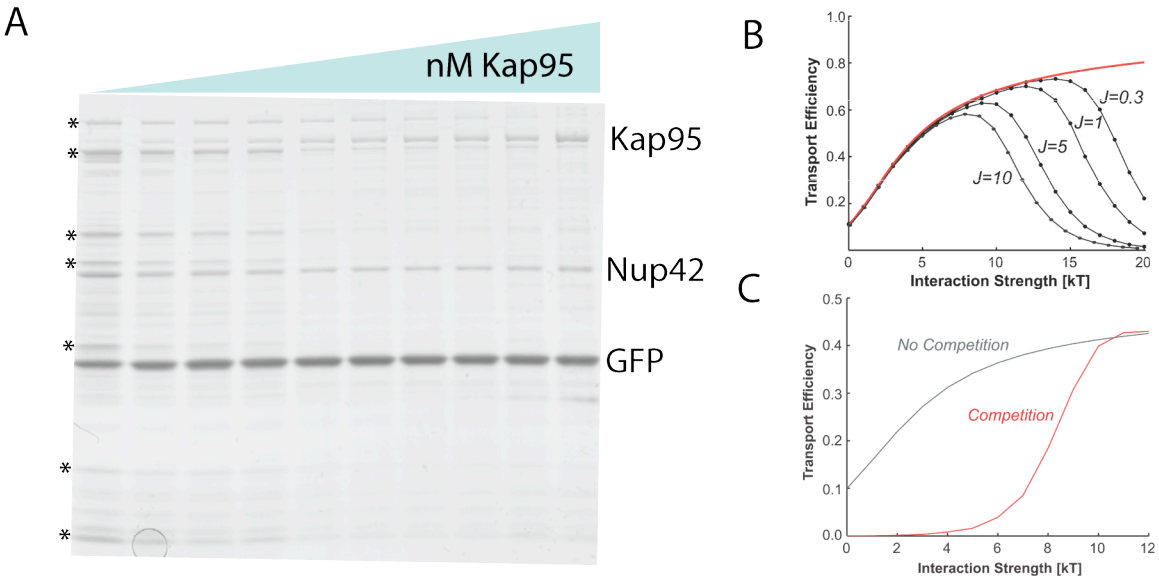

Figure 5-4: Non-specific and specific binders compete for the same binding sites on karyopherins. This competition is predicted to help maintain the selectivity of the NPC. A) Coomassie stained gel of a bead binding assay of Kap95 over Nup42 in the presence of 0.1mg/mL bacterial lysate. Note how non-specific interactions with proteins from the bacterial lysate decrease as the concentration of specifically-interacting Kap95 increases (examples are marked with *) B) Calculated transport efficiency of a molecule versus its interaction strength with the NPC. The different curves are for varying values of J, entrance rate into the pore. The red line indicates the low rate limit. For each value of J (proportional to concentration) there is an optimal interaction strength to get the highest transport efficiency (from (Zilman, Di Talia et al. 2007)). C) Gray line: Transport efficiency as a function of interaction strength in the absence of competition. Red line: transport efficiency as a function of interaction strength in the presence of competitor proteins that bind both weaker and stronger than the protein of interest. Note that the presence of competition increases the interaction strength required for efficient transport, and thus increases the selectivity of the system. (from (Zilman, Di Talia et al. 2007))

In a mathematical model of nucleocytoplasmic transport, Anton Zilman calculated that non-specific competition is part of the selectivity mechanism of the NPC (Zilman, Di Talia et al. 2007). This model was based on the idea that the number of binding sites and physical space within the NPC are limited. Molecules would enter the NPC with a certain flux and move stochastically from one empty binding site to another. If only one type of molecule is present on the cytoplasmic side of the NPC, each copy of that molecule has a certain probability of interacting with the FG-nups and entering the NPC. If its affinity to the NPC is weak, its residence time will be short, and it would have a high probability of exiting back out the cytoplasmic side of the NPC before enough empty binding sites in the channel clear. However, if its affinity for the NPC is higher, it has a greater probability of remaining in the NPC long enough for a path of empty binding sites to clear, allowing it to move through to the nuclear side. Even with the need for some level of interaction with the FG-nups, there is a wide range of different affinities that would be able to successfully cross the NPC (**Figure 5-4 B,** from (Zilman, Di Talia et al. 2007)). On the other hand, if two types of molecules with widely different affinities for FG-nups are present on the cytoplasmic side, then competition for the limited number of binding sites within the NPC becomes a robust yet stringent selectivity mechanism. As shown in **Figure 5-4 C (**from (Zilman, Di Talia et al. 2007)), the presence of transported proteins with high affinities for FG-nups will prevent the passage of proteins that interact weakly and non-specifically with the pore. Thus, our observed interaction

of *E. coli* lysate proteins with FG-nups, and the fact that these *E. coli* proteins are competed off by increasing concentrations of specifically-interacting karyopherin (**Figure 5-4 A**), corresponds very well with this mathematical model of nucleocytoplasmic transport.

Crowding

At the nuclear pore, FG-nups are tightly packed, with at least 128 FG domains occupying the central channel (Strawn, Shen et al. 2004). As the central channel is approximately 38 nm in diameter and 37 nm in height (Yang, Rout et al. 1998; Alber, Dokudovskaya et al. 2007), it has an inner surface area of ~8830 nm^2 and a volume of ~33600 nm^3. Given these dimensions and the estimated copy number of each protein (Rout, Aitchison et al. 2000; Alber, Dokudovskaya et al. 2007), the concentration of FG-nups at the NPC is estimated to be on the order of tens of μM (Gilchrist, Mykytka et al. 2002). This puts multiple FG-repeats within reach of a single Kap molecule as it crosses the pore, allowing for the possibility of cooperativity in Kap/FG-nup binding. In our Kap/FG-nup binding assays, the FG-nups are diluted among a lawn of inert GFP on the surface of the dynabeads TALON. In order to see if there was an avidity or cooperativity effect, we wanted to keep the same ratio of Nup to GFP on the beads, while changing the distribution (**Figure 5-5**). In condition A, the nup is

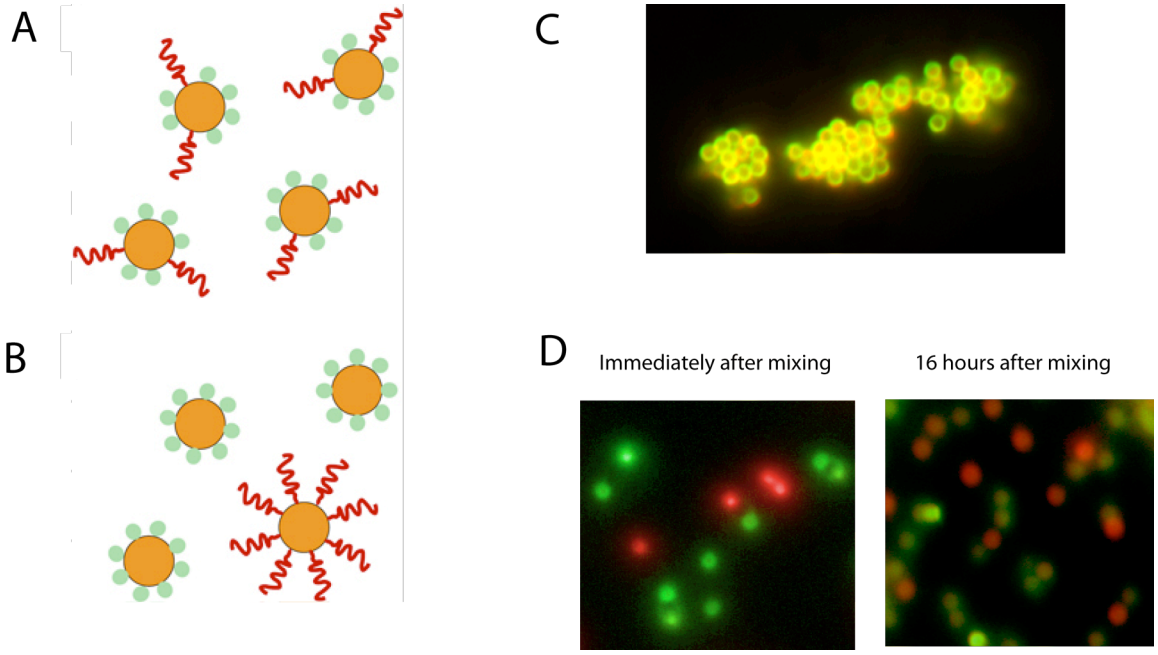

Figure 5-5: FG-nup distribution can be controlled in our binding assays. A and B). Schematic of FG-nups (red squiggles) and GFP (green balls) distributed on Dynabeads TALON (yellow circles) in the regular (A) and crowded (B) conditions C) Image of Alexa633-labeled FG-nup (red) and GFP (green) bound to beads in the "regular" fashion. Co-localization appears yellow. D) Image of Alexa633-labeled FG-nup (red) and GFP (green) bound to beads in the "crowded" fashion.

distributed evenly among the GFP spread out among all the beads. In condition B, the nup is "crowded" on a small subset of the beads, while the GFP is on the rest of the beads. We found that for the FG-nups tested, the apparent affinity for Kap95 was significantly higher in the crowded condition than in the dilute condition (**Figure 5-6)**. It should be emphasized that the amount of FG-nup present on the beads was the same in both conditions – only the *distribution* of the FG-nup changed. This effect was not as consistent for Kap121/FG-nup interactions. The apparent affinity for Nup49 was higher in the crowded condition, while the apparent affinity for Nup57 was not as strongly affected by the change in FG-nup distribution. Future work will explore the nature of this crowding effect and its significance to nucleocytoplasmic transport *in vivo*. As the stoichiometry of Kap/FG-nup interactions is not yet known, it remains to be seen if a Kap can in fact bind more than one FG-nup at a time. However, these findings of the sensitivity of Kap/FG-nup interactions to their environment may help explain the wide range of affinities reported for the same interaction in the literature (**Table 4-1**).

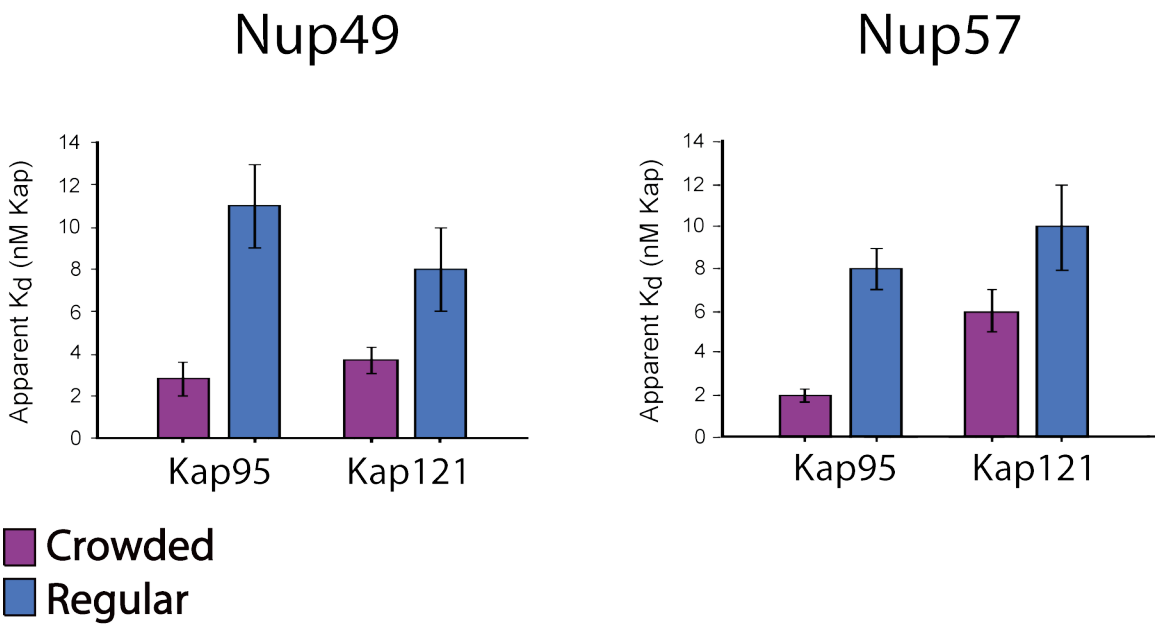

Figure 5-6: Results from bead binding assays of Kap95 and Kap121 over Nup49 or Nup57 in the crowded and regular conditions. Error bars indicate standard deviations. All experiments were performed at least three times.

Chapter Six: Connecting *in vitro* measurements to transport

Quantifying the interactions between karyopherins, their cargo, and the FG-nups has long been a goal of those trying to understand nucleocytoplasmic transport. Results presented thus far indicate that while affinities of such interactions can be measured, the results are only valid for the set of conditions under which the measurement was done. The amount of non-specific competitor protein in the buffer and the way in which the bait proteins are distributed on a surface have been shown to influence the apparent affinities between karyopherins, NLS-cargoes, and FG-nups. As no *in vitro* experiment can exactly duplicate the contents of the cytoplasm or the distribution of FG-nups at the NPC, we wondered how these *in vitro* measurements were relevant to nucleocytoplasmic transport in living cells. I sought to address this question as part of a much larger project by Chait lab postdoc Tijana Jovanovic-Talisman.

The NPC can be considered in its most basic form to consist of a narrow hole lined with transport factor-binding FG-nups. In order to test if this simple arrangement is all that is required to make a selective filter, Tijana designed and built a mimic of the NPC using synthetic materials and recombinant proteins. This device was built upon a 6 μM thick polycarbonate membrane perforated with ~30 nm diameter holes (GE Osmonics). This membrane was coated with a layer of sputtered gold, to which cysteine-containing proteins could be covalently

attached. The FG-domains of Nsp1 (an FxFG nup) and Nup100 (a GLFG nup) were cloned, expressed and enriched as His_6-tagged proteins with an engineered C-terminal cysteine using procedures developed for this thesis work (**Figure 6-1)**. Attaching these cysteine-tagged FG-domains along with small (356 Da) PEG-SH to the sputtered gold surface resulted in a membrane that duplicated many properties of the native NPC (Jovanovic-Talisman, Tetenbaum-Novatt et al. 2009). The ~30 nm pore diameter is similar to the diameter of the central channel of the NPC (**Figure 1-1**) (Yang, Rout et al. 1998; Kiseleva 2003; Alber, Dokudovskaya et al. 2007). The FG-nups are positioned as all evidence indicates they are in the NPC, with their ends anchored around the rim of the central pore and their unfolded domains partially occluding the pore opening. Amino acid analysis of the membranes indicates that the density of FG-nups around these gold-coated holes is similar to the estimated density of FG-nups at the NPC, with approximately 70 molecules per pore. Finally, the functionalized portion of the 6 μm thick polycarbonate membrane is only ~15 nm thick, similar to the ~30 nm thickness of the nuclear envelope (Alber, Dokudovskaya et al. 2007). An illustration of the setup is shown in **Figure 6-2**.

As discussed in Chapter Four, we found a range of affinities between different Kap/FG-nup pairs, although we did not find the large affinity gradient that has been suggested by others (Ben-Efraim and Gerace 2001; Pyhtila and Rexach 2003). In order to test the relevance of changes in Kap/FG-nup binding

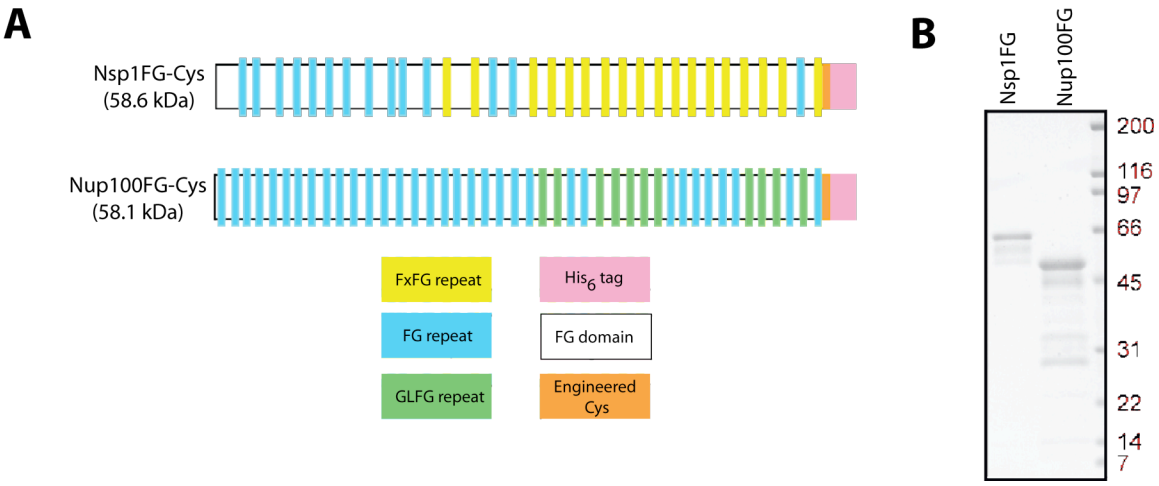

Figure 6-1: FG-nup constructs used in the NPC-mimics. A) Schematic presentation of Ns1pFG-Cys and Nup100FG-Cys sequences. B) Coomassie blue stained SDS-PAGE gels of His6-tagged Nsp1FG-Cys and Nup100FG-Cys (Jovanovic-Talisman, Tetenbaum-Novatt et al. 2009).

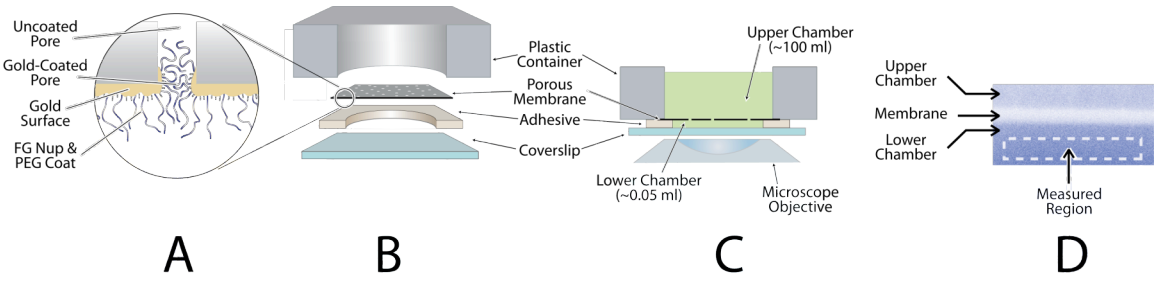

Figure 6-2: Design of the NPC-mimic. A) Schematic of a single pore in the functinoalized membrane. B) Exploded view of the device carrying the membrane. C) Sectional view of the device mounted on a confocal microscope and loaded with a fluorescently labeled protein solution (green). D) Confocal microscopy z-axis section through the lower chamber, membrane and upper chamber showing the fluoresence signal (blue) from a single protein in equilibrium between the two chambers. The measured volume is indicated by the dashed box. (Jovanovic-Talisman, Tetenbaum-Novatt et al. 2009).

affinity on transport through the NPC mimic, we compared the flux of wild type and mutant versions of the transport factor NTF2. NTF2 mediates the transport of Ran across the NPC (as described in the introduction) (Paschal and Gerace 1995; Ribbeck, Lipowsky et al. 1998; Smith, Brownawell et al. 1998) via interactions with FxFG-nups (Paschal, Delphin et al. 1996; Clarkson, Corbett et al. 1997), and this binding is reduced in the mutant NTF2(W7A) due to a change in its phenylalanine binding site (Morrison, Yang et al. 2003). Wild-type and mutant NTF2 were expressed and enriched from *E. coli* as GST-tagged constructs. We used a far western binding assay (Blanar and Rutter 1992) to confirm that binding of the W7A mutant was indeed diminished when compared to wild type. As FG-nups are natively unfolded (Denning, Patel et al. 2003), they will still recognize and bind to transport factors after being run on a denaturing gel and transferred to nitrocellulose (for an example, see (Rout, Blobel et al. 1997)). Thus, equal amounts of Nsp1FG-cys was run in each lane on a gel and transferred to nitrocellulose. Individual lanes were separated, and each membrane strip was probed with a different concentration of fluorescent labeled NTF2-GST, with volumes adjusted such that NTF2-GST was in at least three-fold molar excess over the bait protein at all concentrations. Bound NTF2 was detected by measuring fluorescence on the membrane, and resulting binding curves were analyzed using Equation 1 (Chapter Three) in SigmaPlot. NTF2(WT)-GST was found to bind Nsp1FG-cys with an affinity of 10 +/- 3 nM ,

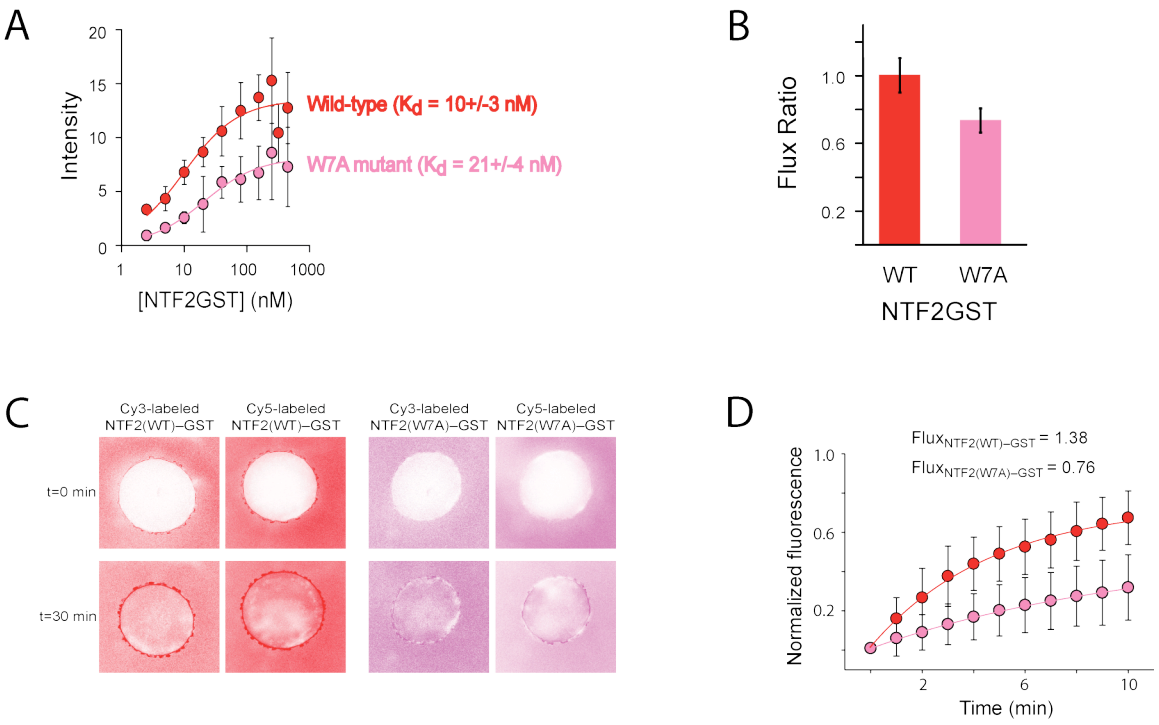

Figure 6-3: Changing transport factor affinity influences transport. A) Results from a far western assay to measure the affinites of NTF2(WT)-GST (red) and NTF2(W7A)-GST (pink) to the engineered Nsp1FG-cys. B) When faced with the Nsp1FG-cys-coated membrane, NTF2(W7A)-GST mutant had a reduced flux ratio compared to NTF2(WT)-GST. No flux difference was seen on the control small-PEG-coated membranes. C) This effect is seen in vivo as well as in vitro. Higher fluorescence intensity is seen around the nuclear envelope of Xenopus oocyte nuclei for Cy3- and Cy5-labelled wild type NTF2GST compared to the mutant, indicating tighter binding of the former. Colors were altered for clarity. D) OSTR experiments with Cy5-labelled NTF2(WT)GST and NTF2(W7A)GST through NPCs in Xenopus laevis oocyte nuclei yielded transport rates of 1.38 (WT protein) and 0.76 (mutant protein) molecules·s^{-1}·NPC^{-1}·μM^{-1}. Standard deviations are shown (Jovanovic-Talisman, Tetenbaum-Novatt et al. 2009).

while NTF2(W7A)-GST bound with an affinity of 21 +/- 4 nM. Nsp1FG-cys also had double the binding capacity for wild type NTF2-GST than for the mutant (see **Figure 6-3 A**).

To see if this change in affinity for Nsp1FG-cys affected transport, we monitored the flux of wild type and mutant NTF2-GST through the NPC mimic. For all proteins tested, we compared the rate of transport through an FG-nup-coated membrane to the rate of transport through a membrane coated only with small (356 Da) PEG-SH. The small PEG-SH provided a non-fouling surface, preventing non-specific binding of proteins to the gold layer. The small-PEG-coated membranes were thus simply inert surfaces perforated with open holes. Transport rates were reported as flux ratios – the ratio of flux through the Nsp1FG-coated membrane to the flux through the control small PEG-coated membrane. A flux ratio of 1 signifies equal rates of transport through Nsp1FG-coated and small-PEG-coated membranes. A flux ratio of zero indicates that the functionalized membrane selectively stopped transport of the molecule. As shown in **Figure 6-3 B**, when the two proteins are combined in equimolar ratios, the flux ratio of mutant NTF2-GST is significantly lower than wild type. This change was due to a decrease in flux of mutant NTF2-GST through the Nsp1FG-coated membranes, as there was no significant difference in flux between wild type and mutant NTF2-GST through the small-PEG-coated membranes (Jovanovic-Talisman, Tetenbaum-Novatt et al. 2009).

With the help of Professor Reiner Peters, we next asked if this difference in affinity affected transport factor interaction with intact NPC. *Xenopus laevis* oocyte nuclei were isolated and exposed to fluorescent-labeled wild type or mutant NTF2-GST. Localization of the protein was monitored as fluorescence intensity. As shown in **Figure 6-3 C**, mutant NTF2-GST has reduced affinity for the nuclear envelope of isolated intact nuclei, which contain all endogenous FG-nups. This *ex vivo* observation agrees with the *in vitro* finding of a reduction in affinity of NTF2-GST for Nsp1FG caused by the W7A mutation (Figure 6-3a). Optical single transporter recording (OSTR) (Tschodrich-Rotter and Peters 1998; Peters 2003; Peters 2006) was then used to measure the flux of fluorescent-labeled proteins through isolated nuclear envelopes. Results from this experiment are shown in **Figure 6-3 D**. Wild type NTF2-GST was seen to travel nearly twice as fast as the mutant through intact *Xenopus* NPCs, with transport rates of 1.38 and 0.76 molecules per pore per second per μM protein respectively (Jovanovic-Talisman, Tetenbaum-Novatt et al. 2009). Thus, differences in affinity found *in vitro* influence transport rates through NPC mimics *in vitro* and through intact *Xenopus* NPCs *ex vivo*. It's important to note that this assay measures transport through the intact NPC, which contains a variety of FG-nups.

We next wanted to test if changing the identity of the FG-domain used to line the pore will influence transport, because different types of FG-domain have different affinities for a given transport factor. For example, NTF2 has a weaker

affinity to Nup100FG than for Nsp1FG (Clarkson, Corbett et al. 1997; Strawn, Shen et al. 2001; Bayliss, Littlewood et al. 2002), but Kap95 binds well to both. (Chapter Four and **Table 4-2**). We confirmed that the addition of fluorescent labels to probe proteins did not alter the binding behavior and specificity of FG-nups using the binding assay described in Chapter Four (**Figure 6-4 A**). When incubated with TALON dynabeads coated with Nup100FG-cys-his_6 and GFP-his_6, equal concentrations of labeled and unlabeled Kap95 were seen to bind Nup100FG to the same extent, while labeled and unlabeled BSA did not bind. We then verified that the affinity relationships between Kap95, NTF2, Nsp1 and Nup100 held for the fluorescent-labeled proteins using a far western assay (**Figure 6-4 B and C**). We proceeded to monitor flux of Kap95 and NTF2-YFP in the presence of non-binding proteins of similar size through membranes functionalized with either Nsp1FG or Nup100FG. Kap95 was visualized via its fluorescent cargo, the Importin β binding domain of Kap60 fused to GFP (Ibb-GFP). Ibb-GFP-his_6 was cloned, expressed and enriched as described for other GFP-NLSs in Chapter Three. Size exclusion chromatography indicated that all Ibb-GFP was in complex with Kap95 under our experimental conditions (Jovanovic-Talisman, Tetenbaum-Novatt et al. 2009). As predicted, the IbbGFP-Kap95 complex was seen to accumulate significantly on both Nsp1FG and Nup100FG membranes, while NTF2YFP only accumulated significantly on the Nsp1FG membrane (**Figure 6-4 D**). This interaction was indeed specific, as BSA

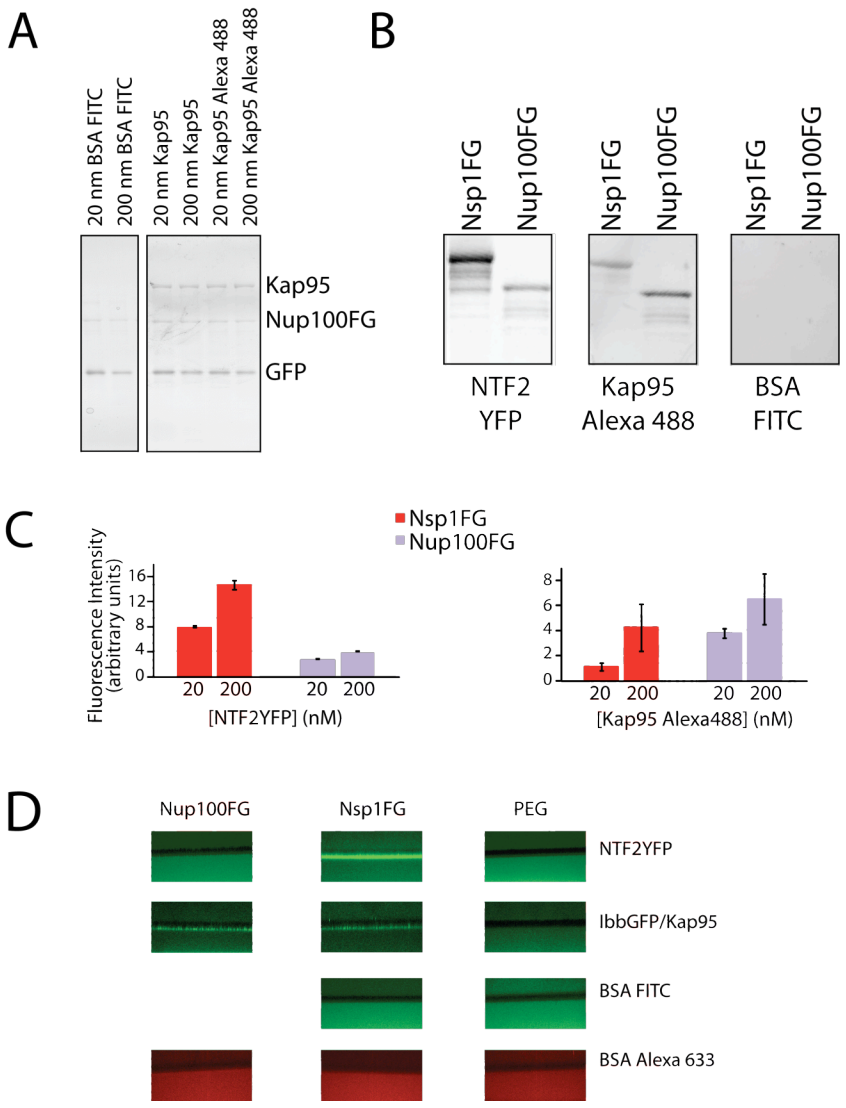

Figure 6-4: Nsp1FG vs Nup100FG. A) The fluorescent label does not affect protein interactions. Coomassie stained gel of a bead binding assay for either FITC-labelled BSA, unlabelled Kap95, or Alexa488-labelled Kap95 with Nup100FG. B) Fluorescent scans of far western blots obtained after binding of 200nM NTF2YFP, Alexa488-labelled Kap95 over Nsp1FG and Nup100FG using a far western binding assay. C) Observed relative binding for NTF2YFP and Alexa488-labelled Kap95 over Nsp1FG and Nup100FG using a far western binding assay. D) Visible accumulation layers are seen with transport factors that bind strongly to the FG-nup membranes, but never on the control PEG membranes. (Jovanovic-Talisman, Tetenbaum-Novatt et al. 2009).

was not seen to accumulate significantly on either functionalized membrane, and none of the proteins tested accumulated on a membrane coated only with PEG-SH (**Figure 6-4 D**) (Jovanovic-Talisman, Tetenbaum-Novatt et al. 2009).

In all of the experiments described thus far, the flux of transport factors was monitored in the presence of non-transport proteins of similar size. The transport factors moved easily through membranes where they interacted specifically with the FG-nup coating the surface. The non-transport proteins were significantly retained by the FG-nup-coated membrane in the presence of an FG-binding transport factor, but were not retained by the small PEG-coated membrane (Jovanovic-Talisman, Tetenbaum-Novatt et al. 2009). We next monitored the flux of an FG-binding transport factor (NTF2-GST) and a non-transport protein (BSA) through functionalized membranes individually and compared this to their respective fluxes when in combination. Experiments showed that flux of a transport factor was not significantly affected by the presence or absence of a non-transport protein. However, the flux of a non-transport control protein (such as BSA) through an Nsp1FG membrane was affected by the presence or absence of an FG-binding transport factor. Flux of BSA was inhibited in the presence of a transport factor that binds specifically to the Nsp1FG (such as NTF2). Without the transport factor, the FG-nup membrane only slightly impeded the flux of non-binding molecules such as BSA (**Figure 6-5**, left). To ensure that this effect was due to specific binding to FG

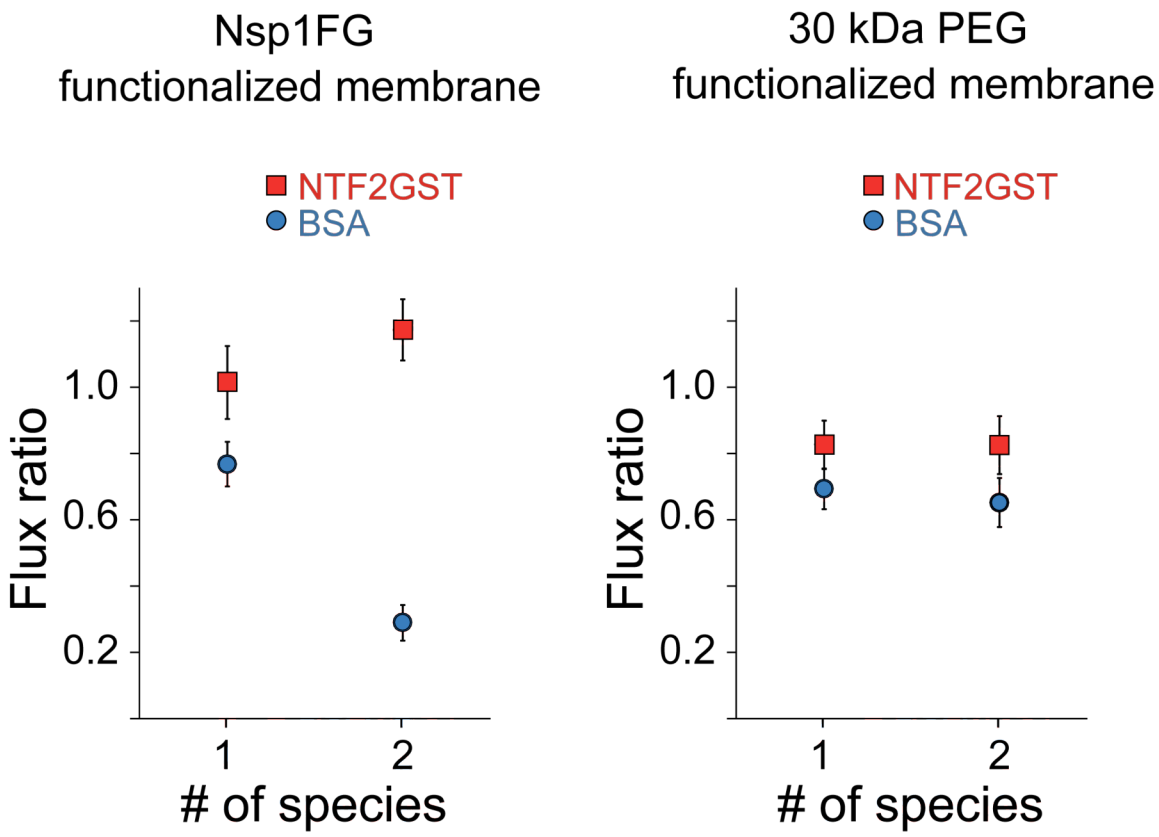

Figure 6-5: Presence of transport factors enhances the selectivity of the FG-nup-coated membranes. Strong selectivity of NTF2-GST transport over BSA is observed for the Nsp1FG-functionalized membrane (left), but not for the "inert" 30kDa PEG-functionalized membrane (right). Flux ratios are plotted for BSA and NTF2-GST alone (one species at a time) or in combination with each other (two species facing the membrane at the same time) through either Nsp1FG or 30kDa PEG membranes versus small PEG coated membranes. The only molecule showing a significant difference between conditions is BSA flux through an NspFG-coated membrane with and without NTF2-GST. Standard errors are shown (Figure modified from (Jovanovic-Talisman, Tetenbaum-Novatt et al. 2009)).

repeats, we monitored flux of these proteins through a membrane functionalized with large 30 kDa PEG-SH. This large PEG is similar to Nsp1FG both in size and in (lack of) secondary or tertiary structure, but it does not contain the specific FG binding sites. As with the Nsp1FG-coated membranes, flux ratios were obtained, relating flux through the 30 kDa PEG membrane to flux through the small 356 Da PEG membrane. Fluxes of NTF2-GST and BSA were both moderately reduced by the physical barrier of the large PEG-SH, and there was no difference in flux if the proteins were alone or in combination (**Figure 6-5**, right).

Changing the affinity of transport factor to FG-nup not only affected flux of the transport factor, but it affected the ability of the transport factor to prevent passage of a non-transport protein. As expected from the binding affinity measurements and the observed accumulation on functionalized membranes, Nsp1FG- or Nup100FG-coated membranes selectively transport Kap95 over a control protein. In contrast, the presence of NTF2 only slightly reduced the flux of a control protein when faced with a Nup100FG-coated membrane, but it significantly reduced the flux of a control protein through a Nsp1FG-coated membrane (Jovanovic-Talisman, Tetenbaum-Novatt et al. 2009). Thus, the FG-nup membrane only proves a substantial barrier to the flux of non-binding proteins when a *specifically-binding* transport factor is present. This effect could be explained by the specifically and non-specifically binding proteins competing for a limited amount of FG-binding sites in the NPC, as predicted by Zilman et al

(Zilman, Di Talia et al. 2007), or by changes in the configuration of the FG-nup barrier upon transport factor binding (for example see (Lim, Fahrenkrog et al. 2007)). These two explanations are not necessarily mutually exclusive.

In summary, we have used *in vitro* binding assays to examine the binding behaviour between different transport factors and FG-nups, and have shown that the findings from these assays are relevant to transport through an NPC mimic and to interactions between transport factors and isolated nuclei. Our NPC mimic is a minimal assembly based upon the essential features of NPC architecture - a simple pore ~30 nm in diameter coated with a layer of FG-nups. Strikingly, this assembly exhibits key features of nucleocytoplasmic transport, selectively discriminating against control proteins while permitting passage of transport factors and cargo/transport factor complexes. Changing the affinity of a transport factor to FG-nups by mutating its binding site was shown to influence its transport efficiency. Changing the FG-motif lining the pore from one with high affinity to a transport factor to one with lower affinity was also shown to influence transport efficiency. These studies also provide insight into the role of transport factors in the NPC selectivity mechanism. The presence of an FG-binding transport factor is required for an FG-nup functionalized membrane to act as a selective filter and prevent the passage of non-specifically interacting proteins. In

a sense, transport factors may be considered transient components of the NPC that help discriminate against the passage of non-specific material across the nuclear envelope.

Chapter Seven: Conclusions and Future Directions

In this work, the protein-protein interactions involved in nucleocytoplasmic transport were examined *in vitro*. Recombinant full-length FG-nups, karyopherins, and fluorescent proteins containing nuclear localization sequences were expressed and enriched from bacteria. Solid phase binding assays were developed to measure the affinities between karyopherins, their cargo, and the FG-nups that make up the nuclear pore complex. The significance of these *in vitro* measurements to transport was explored using nuclei from *Xenopus* oocytes and a synthetic NPC-like filter consisting of small pores lined with a layer of FG-nups.

Expression and enrichment of protease-sensitive proteins

Obtaining enough full-length protein to measure was the first hurdle we faced in this work and, judged by discussion with other research groups and the published literature, a problem common to this field. Purifying endogenous or even over-expressed proteins from yeast resulted in full-length, functional proteins, but the yields were very low. 36 litres of yeast produced only several hundred micrograms of Kap123, which is the most abundant of all proteins we are interested in. Our assays require milligram quantities of enriched protein,

therefore trying to obtain other karyopherins or FG-nups from yeast was impractical.

As discussed in Chapters Two and Four, obtaining full-length FG-nups from bacteria was a challenge. FG-nups are natively unfolded (Denning, Patel et al. 2003), and therefore highly protease sensitive. For this reason, most previously published work examining FG-nups used small, well-behaved portions of the protein of interest rather than the full-length protein (for examples see (Bayliss, Littlewood et al. 2000; Allen, Patel et al. 2002; Bayliss, Leung et al. 2002; Bayliss, Littlewood et al. 2002; Denning, Patel et al. 2003; Pyhtila and Rexach 2003; Berke, Boehmer et al. 2004; Melcak, Hoelz et al. 2007; Schrader, Stelter et al. 2008). However, as different FG-nup fragments exhibit different behaviors (Pyhtila and Rexach 2003), we considered it important to measure interactions with full-length FG-nups. We found that, of the various strains tested, BL21 DE3 GOLD cells produced the most full-length protein with the least pre-lysis cleavage. Induction time and temperature was optimized for each individual FG-nup, as these parameters were clearly found to influence the yield of full-length protein. Solubility of the expressed FG-nup was increased by performing as much of the purification as possible at room temperature. Post-lysis proteolysis was inhibited by the addition of 5mg/mL 6-amino-n-caproic acid to the lysate. This lysine analog prevented lysine-specific proteases from

digesting the natively unfolded FG-nups. In many cases, co-expression with Kap95 in BL21DE3 RIL cells improved the yield of full-length FG-nup.

Protease sensitivity was also a problem with our NLS-GFP constructs. In that case, re-designing the constructs enabled us to do the entire purification in the presence of protease inhibitors, and including 0.1 mM EDTA in the lysis buffer inhibited the relevant proteases without interfering with the affinity purification. These adaptations of the protocol helped us with expression and purification of FG-nups and GFP-NLSs, but they can also be useful for expression and purification of any protease-sensitive protein.

Interactions between karyopherins, their cargo, and FG-nups

Karyopherins were found to recognize their respective NLSs with affinities ranging from ~30-~300 nM (**Table 3-1**). Our values are comparable to the published affinity of Kap104 for the Nab2NLS (Suel, Gu et al. 2008). In most cases we observed a significant difference in binding between Kaps and the NLSs that they do and do not transport *in vivo*, possibly explaining how Kaps selectively bind to their cargos. However, this clear distinction between Kap cargo and non-cargo affinities was not present in all cases. For example, the Nab2NLS bound significantly to all Kaps tested (**Table 3-1**), even though it is only carried *in vivo* via Kap104 (Lee and Aitchison 1999). It remains to be seen if

the distinction between cargo and non-cargo affinities becomes clearer in the presence of specific or non-specific competitor proteins.

We found Kap/FG-nup interactions to be strong, exhibiting apparent K_ds ranging from <1 to ~50 nM, with most under 10 nM (**Table 4-2**). Previous published measurements of interaction strength between Kaps and FG-nups report K_ds ranging from <50pM to >100nM, with as much as an order of magnitude difference in apparent K_d for the same interaction reported by different authors (**Table 4-1**) (Ben-Efraim and Gerace 2001; Bayliss, Littlewood et al. 2002; Gilchrist, Mykytka et al. 2002; Pyhtila and Rexach 2003). In contrast to previous reports (Ben-Efraim and Gerace 2001; Pyhtila and Rexach 2003), we found no clear correlation between affinity for Kaps and location of the FG-Nup within the NPC, and we found no clear distinct subset of "favored" FG-nups for the two Kaps we measured. Each karyopherin bound significantly to each FG-nup tested. The apparent discrepancies could be due to the fact that different researchers used different portions of FG-nups and/or they could be due to environmental influences as discussed below.

Environmental influences

It is important to note that karyopherin concentrations *in vivo* are on the order of μM (Timney, Tetenbaum-Novatt et al. 2006). This is much higher than

the apparent Kap/Cargo and Kap/FG-Nup K_ds as measured with *in vitro* binding assays, including our results and the work of others (Ben-Efraim and Gerace 2001; Bayliss, Littlewood et al. 2002; Gilchrist, Mykytka et al. 2002; Pyhtila and Rexach 2003), indicating that these interactions should be constantly saturated *in vivo*. Constantly saturated Kap/FG-nup interactions would not allow for an effective transport system in which Kaps move through the NPC, because the binding sites in the pore would be continuously occupied. This observation, the wide range of affinities in the literature (**Table 4-1**), and other observations (Timney, Tetenbaum-Novatt et al. 2006) led us to explore the effect of environment on Kap/NLS and Kap/FG-Nup interactions. We found that proteins will interact non-specifically with FG-nups, but that these interactions are competed off by the presence of a specifically-interacting transport factor (**Figure 5-4**). We also observed that apparent affinities of Kap/FG-nup and Kap/NLS interactions are significantly decreased in the presence of non-specific competitor proteins. The distribution of FG-nups on a surface can, in some cases, also influence the apparent K_d as measured by *in vitro* assays.

This vulnerability of Kap/FG-nup interactions to their environment could be partially caused by the natively unfolded nature of the FG-repeat domains. A canonical lock-and-key mechanism for protein-protein interactions would not necessarily be affected by non-specifically interacting proteins to this extent. If a globular background protein “key” does not fit into the “lock” created by the

globular protein of interest, it will not non-specifically bind. However, the native disorder that allows FG-nups to bind specifically to a wide range of transport factors will also allow these proteins to bind non-specifically to almost any protein they come in contact with. The unfolded FG-repeat regions can move relatively freely, allowing the phenylalanines to interact with hydrophobic pockets on almost any protein. In addition, the exposed positive and negative amino acid side chains on FG-nups can interact with surface-exposed charged residues on any other protein. The long FG-repeat region can extend as far as ~60nm (Lim, Huang et al. 2006), while the globular Kaps are much smaller, at ~9 nm diameter (measured from the structures in (Cingolani, Petosa et al. 1999) and (Bayliss, Littlewood et al. 2002)) (**Figure 7-1**). Selectivity has been proposed to come from the density and distribution of hydrophobic pockets along the surface of specifically-binding transport factors (Isgro and Schulten 2007).

The wide range of measured Kap/FG-nup affinities in the literature, along with preliminary data from Tijana Jovanovic-Talisman (personal communication), indicate that the surface to which the FG-nups are bound may also have an effect on apparent affinity. When the FG-domain of Nsp1 was immobilized on the gold-sputtered membrane used to make the NPC-mimic, preliminary data indicate that the apparent affinities of transport factors to that immobilized Nsp1FG were weaker than indicated by the bead binding assays and far western assays described in this work. While the bead binding assays used full-length Nsp1, the

far western assay and the NPC-mimic both used the same Nsp1FG construct. This discrepancy supports our previous conclusion that environmental factors and experimental conditions are important when describing apparent affinities.

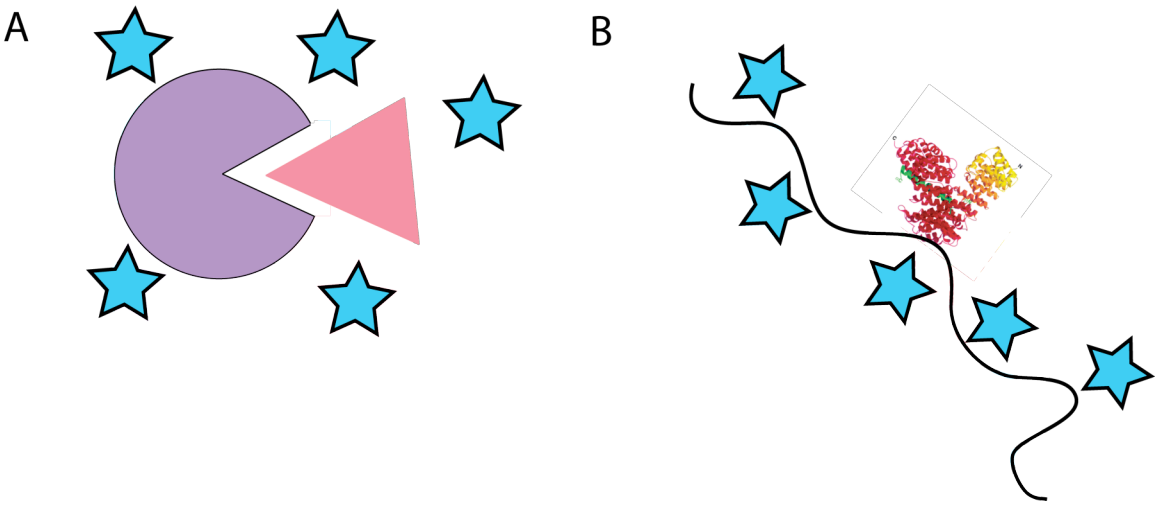

Figure 7-1: Lack of secondary or tertiary structure makes FG-nup interactions more vulnerable to non-specific competition. A) Schematic of an interaction involving two globular proteins with a structured interaction surface. Non-specific competitor proteins are represented by the blue stars. As the stars are the wrong shape to bind to the opening in the purple circle, they are not expected to effect the interaction between the purple and pink proteins. B) A schematic of an FG-nup interacting specifically and non-specifically with proteins in its surroundings. Again, non-specific proteins are represented by the blue stars, and a specific transport factor (importin beta) is represented by its crystal structure (Cingolani, Petosa et al. 1999). Because the FG-nup has no defined secondary structure, we propose that the hydrophobic FG repeats and the charged amino acids separating them can interact with hydrophobic pockets or charged residues on a wide range of proteins.

Comparing binding behavior of different karyopherins

An inverse relationship between karyopherin concentration and affinity for the nuclear pore complex was predicted by a mathematical model of nucleocytoplasmic transport (Zilman, Di Talia et al. 2007). This model noted that more abundant karyopherins have a higher probability of interacting with the NPC due to their higher concentration, but this higher entrance flux must come at the expense of residence time at the NPC. If affinities of abundant karyopherins for nucleoporins are not lowered, then the increased probability of interaction combined with a long residence time would result in a barrier preventing other less-abundant karyopherins from crossing the NPC. Agreeing with this prediction, we did find a potential inverse relationship between Kap abundance *in vivo* and affinity for NLS-cargo and FG-Nups (**Figures 3-6** and **4-6**). We also found a possible dependence of affinity to Kap95 on the number of phenylalanines present in a given FG-nup (**Figure 4-5**). This trend was not seen for Kap121, indicating that despite the clear homology between the two members of the Karyopherin β family, Kap121 may interact with FG-nups via a somewhat different mechanism than Kap95. Currently, the only karyopherin whose structure has been solved in complex with FxFG- and GLFG-repeat peptides is importin β/Kap95 (Bayliss, Littlewood et al. 2000; Bayliss, Littlewood et al. 2002; Liu and Stewart 2005). FxFG and GLFG repeats have been shown to bind to the same site on importin β, via interactions between the phenylalanine side chains and hydrophobic pockets on the karyopherin (Bayliss, Littlewood et al. 2000;

Bayliss, Littlewood et al. 2002). The structure of FxFG repeats bound to the transport factor NTF2 (not a member of the importin β family) indicates that it has common features to the interaction of FxFG with importin β. For example, in both cases, the phenylalanine side chains of FG repeats are buried in hydrophobic pockets of the transport factor, and the unfolded FG domains are seen to form a β-like conformation upon binding (Bayliss, Leung et al. 2002). However, there are differences in how each transport factor interacts with FG-nups. The hydrophobic binding pockets are not necessarily conserved between transport factors (**Figure 7-2** and (Bayliss, Leung et al. 2002)). Also, unlike importin β, NTF2 does not appear able to interact well with GLFG peptides. This difference in behavior is possibly due to differences in spacing between hydrophobic pockets on the different transport factors or differences in interactions with the amino acids in between the FG repeats (Clarkson, Corbett et al. 1997; Bayliss, Leung et al. 2002). Therefore, it is not unexpected that different transport factors will bind differently to the FG-nups. A structure of Kap121 in complex with FG repeats will hopefully ultimately address this difference in binding behavior.

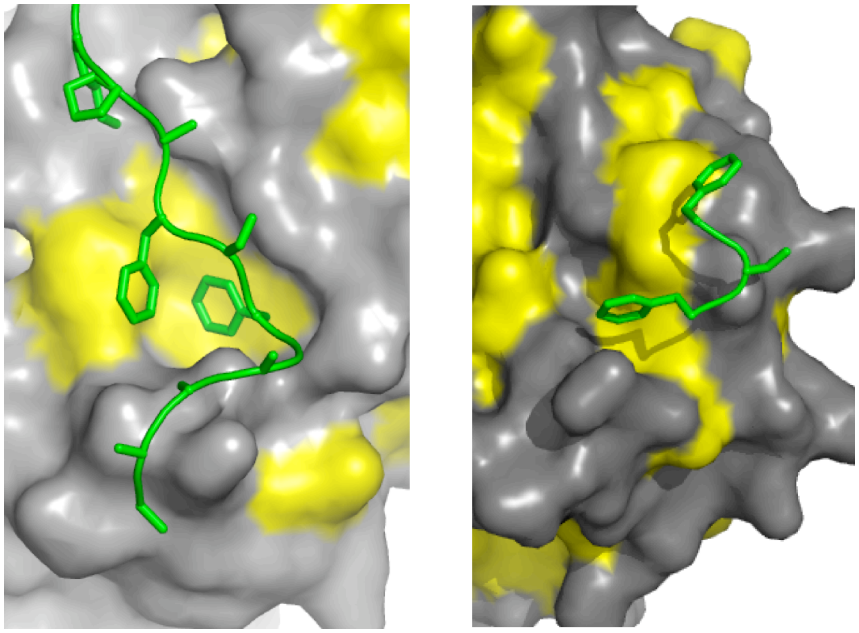

Figure 7-2: Surface representations comparing the binding of FxFG peptides to different transport factors. (Left) Importin β, PDB 1F59 (Bayliss, Littlewood et al. 2000) NTF2, PDB 1GYB (Bayliss, Leung et al. 2002); In each case the Phenylalanine rings bind to hydrophobic depressions on the transport factor surface, but the overall structure of each site is different. Transport factors are depicted in gray (hydrophilic) and yellow (hydrophobic). The FxFG peptide is in green.

Significance of *in vitro* measurements to transport through natural and artificial NPCs

We have shown that affinity differences measured *in vitro* can predict binding to and transport through *Xenopus* oocyte NPCs *ex vivo* (**Figure 6-3**). We also used a synthetic NPC-like filter that we developed to understand the significance of our measurements to transport. Affinity to FG-nup was found to influence filter selectivity, and the presence of specifically-binding transport

factors was found to be an integral part of the selectivity mechanism of the NPC-mimics (**Figure 6-5**). This device has proven to be a useful testbed, and provides a basis for fascinating future studies.

Future directions

We have now developed a method to produce relatively large amounts of full-length, functional karyopherins, cargo, and FG-nups. We have also shown that a bead-binding assay is an informative way to examine interactions between these proteins, and that these *in vitro* observations are relevant to transport through natural NPCs and an NPC-based filter. We have recently found that a custom codon-optomised gene (Integrated DNA Technologies) greatly increases yield and purity of recombinant Nsp1FG (Loren Hough, personal communication). This new method shows great promise for increasing yield and expression of full-length FG-nups and karyopherins. It may enable us to finally obtain full-length recombinant Kap123. Now that these methods are in place, and with the hope that codon-optimization may lead to further improvements, there are many interesting questions we can explore.

Kap123

Although it is the most abundant karyopherin in yeast (Timney, Tetenbaum-Novatt et al. 2006), Kap123 was not included in the majority of our study because we were unable to obtain large amounts of full-length protein (Chapter Two). If codon optimization results in full-length recombinant Kap123, we will be able to test the significance of our observed trends. A third Kap will enable us to determine if there Is in fact an inverse relationship between affinity to FG-nups and *in vivo* Kap concentration. We would also check how the presence of non-specific competitor proteins or changes in FG-nup distribution affect interactions with Kap123. These results will add to the significance of our current findings.

Surface

Kap/FG-nup interactions as measured by bead binding assay are too tight for effective transport to occur (discussed in Chapter Five). The fact that transport occurs in vivo may be explained by the effect of FG-nup distribution, the presence of non-specific bulk proteins in the cytoplasm, and/or any number factors yet to be identified. However, selective transport also can occur in vitro (Jovanovic-Talisman et al, 2009), indicating that this ability is not unique to native NPCs. Preliminary data indicates that the apparent affinity of transport factors to

Nsp1FG bound to the gold sputtered surface of the NPC-mimic is weaker than the apparent affinities of these Kaps to Nsp1 as measured by the bead binding assay and the far western binding assay (Tijana Jovanovic-Talisman, personal communication). This discrepancy, while explaining how the NPC-mimics are capable of transport, leads to further questions. The differences in apparent affinities between Nsp1 bound to the gold surface and to the Dynabeads or nitrocellulose could be due to a wide variety of factors. One possible factor is the surface upon which the FG-nups are immobilized. The surface of the Dynabeads is saturated with GFP (Chapter Four), the gold-sputtered surface is saturated with PEG-SH (Chapter Six), and the nitrocellulose surface only contains the Nsp1FG (Chapter Six). Perhaps the change in apparent affinities is due to differences in FG-nup behavior on these different surfaces. Future work will explore this question of a possible surface effect. For example, we could examine the binding behavior of FG-nups diluted in a lawn of negatively charged GFP (Dashevskaya, Kopito et al. 2008), or repeat some affinity measurements using Dynabeads TALON with larger or smaller radii. These experiments will hopefully further our understanding of the effect of surface properties on apparent affinity.

Orientation

FG-Nups are long proteins with a natively unfolded FG domain anchored to the NPC *in vivo* via a terminal structured domain (Devos, Dokudovskaya et al. 2006). The FG-domains range in size and in the fraction of the FG-nup they occupy (see **Figure 1-3**). To try and understand the reason for this variety of FG-nup composition and structure, and if the location of the FG-domain on the nup is important for Kap recognition, we are checking to see if the orientation of FG-nups influence their interaction with karyopherins. To do this, we have cloned an FxFG nup (Nsp1) and a GLFG nup (Nup100) with His-tags on the FG-end and compared the behavior of those constructs to the same proteins with His-tags on the structured end. Experiments are currently in progress to examine the effect of orientation on Kap/FG-nup interactions. Initial results indicate that orientation influences the apparent affinity of karyopherins to Nsp1, but not to Nup100.

Nsp1 and Nup100 are the nups whose FG domains were used to line the gold-coated pores of the synthetic NPC-mimic. It would be interesting to see if switching the cysteine tag to the other end of the FG-domain, thus turning the domains upside down on the surface, would influence their binding behavior.

Stoichiometry

The stoichiometry of Kap/NLS and Kap/FG-nup interactions is not known. Simulations and crystal structures indicate multiple FG-binding sites on a single karyopherin (Bayliss, Littlewood et al. 2000; Bayliss, Littlewood et al. 2002; Isgro and Schulten 2005; Liu and Stewart 2005), but it is not known if these sites are occupied *in vivo* by multiple FGs from the same FG-nup, or by single FGs from multiple FG-nups. Experiments are currently in progress to determine the stoichiometry of Kap/FG-nup and Kap/NLS interactions. These experiments consist of bead binding assays and native mass spectrometry.

In bead binding assays, FG-nups immobilized on beads are incubated with saturating concentrations of Kap. Beads are washed, and bound proteins are visualized with Coomassie blue, as in Chapter 4. We are currently in the process of calibrating Coomassie intensity to μg protein using amino acid analysis (J. Myron Crawford, Keck Facility, Yale University). We then hope to be able to quantify how many μg of karyopherin saturates how many μg of FG-nup, and this will provide stoichiometry of the interaction on beads.

Native mass spectrometry is a relatively new technique where native-like proteins and protein complexes can be investigated via a mass spectrometer. Additionally, individual subunits can be dissociated from a complex via tandem

MS. Information gained from these experiments can confirm stoichiometry or determine subunit interaction maps for large complexes. The technique of native MS is currently being developed and optimized by Zachary Quinkert in Brian Chait's laboratory and others (Sharon and Robinson 2007; Heck 2008). Relatively gentle electrospray ionization (ESI) generates ions directly from solution and thus can preserve certain non-covalent interactions. Stoichiometry can then be determined from the measured mass/charge ratio (m/z) of an intact complex. This technique can tolerate heterogeneity in complex composition and can thus detect multiple forms of a complex simultaneously (Sharon and Robinson 2007). However, finding buffer conditions that are compatible with both protein complex purification and mass spectrometry has proven to be a major challenge (Heck 2008). For example, salts and detergents are often required to maintain protein and complex integrity, and these reagents are often incompatible with ESI-MS. Our own experience has shown that detergents are very difficult to completely remove from a solution once added, and even the smallest amount of remaining detergent results in a heterogenous mixture of adducts in the final spectra (**Figure 7-3**). High concentrations (~10 μM) of full-length proteins or protein complexes in a salt- and detergent-free ammonium acetate buffer are required (Heck 2008). Spectra have been obtained for both Kap95 and Nsp1FG (**Figure 7-3**), although some optimization is still needed. However, we have not yet been able to observe the intact Kap/FG-nup complex. The process of ionization by electrospray, even though it is relatively gentle, may

disrupt the non-covalent interaction between Kap and FG-nup. We are planning to obtain a mutant version of the transport factor NTF2 that has an increased affinity to FG-nups (Lane, Cushman et al. 2000). Perhaps this tightly-binding mutant will enable the transport factor/FG-nup complex to hold up to the ionization required for native mass spectrometry.

Knowing the stoichiometry may help us understand how FG-nups move across the pore. Must they unbind from one FG-nup completely before "hopping" over to the next? Do they bind multiple FG-nups at a time, moving along in a hand-over-hand fashion? This is currently unknown. Also, based on our findings, we must ask if the presence of non-specific competitor proteins affects stoichiometry. It is possible that the multiple FG-binding sites are not fully occupied *in vivo* because they are "distracted" by the non-specific proteins in the cellular milieu. This would help explain how such apparent tight interactions with multiple binding sites can function as an effective transport system with rapid on/off rates.

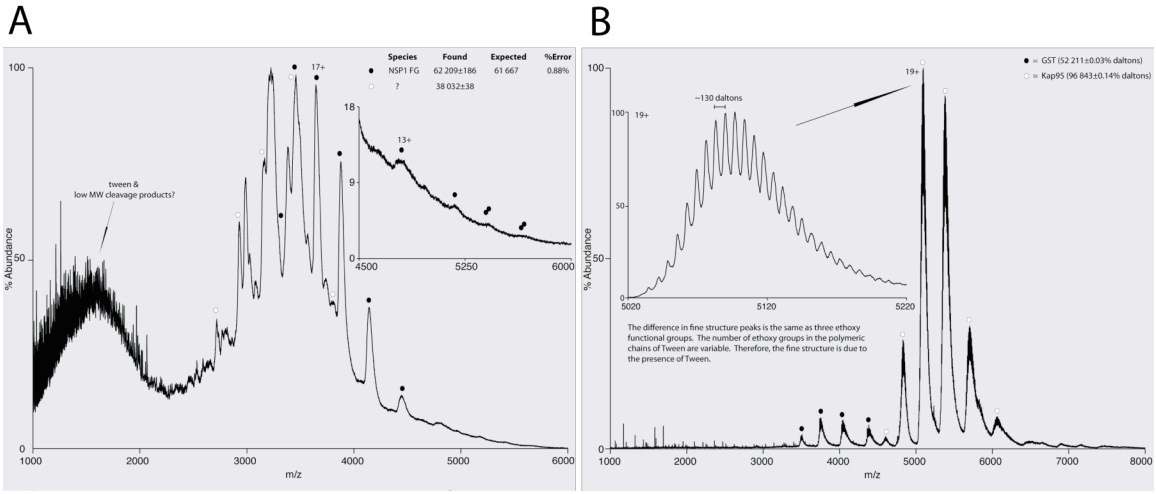

Figure 7-3: Initial results from native mass spectrometry. A) Native MS of codon-optimized Nsp1FG. The Tween present in the protein purification buffer is difficult to remove, and remains even after three buffer changes through a desalting column. The Nsp1FG is also not entirely full-length, as some cleavage products remain. The presence of Tween-20 and cleavage products contribute to the noisy spectrum and high baseline. B) Native MS of Kap95. Again, the small amount of Tween remaining after multiple buffer exchanges causes the multiple peaks seen in the spectra. The Tween forms adducts with Kap95, leading to the pattern of peaks seen in the inset. Further work must be done to obtain the yield, purity, and concentration of full-length protein needed for these experiments. (Native MS performed by Zachary Quinkert)

Solution binding assays

This work has examined the behavior of FG-nups immobilized on the surface of the beads. Although the native environment of these proteins is on the surface of the NPC, it would be beneficial to study their interactions in solution. Full-length FG-nups are not compatible with solution-based assays. As these proteins are normally anchored to the NPC, their structured domains are often insoluble and either precipitate out or aggregate under non-denaturing conditions. However, the Nsp1FG-cys-his and Nup100FG-cys-his constructs used in the NPC mimic device (Chapter Six) do not contain the structured anchor domain and are thus more soluble in solution. The increased yield of full-length Nsp1FG obtained from the codon-optimized gene now allows us to plan solution-based assays.

Fluorescence anisotropy could be used to monitor the binding of Kaps to FG-nups in real time. Kaps and FG-nups are both nearly 100kD in size. The change in mass upon complex formation would therefore be a two-fold change, which would normally not cause a not a large enough change in tumbling rate to be visible by fluorescence anisotropy. However, unlike most 100kD proteins, the FG-nups are natively unfolded. This means that their N- and C-terminal ends are not restrained by secondary structure and thus will likely behave as nearly free amino acids in solution (i.e. fast tumbling rates). The observed tumbling will likely

change drastically upon binding to karyopherin, and this will hopefully be measurable using fluorescence anisotropy allowing us to measure Kap interactions in real time. Different FG-repeat constructs can be tested, containing different numbers of FG repeats and/or different mutations in the FG or spacer amino acids. This would further our understanding of the requirements for Kap/FG-nup interactions.

Nuclear magnetic resonance (NMR) has recently been used to examine the interaction between intrinsically unfolded proteins and their substrates. For example, the intrinsically unfolded kinase inhibitor Sic1 was studied along with its cognate receptor Cdc4 (Mittag, Orlicky et al. 2008). Unfolded proteins such as Sic1 tend to have fast internal motions and short effective correlation times, thus producing sharp NMR resonances. Analogous to the changes visualized in fluorescence anisotropy, a larger effective correlation time and a restriction in local motion will be observed upon interaction with a large globular protein, leading to broader NMR resonances (Mittag, Orlicky et al. 2008). Sic1 has six residues that can be phosphorylated, and this phosphorylated version binds to Cdc4. NMR results indicate that Sic1 and pSic1 are both natively unfolded (Mittag, Orlicky et al. 2008). By monitoring changes in resonances assigned to specific amino acids, the authors were able to identify which residues were interacting with Cdc4. In an NMR experiment, proteins are expressed in bacteria grown in synthetic media supplemented with ^{15}N, or ^{13}C. The resonances of

these isotopes, along with protons (^{1}H), are determined primarily by the atom and its local environment. Chemical shifts of the resonances can be assigned to specific atoms within the protein as chemical shifts of the different protons of nonterminal amino acid residues in random coil peptides is known (Bundi and Wuthrich 1979; Reid, MacLachlan et al. 1997). Deviations from these chemical shifts due to the nonbonded environment of secondary, teriary, and quaterniary structure provide information about the folded state of the protein. NMR resonance linewidths are inversely proportional to the spin-spin relaxation times, and thus provide information about molecular mobility (reviewed in (Reid, MacLachlan et al. 1997)). To separate overlapping peaks in NMR spectra, two-dimensional and three-dimensional experiments are used (reviewed in (Wuthrich 1990)). We would like to explore the use of this technique to study Kap/NLS and Kap/FG-nup interactions. If better resolution is needed to assign resonances to particular amino acids, proteins could be expressed in media where only select amino acids (for example, only phenylalanines) contain ^{15}N, or ^{13}C. Peptide synthesis can also be used to incorporate the isotope-labeled amino acids in select sites. By monitoring the changes in NMR resonances of FG-nup or NLS residues upon binding to Kap, we might be able to identify which residues on the FG-nup or NLS are interacting with Kap and could possibly identify order or processivity in the interactions if any exists. We could also determine how many FG repeats are involved in an interaction at a given time.

Protease mapping of Kap binding sites

Exactly which residues on each FG-nup interact with a Kap? How many FG repeats are required? These and other questions remain unanswered. Protease accessibility laddering (PAL) has been developed and used by members of our laboratory to confirm secondary structure predictions of nucleoporins (Devos, Dokudovskaya et al. 2004; Devos, Dokudovskaya et al. 2006). In this technique, full-length proteins are immobilized by a terminal tag and partially digested with a specific protease. Beads are then washed, and bound fragments are separated by SDS-PAGE. The fact that each fragment begins at the tagged terminus, combined with the known amino acid sequence of the bound protein and the known specificity of the protease allows the amino acid composition of each cleavage product to be estimated from the molecular weight. This method is depicted in **Figure 7-4 A**. We hope to combine this method with the far western or overlay assay to determine which portions of the FG-nups interact with Kaps. Results from an initial experiment are shown in **Figure 7-4 B** and **C**. These initial results indicate the feasibility and value of this technique. As expected, it appears that Kap95 does bind specifically to the FG-repeat region of Nsp1 and that approximately four FG repeats are required for Kap binding. This technique can be applied to Kap/FG-nup interactions as well as any other interaction where one partner is natively unfolded. Findings from these experiments can be confirmed using bead binding assays with recombinant

proteins containing different numbers of FG repeats produced from codon optimized genes.

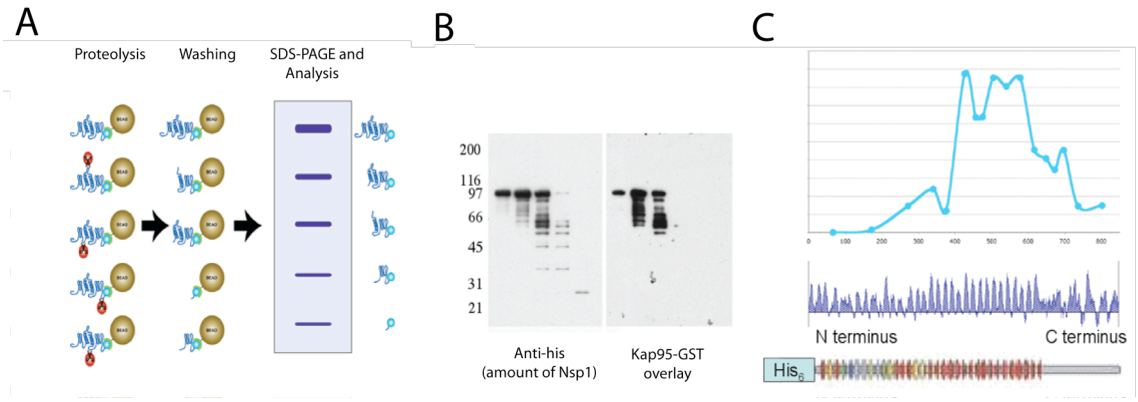

Figure 7-4: Protease mapping of the Nsp1-Kap95 interaction. A. Schematic of protease mapping experiment. B. The anti-his blot of the Nsp1 ladder and Kap95-GST overlay blot. C) A plot of the GST/HIS ratio vs Amino Acid number, indicating that the relative binding ability for Kap95 is highest in the central FG region of Nsp1.

Concluding remarks and final thoughts

This work has provided novel insight into the protein-protein interactions involved in karyopherin-mediated transport across the NPC. Techniques have been developed to obtain full-length recombinant versions of natively unfolded and often insoluble proteins. A potential trend was found where less abundant transport factors interact more tightly with their cargoes and with FG-nups. Interactions involving FG-nups have been shown to be preternaturally sensitive to factors in their environment, including the presence of non-specifically interacting proteins and the distribution of the FG-nups along a surface. Transport factors that specifically interact with FG-nups have been shown to compete with and prevent binding of non-specific interactions, and this competition was shown to be crucial to the selectivity of an NPC-like synthetic filter. While this work has led to many new questions, much has been learned about the unusual behavior of these FG-nups, and some of the disparity in the literature may be explained. With the additional experiments made possible by the codon-optimized genes, we hope to paint a more complete picture of how the natively unfolded FG-repeat domains interact with transport factors and other proteins in their environment to create the robust, selective and efficient filter that is the nuclear pore complex.

While we do not have the data yet to fully understand how Kap-mediated transport is accomplished, I believe that my data and the data in the literature are consistent with the following model. When I picture the FG-nups within the NPC, I see them moving, similar to the tentacles of a sea anemone. Some FG-nups (perhaps those containing cohesive GLFG repeats (Patel, Belmont et al. 2007)) tangle and interact with each other, while others (perhaps those containing non-cohesive FxFG repeats (Patel, Belmont et al. 2007)) are extended and interacting with cytoplasmic or nucleoplasmic proteins, either specifically or non-specifically. I believe that the phenylalanines of FG-nups interact with hydrophobic pockets on all proteins they encounter, meaning that almost any protein can get through the NPC to some extent. Selectivity in transport comes from strongly binding transport factors competing off the weakly-binding non-specific proteins (**Figure 5-4**). The stronger binding of transport factors results from the presence of multiple, correctly spaced phenylalanine-interacting hydrophobic pockets over the surface of the transport factors (Isgro and Schulten 2005; Isgro and Schulten 2007; Isgro and Schulten 2007). I believe transport factors move through the NPC by passing from FG-nup to FG-nup in a hand-over-hand manner. The presence of multiple FGs spaced out over a single FG-nup may enable transport selectivity (by specifically binding only those proteins with the proper distribution of hydrophobic pockets to correspond with the spacing between Phe-s within the FG-nup), and that multiple binding pockets on the transport factor are also required to enable the hand-over-hand passage from FG-nup to FG-nup. This

mechanism might explain how the NPC can transport such a variety of proteins with very high selectivity. Experiments in which binding sites on Kaps and FG-nups are systematically modified will be useful in testing this model, and the NPC mimic membranes will also be a valuable resource. These membranes allow much more experimental flexibility than isolated nuclei or living cells. Therefore, this thesis work has provided insight into the role of non-specific competition in determining the selectivity of transport, and has also developed methods to obtain the starting materials and testbeds needed to further explore the mechanisms of selective nucleocytoplasmic transport.

Chapter Eight: Materials and Methods

Expression and purification of karyopherins

Plasmids encoding Kap95 in pGEX-2TK and Kap121 in pGEX -4T1 were a kind gift from John Aitchison (see **Table 2-1** for a list of Kap plasmids). Kap123 was cloned with a flu tag into the SalI site of pGEX-4T3. These plasmids were transformed into BL21DE3 pLys or RIL cells and grown with the following protocol. Buffers are TB (0.253% Tryptone, 0.51% Yeast extract, 0.113% glycerol) and TBB (11.5 g KH_2PO_4 and 62.5 g K_2HPO_4 per 500 mL). One colony of cells is inoculated into 27 mL TB + 3 mL TBB + antibiotics and incubated overnight shaking at 37 ºC. That pre-culture is spun down, resuspended in 45 mL TB + 5 mL TBB + antibiotics and incubated shaking at 37 ºC for 8 hours. The 50mL culture is spun down, resuspended into 1-2 mL TB and inoculated into 900 mL TB + 100 mL TBB + antibiotics. This 1 L culture is incubated shaking at 37 ºC for 5 hours. Cells are then induced with 1 mM isopropyl-1-thio-b-D-galactopyranoside (IPTG) and incubated for 16 hours at 30 ºC. Cells were pelleted and stored at -80 ºC until ready for use.

Cell pellets from 1 L of culture were thawed and resuspended in 20 mL transport buffer (TBT; 20 mM Hepes pH 7.4, 110 mM KOAc, 2 mM $MgCl_2$, 0.1% Tween20, 10 μM $CaCl_2$, 10 μM $ZnCl_2$) plus 1 mM DTT and protease inhibitors.

Cells were lysed by passing several times through a microfluidizer ® (Microfluidics), and cell membranes were pelleted by spinning 90 minutes at 40,000 rpm (145,000 x g_{av}) in a Ti50.2 rotor (Beckman) at 4 ºC. The lysate was then filtered through a 0.22 μm filter, and incubated with 25-50 mL of Glutathione Sepharose Fast Flow (GE Healthcare) for 2 hours at 4 ºC. The resin was then washed with 5 bed volumes of cold (4 ºC) TBT + 1 mM DTT + protease inhibitors, once with 5 bed volumes of cold (4 ºC) TBT + 1 M NaCl + 1 mM DTT + protease inhibitors, once with 5 bed volumes of room temperature TBT + 100 μM ATP + 1 mM DTT + protease inhibitors, and once with 5 bed volumes of cold (4 ºC) TBT + 1 mM DTT (no protease inhibitors). GST-Kaps were eluted from the Glutathione Sepharose resin with 10 mM reduced glutathione (Sigma) in 100 mM Tris pH 7.4. Buffer was changed to TBT without glutathione, and the GST was cleaved off using the thrombin cleavage capture kit (Novagen) following the manufacturer's instructions. Glycerol was added to 10%, and the cleaved Kap was aliquoted and stored at -80 ºC until ready for use. Thawed Kaps were centrifuged for 2 hours at 55,000 rpm (112,000 x g_{av}) in a TLA55 rotor (Beckman) at 4 ºC immediately prior to use to ensure that no micro-aggregates were present. When fluoresecent labeled proteins were required, Kaps were labeled with the Alexa 488 or Alexa 633 protein labeling kit (Invitrogen) as per the manufacturer's instructions, and spun again at 112,000 g_{av} for 60 minutes in a TLA55 rotor. Labeled Kap121 was further enriched using a Superose 6 column equilibrated in

TBT. Dye content was measured by absorbance, and was usually between 0.5-2 dye molecules per molecule of Kap.

Expression and purification of NTF2

Human NTF2(WT)GST in pGEX-2T, NTF2(W7A)GST in pGEX-2T, and NTF2(WT)YFP-His_6 in pET21b were transformed into BL21DE3 cells. Cells grown in LB medium with antibiotic selection were induced with 0.1 mM IPTG at OD_{600} = ~0.8 and protein was expressed for ~12 hours at 30 °C and 23 °C for GST and YFP tagged proteins respectively. Cells were harvested, resuspended in the appropriate buffer (listed below), and lysed in a microfluidizer. GST-tagged species were enriched from the clarified lysate using a Glutathione Sepharose column in PBS buffer (140 mM NaCl, 2.7 mM KCl, 10 mM Na_2HPO_4, 1.8 mM KH_2PO_4, pH 7.4) supplemented with 0.1% Tween 20. The NTF2-YFP-His6 was enriched using a HisTrapFF (GE Healthcare) in 50 mM NaH_2PO_4 pH 8, 300mM NaCl followed by a Superose 6 column in TBT buffer. The GST tagged proteins were dialyzed into 20 mM TRIS pH 7.1, 50 mM NaCl, 2 mM $MgCl_2$, 0.1% Tween 20, allowing the proteins to be labeled with Cy dyes according to the manufacturer's instructions. Unreacted dye was removed via size exclusion Biogel P30 resin (Bio-Rad) equilibrated with TBT or mock3 buffer (90 mM KCl, 10 mM NaCl, 2 mM $MgCl_2$, 0.1 mM $CaCl_2$, 1.0 mM N-(2-hydroxyethyl)ethylene-

diaminetriacetic acid, 10 mM HEPES, pH 7.2). After labeling, Cy dye labeled proteins were spun down at 72,000 g_{av} for 45 minutes in TLA55 rotor (Beckman) and the supernatant was passed through a 100 kDa nanosep concentrator (Pall Corporation) to remove micro-aggregates. (Jovanovic-Talisman, Tetenbaum-Novatt et al. 2009). The flow-through from the concentrator was used for flux experiments (Chapter 6).

Expression and purification of NLS-GFP constructs

eGFP-His_6, Rpl25NLS-eGFP-His_6, Pho4NLS-eYFP-His_6, Nab2NLS-eGFP-His_6, and Ibb-eGFP-His_6 were cloned into pET21b were transformed into BL21DE3 gold cells (see **Table 2-1** for NLS plasmids, and **Table 2-2** for NLS sequences). Cells were grown in LB with antibiotic selection at 37 °C to an OD_{600} of 0.8, induced with 1mM IPTG, incubated for 4 hours at 30 °C, harvested by centrifugation, and stored at -80 °C. Cell pellets were defrosted and resuspended in 50 mM NaH_2PO_4 pH 7, 300mM NaCl supplemented with 0.1mM EDTA and protease inhibitors. Cells were lysed in a microfluidizer, and debris was pelleted by a 145,000 g_{av} spin in a Ti50.2 rotor (Beckman) at 4 °C. GFP-his_6 and all NLS-GFP-his_6 were enriched from the lysate using TALON Sepharose (Clontech) according to the manufacturer's instructions. As much of the purification as possible was performed at 4ºC. This was necessary to prevent

the unfolded NLS domains from getting cleaved. Enriched protein was stored at 4 ºC until ready for use.

Expression and purification of FG-nups

FG-nups are natively unfolded (Denning, Patel et al. 2003), and thus highly sensitive to proteolysis. Therefore these proteins are difficult to express and purify full-length. The genes encoding for FG-nups were amplified from either genomic DNA or a plasmid containing the gene, and inserted into vectors of the pET family. Unless otherwise noted, the his_6 tag was positioned on the coiled-coil end of the FG-nups. These plasmids were then transformed into BL21DE3 Gold cells, which were found to give the best expression with the least cleavage. Expression conditions were determined for each individual protein, varying induction times from 1-16 hours and induction temperatures from 22-37ºC. Some FG-nups cleaved *in vivo* at all expression conditions tested. Many of these nups expressed full-length when co-expressed with Kap95. Nups in a Kanamycin-resistant plasmid were co-expressed with Kap95 in pGEX-2TK, while Nups in an Ampicillin-resistant plasmid were co-expressed with Kap95 in pET24. After the appropriate induction, cells were harvested and stored at -80ºC until ready for purification (see **Table 2-3** for FG-nup plasmids and **Table 2-4** for FG-nup expression conditions).

Cell pellets were defrosted and resuspended in 4 volumes of lysis buffer (50mM NaH_2PO_4 pH 8, 300mM NaCl) plus 8M urea plus protease inhibitors. The FG-nups are natively unfolded, so the denaturing conditions required to keep them soluble is not a problem, because there is no secondary or tertiary structure to denature. The urea also enables the FG-nups that are co-expressed with Kap95 to be enriched without the Kap. Cells were lysed by passing several times through a microfluidizer ® (Microfluidics). 6-amino-n-caproic-acid (Sigma) was added to a final concentration of 5 mg/mL, and cell debris was spun down in a Ti50.2 Rotor (Beckman), 40,000 rpm at room temperature. The supernatant was put through a 0.22 μm filter, and the clarified lysate was incubated for >2 hours at room temperature with TALON Sepharose resin (Clontech). The resin was washed with >5 bed volumes of lysis buffer + 0.8M urea + protease inhibitors, and protein was eluted in lysis buffer + 0.8M urea + protease inhibitors + 150mM imidazole. Glycerol was added to 10%, and the enriched FG-nups were stored at -80^{o}C until ready for use. When necessary, a second purification step was done using a Superose 6 size exclusion column (GE Healthcare) or electropurification (described below).

Nsp1FG-Cys-His_6 (residues 30-591) in pET21b was transformed into BL21DE3 gold cells. Nup100FG-Cys-His_6 (residues 1-570) in pET21b was co-transformed with untagged Kap95 in pET24a into BL21DE3 RIL cells. Cells grown in LB (Luria Bertani) medium with antibiotic selection were induced with

1 mM IPTG (Isopropyl-Thio-β-D-galactopyranoside, from RPI) at optical density (OD) ~0.8 and harvested after a 2 hour incubation at 30 °C (Nsp1FG) or 4 hour incubation at 22 °C (Nup100FG). Cells were resuspended in 50 mM NaH_2PO_4 pH 8, 300mM NaCl supplemented with 8M urea and protease inhibitors, and lysed in a microfluidizer. Cell debris was removed with a 90 minute spin at 145,000 g_{av} in a Ti50.2 rotor (Beckman) at 4 ºC. The his-tagged nup proteins were enriched in two steps using TALON resin (Clontech) or a HisTrapFF column (GE Healthcare) and a Superose 6 column (GE Healthcare) equilibrated with 50 mM HEPES pH 7.4, 300 mM NaCl, 1 mM EDTA, 50 μM TCEP or TBT buffer supplemented with 50 μM TCEP.

When completely pure, full-length protein was needed, electropurification was used. This method takes advantage of the fact that FG-nups are natively unfolded, and are thus fully functional after being run on an SDS-PAGE gel. ~500 μg of TALON-enriched FG-nup was boiled in gel loading buffer and loaded into the large well of a 10% Tris-Glycine 2D gel (Invitrogen). Proteins were visualized with via zinc staining as follows. Gels were washed quickly with water, and incubated for 15 minutes at room temperature in 200mM imidazole, 0.1% SDS. After another quick wash with water, gels were incubated in 200mM $ZnSO_4$ until protein bands were visible. A wash with water stopped the staining. A scalpel was used to excise the portion of gel containing full-length protein (**Figure 8-1**). The excised band was placed into dialysis tubing (Spectra/Por) with ~5mL

of Elution Solution (50 mM Tris pH 9, 0.5 mM DTT, 1 mM EDTA, 0.1% SDS). The tubing was then placed in a flat DNA gel box filled with elution solution, and weighted down with a glass plate. A schematic of this set-up is shown in **Figure 2-7**. The system was run in the cold room (4 ºC) at 80 V (33 mA). After 16 hours the protein was eluted from the gel band and was in solution in the dialysis tubing. This elution was concentrated and stored at -80 ºC until ready for use.

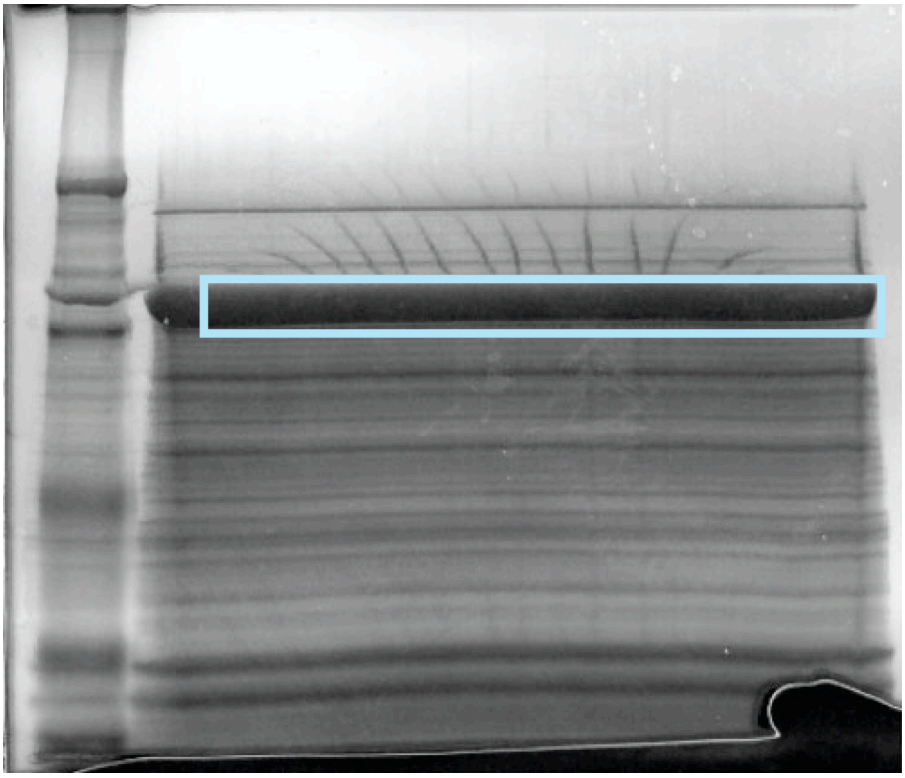

Figure 8-1: Zinc-stained gel of Nsp1-His_6. A scalpel was used to cut out the band marked by the blue rectangle. Protein was eluted from this band using the electropurification setup shown in Figure 2-7.

Preparation of His-depleted *E. coli* lysate

As bacteria are prokaryotes, their cytoplasm contains many components of the yeast cytoplasm without any of the molecules involved in nucleocytoplasmic transport. Thus, *E. coli* lysate was used as non-specific competitor protein to see how environment influences Kap interactions. 1 L of BL21 DE3 RIL cells were grown to an OD_{600} of 0.8 and incubated for 4 hours at 30ºC. Cells were harvested, resuspended in TBT plus protease inhibitors, and lysed by passing through a microfluidizer. Cell debris was removed with a 90 minute spin at 145,000 x g_{av} in a Ti50.2 rotor (Beckman) at 4 ºC. In order to ensure that no non-specific interactions to the Dynabeads TALON would occur, this clarified lysate was incubated with 3 x 3 mL TALON Sepharose. Lysate was then stored at 4ºC until ready for use. Immediately before each use the lysate was passed through a 0.22 μm filter and spiked with protease inhibitors.

Resin binding assay to measure Kap/cargo affinity

Binding assays were performed in TBT plus 1 mM DTT, and protease inhibitors. A custom high titer anti-GFP rabbit polyclonal antibody (Convance; (Cristea, Williams et al. 2005)) was affinity purified and conjugated to CNBr Sepharose by standard methods (Harlow and Lane 1988). For each experiment, 0.5 μg of enriched NLS-GFP-His_6 was incubated per μL (bed volume) of anti-

GFP-conjugated Sepharose, generating immobilized NLS-GFP-His_6 resin. 10 μL aliquots of this resin were dispensed into 10 mL of TBT plus 2.5% milk, and containing a particular concentration of enriched Kap – volumes were adjusted such that Kap was always in molar excess to the NLS. NLSs were allowed to reach binding equilibrium with the Kap overnight at 4 ˚C, with mixing. The resin, with bound Kap, was harvested and transferred to mini-centrifugation columns. Binding buffer was removed by centrifugation and the resin was washed with 500 μL of ammonium acetate buffer (0.1 M NH_4OAc, 0.1 mM $MgCl_2$, 0.02% Tween-20). All proteins were eluted from the resin by incubation with ammonium hydroxide solution (0.5 M NH_4OH, 0.5 mM EDTA). Evaporated protein samples were prepared for SDS-PAGE and proteins observed via Coomassie blue staining. The total, background-subtracted, pixel intensities of bands from scanned gels were measured using OpenLab (*Improvision*) image analysis software. Dissociation constants were calculated from the resulting binding curves by fitting the data to Equation 1 (Chapter 3).

Bead binding assay to measure Kap/FG-nup affinity.

Dynabeads TALON (Dynal Biotech, Invitrogen) were equilibrated in TALON wash buffer (50mM NaH_2PO_4, 300mM NaCl, 0.1% Tween20). 0.5 mg beads were used per data point, or 6.5 mg beads for a 13-point curve. Beads

were then resuspended in TALON wash buffer + 0.8M urea + 25% saturated ammonium sulfate + 1/100 solution P, and protein was added as appropriate. For "regular" assays, 15-50 pmoles FG-nup per data point and 25 μg of GFP-his_6 per data point were combined and added to the beads. The large amount of GFP ensured that no empty TALON surface remained. For "crowded" assays, the beads were separated into two aliquots. Assuming 1 μg protein/μL beads (this will result in super-saturated beads), "x" μL of TALON dynabeads were incubated with "x" μg of FG-nup to result in beads for 13 data points saturated with 15-50 pmoles FG-nup as appropriate. The remaining beads were then saturated with 25 μg GFP-his per data point. In all cases, beads were incubated with the protein for >10 minutes at room temperature to bind the his-tagged proteins to the beads. Beads were then washed 3x with TALON wash buffer + 1/100 solution P, combined if necessary (for "crowded"), and divided equally among tubes of Kap solutions of various concentrations. Kap solutions were made in GST-TBT + 0.3% PVP + protease inhibitors (plus competitor proteins when appropriate), and volumes were adjusted so that at all concentrations there is no less than 3-fold molar excess of Kap over Nup. To ensure adequate mixing, volume was never below 0.3 mL. Beads were incubated with Kap solutions overnight on a rotating wheel at 4 ºC. After incubation, the beads from each data point were washed twice with 1mL GST-TBT + 1/100 solution P, and resuspended in 20μL SDS-PAGE sample buffer. The beads were heated 10 minutes to 95ºC, and 15μL of the supernatant was loaded on a Novex 4-20% TG

gel. The gels were stained with Coomassie Blue R-250, images were digitized and band intensities were quantified using ImageJ (Abramoff, Magelhaes et al. 2004). Background bands of the same size were measured and subtracted from the signal bands. K_ds were calculated by fitting the resulting curves to Equation 1 in SigmaPlot (Systat Software)

In order to confirm the distribution of FG-nup and GFP on the beads, fluorescence microscopy was used. Nsp1FG-cys-His_6 was dialyzed into PBS and labeled with Alexa633 (Invitrogen) according to the manufacturers instructions. Beads were prepared as described above for visual examination. Images were collected with a Hamamatsu C4742-95 cooled CCD camera attached to a Zeiss Axioplan 2 microscope, using a 63x objective lens (NA 1.4). GFP and Alexa633 were imaged using FITC and CY5 excitation/dichroic/emission filter sets respectively, by Chroma. Images were acquired, colorized and combined using OpenLab microscopy software (Improvision). Levels were optimized using Photoshop (Adobe).

Far western assays

As FG-nups are natively unfolded (Denning, Patel et al. 2003), they can be boiled in SDS, run on a gel, transferred to nitrocellulose, and still be recognized by karyopherins. We took advantage of this ability to probe the interactions

between transports and nups. For these assays, enriched Kaps were dialyzed into PBS buffer, and labeled with Alexa Fluor 488 or 633 (Invitrogen) according to the manufacturer's instructions. FG-nups were diluted to 0.05 mg/mL in SDS-PAGE sample buffer, and heated 10 minutes at 95ºC. 10 μL (0.5 μg) was loaded per lane in 10 well 4-20% Novex TG gels (Invitrogen). Proteins were transferred to nitrocellulose overnight at 35V. Membranes were stained with Ponceau to mark the location of the FG-nup bands. Ponceau was used as leftover amido black would be visible during scans of AlexaFluor 633. Membranes were dried and cut into strips with two lanes per strip. Strips were blocked with 2mL of GST-TBT + 0.3% PVP for > 1 hour at room temperature. Strips were then incubated overnight in the dark on a rocker at 4ºC with solutions of fluorescent karyopherin. Kap solutions were made in GST-TBT + 0.3% PVP, and volumes were adjusted so that there was never any less than three-fold molar excess of Kap over Nup. To ensure proper coverage of the membrane strip, Kap volume was never less than 900μL. Membranes were washed three times quickly, and three times five minutes with GST-TBT + 0.3% PVP. Strips were then scanned at on a Typhoon 9400 Variable Imager (Amersham Biosciences, Rockefeller University Proteomics Resource Center) at the appropriate settings for Alexa 488 or 633. Band intensities were quantified in ImageJ.

Experiments performed by others

In vivo import assays were performed by Benjamin Timney using methods described in (Timney, Tetenbaum-Novatt et al. 2006).

The NPC-mimic nanopores were prepared and used by Tijana Jovanovic-Talisman as described in (Jovanovic-Talisman, Tetenbaum-Novatt et al. 2009).

OSTR measurements were performed by Reiner Peters as described in (Peters 2003; Jovanovic-Talisman, Tetenbaum-Novatt et al. 2009).

References

Abramoff, M., P. Magelhaes, et al. (2004). "Image Processing with ImageJ." Biophotonics International **11**(7): 36-42.

Adam, E. and S. Adam (1994). "Identification of Cytosolic Factors Required for Nuclear Location Sequence-mediated Binding to the Nuclear Envelope." J Cell Biol **125**(3): 547-55.

Adam, S. and L. Gerace (1991). "Cytosolic Proteins That Specifically Bind Nuclear Localization Signals are Receptors for Nuclear Import." Cell **66**: 837-47.

Aitchison, J. D., G. Blobel, et al. (1996). "Kap104p: a karyopherin involved in the nuclear transport of messenger RNA binding proteins." Science **274**(5287): 624-7.

Akey, C. W. (1990). "Visualization of transport-related configurations of the nuclear pore transporter." Biophys J **58**(2): 341-55.

Akey, C. W. and D. S. Goldfarb (1989). "Protein import through the nuclear pore complex is a multistep process." J Cell Biol **109**(3): 971-82.

Akey, C. W., Radermacher, M. (1993). "Architecture of the *Xenopus* nuclear pore complex revealed by three-dimensional cryo-electron microscopy." J Cell Biol **122**: 1-19.

Alber, F., S. Dokudovskaya, et al. (2007). "Determining the architectures of macromolecular assemblies." Nature **450**(7170): 683-94.

Alber, F., S. Dokudovskaya, et al. (2007). "The molecular architecture of the nuclear pore complex." Nature **450**(7170): 695-701.

Allen, N., Huang, L, Burlingame, A, Rexach, M (2001). "Proteomic analysis of nucleoporin interacting proteins." J Biol Chem **276**(31): 29268-74.

Allen, N. P., S. S. Patel, et al. (2002). "Deciphering networks of protein interactions at the nuclear pore complex." Mol Cell Proteomics **1**(12): 930-46.

Alvarez, C., I. F. Pazos, et al. (2001). "Effect of pH on the conformation, interaction with membranes and hemolytic activity of sticholysin II, a pore forming cytolysin from the sea anemone Stichodactyla helianthus." Toxicon **39**(4): 539-53.

Arts, G. J., M. Fornerod, et al. (1998). "Identification of a nuclear export receptor for tRNA." Curr Biol **8**(6): 305-14.

Bailer, S. M., C. Balduf, et al. (2000). "Nup116p associates with the Nup82p-Nsp1p-Nup159p nucleoporin complex." J Biol Chem **275**(31): 23540-8.

Bailer, S. M., S. Siniossoglou, et al. (1998). "Nup116p and nup100p are interchangeable through a conserved motif which constitutes a docking site for the mRNA transport factor gle2p." Embo J **17**(4): 1107-19.

Bayliss, R., A. H. Corbett, et al. (2000). "The molecular mechanism of transport of macromolecules through nuclear pore complexes." Traffic **1**(6): 448-56.

Bayliss, R., H. M. Kent, et al. (2000). "Crystallization and initial X-ray diffraction characterization of complexes of FxFG nucleoporin repeats with nuclear transport factors." J Struct Biol **131**(3): 240-7.

Bayliss, R., S. W. Leung, et al. (2002). "Structural basis for the interaction between NTF2 and nucleoporin FxFG repeats." Embo J **21**(12): 2843-53.

Bayliss, R., T. Littlewood, et al. (2000). "Structural basis for the interaction between FxFG nucleoporin repeats and importin-beta in nuclear trafficking." Cell **102**(1): 99-108.

Bayliss, R., T. Littlewood, et al. (2002). "GLFG and FxFG nucleoporins bind to overlapping sites on importin-beta." J Biol Chem **277**(52): 50597-606.

Beck, M., Forster, F, Ecke, M, Plitzko, JM, Melchior, F, Gerisch, G, Baumeister, W, Medalia, O (2004). "Nuclear Pore Complex Structure and Dynamics Revealed by Cryoelectron Tomography." Science **306**(5700): 1387-90.

Belgareh, N., C. Snay-Hodge, et al. (1998). "Functional characterization of a Nup159p-containing nuclear pore subcomplex." Mol Biol Cell **9**(12): 3475-92.

Ben-Efraim, I. and L. Gerace (2001). "Gradient of increasing affinity of importin beta for nucleoporins along the pathway of nuclear import." J Cell Biol **152**(2): 411-7.

Berke, I. C., T. Boehmer, et al. (2004). "Structural and functional analysis of Nup133 domains reveals modular building blocks of the nuclear pore complex." J Cell Biol **167**(4): 591-7.

Bischoff, F. R., H. Krebber, et al. (1995). "Co-activation of RanGTPase and inhibition of GTP dissociation by Ran-GTP binding protein RanBP1." Embo J **14**(4): 705-15.

Blanar, M. A. and W. J. Rutter (1992). "Interaction cloning: identification of a helix-loop-helix zipper protein that interacts with c-Fos." Science **256**(5059): 1014-8.

Boehmer, T., S. Jeudy, et al. (2008). "Structural and functional studies of Nup107/Nup133 interaction and its implications for the architecture of the nuclear pore complex." Mol Cell **30**(6): 721-31.

Bradley, K. J., M. R. Bowl, et al. (2007). "Parafibromin is a nuclear protein with a functional monopartite nuclear localization signal." Oncogene **26**(8): 1213-21.

Brohawn, S. G., N. C. Leksa, et al. (2008). "Structural evidence for common ancestry of the nuclear pore complex and vesicle coats." Science **322**(5906): 1369-73.

Brunet, S., P. Thibault, et al. (2003). "Organelle proteomics: looking at less to see more." Trends Cell Biol **13**(12): 629-38.

Bundi, A. and K. Wuthrich (1979). "Proton NMR parameters of the common amino acid residues measured in aqueous solutions of the linear tetrapeptides H-Gly-Gly-X-L-Ala-OH." Biopolymers **18**: 285-297.

Byers, B. (1981). Cytology of the yeast life cycle. The Molecular Biology of the Yeast Saccharomyces: Life Cycle and Inheritance. J. Strathern, E. Jones and J. Broach. Cold Spring Harbor, NY, Cold Spring Harbor Laboratory Press.

Cansizoglu, A. E. and Y. M. Chook (2007). "Conformational heterogeneity of karyopherin beta2 is segmental." Structure **15**(11): 1431-41.

Cansizoglu, A. E., B. J. Lee, et al. (2007). "Structure-based design of a pathway-specific nuclear import inhibitor." Nat Struct Mol Biol **14**(5): 452-4.

Catimel, B., T. Teh, et al. (2001). "Biophysical characterization of interactions involving importin-alpha during nuclear import." J Biol Chem **276**(36): 34189-98.

Chook, Y. M. and G. Blobel (1999). "Structure of the nuclear transport complex karyopherin-beta2-Ran x GppNHp." Nature **399**(6733): 230-7.

Cingolani, G., C. Petosa, et al. (1999). "Structure of importin-beta bound to the IBB domain of importin-alpha." Nature **399**(6733): 221-9.

Clarkson, W. D., A. H. Corbett, et al. (1997). "Nuclear protein import is decreased by engineered mutants of nuclear transport factor 2 (NTF2) that do not bind GDP-Ran." J Mol Biol **272**(5): 716-30.

Clayton, R. A., O. White, et al. (1997). "The first genome from the third domain of life." Nature **387**(6632): 459-62.

Conti, E., C. W. Muller, et al. (2006). "Karyopherin flexibility in nucleocytoplasmic transport." Curr Opin Struct Biol **16**(2): 237-44.

Cristea, I. M., R. Williams, et al. (2005). "Fluorescent proteins as proteomic probes." Mol Cell Proteomics **4**(12): 1933-41.

Cronshaw, J. M., A. N. Krutchinsky, et al. (2002). "Proteomic analysis of the mammalian nuclear pore complex." J Cell Biol **158**(5): 915-27.

D'Angelo, M. A., D. J. Anderson, et al. (2006). "Nuclear pores form de novo from both sides of the nuclear envelope." Science **312**(5772): 440-3.

D'Angelo, M. A. and M. W. Hetzer (2008). "Structure, dynamics and function of nuclear pore complexes." Trends Cell Biol **18**(10): 456-66.

Dashevskaya, S., R. B. Kopito, et al. (2008). "Diffusion of anionic and neutral GFP derivatives through plasmodesmata in epidermal cells of Nicotiana benthamiana." Protoplasma **234**(1-4): 13-23.

Debler, E. W., Y. Ma, et al. (2008). "A fence-like coat for the nuclear pore membrane." Mol Cell **32**(6): 815-26.

Delphin, C., T. Guan, et al. (1997). "RanGTP targets p97 to RanBP2, a filamentous protein localized at the cytoplasmic periphery of the nuclear pore complex." Mol Biol Cell **8**(12): 2379-90.

Denning, D. (2007). "Repid evolution exposes the boundaries of domain structure and function in natively unfolded FG nucleoporins." Mol Cell Proteomics **6**(2): 272-82.

Denning, D., S. Patel, et al. (2003). "Disorder in the nuclear pore complex: the FG repeat regions of nucleoporins are natively unfolded." Proc Natl Acad Sci U S A **100**(5): 2450-5.

Devos, D., S. Dokudovskaya, et al. (2004). "Components of coated vesicles and nuclear pore complexes share a common molecular architecture." PLoS Biol **2**(12): e380.

Devos, D., S. Dokudovskaya, et al. (2006). "Simple fold composition and modular architecture of the nuclear pore complex." Proc Natl Acad Sci U S A **103**(7): 2172-7.

Dingwall, C. and R. A. Laskey (1986). "Protein import into the cell nucleus." Annu Rev Cell Biol **2**: 367-90.

Dokudovskaya, S., R. Williams, et al. (2006). "Protease accessibility laddering: a proteomic tool for probing protein structure." Structure **14**(4): 653-60.

Doye, V. and E. Hurt (1997). "From nucleoporins to nuclear pore complexes." Curr Opin Cell Biol **9**(3): 401-11.

Dunker, A. K., J. D. Lawson, et al. (2001). "Intrinsically disordered protein." J Mol Graph Model **19**(1): 26-59.

Dworetzky, S. I. and C. M. Feldherr (1988). "Translocation of RNA-coated gold particles through the nuclear pores of oocytes." J Cell Biol **106**(3): 575-84.

Enenkel, C., Blobel, G, Rexach, M (1995). "Identification of a Yeast Karyopherin Heterodimer That Targets Import Substrate to Mammalian Nuclear Pore Complexes." J Biol Chem **270**(28): 16499-16502.

Fabre, E. and E. Hurt (1997). "Yeast genetics to dissect the nuclear pore complex and nucleocytoplasmic trafficking." Annu Rev Genet **31**: 277-313.

Fahrenkrog, B., J. P. Aris, et al. (2000). "Comparative spatial localization of protein-A-tagged and authentic yeast nuclear pore complex proteins by immunogold electron microscopy." J Struct Biol **129**(2-3): 295-305.

Fahrenkrog, B., E. Hurt, et al. (1998). "Molecular architecture of the yeast nuclear pore complex: localization of Nsp1p subcomplexes." J Cell Biol **143**(3): 577-88.

Feldherr, C., D. Akin, et al. (2002). "The molecular mechanism of translocation through the nuclear pore complex is highly conserved." J Cell Sci **115**: 2997-3005.

Feng, W., A. L. Benko, et al. (1999). "Antagonistic effects of NES and NLS motifs determine S. cerevisiae Rna1p subcellular distribution." J Cell Sci **112 (Pt 3)**: 339-47.

Floer, M. and G. Blobel (1996). "The nuclear transport factor karyopherin beta binds stoichiometrically to Ran-GTP and inhibits the Ran GTPase activating protein." J Biol Chem **271**(10): 5313-6.

Floer, M., G. Blobel, et al. (1997). "Disassembly of RanGTP-karyopherin beta complex, an intermediate in nuclear protein import." J Biol Chem **272**(31): 19538-46.

Frey, S. and D. Gorlich (2007). "A saturated FG-repeat hydrogel can reproduce the permeability properties of nuclear pore complexes." Cell **130**(3): 512-23.

Frey, S., R. P. Richter, et al. (2006). "FG-rich repeats of nuclear pore proteins form a three-dimensional meshwork with hydrogel-like properties." Science **314**(5800): 815-7.

Fuxreiter, M., P. Tompa, et al. (2008). "Malleable machines take shape in eukaryotic transcriptional regulation." Nat Chem Biol **4**(12): 728-37.

Garner, M. M. and M. B. Burg (1994). "Macromolecular crowding and confinement in cells exposed to hypertonicity." Am J Physiol **266**(4 Pt 1): C877-92.

Gelamo, E. L. and M. Tabak (2000). "Spectroscopic studies on the interaction of bovine (BSA) and human (HSA) serum albumins with ionic surfactants." Spectrochim Acta A Mol Biomol Spectrosc **56A**(11): 2255-71.

Gilchrist, D., B. Mykytka, et al. (2002). "Accelerating the rate of disassembly of karyopherin.cargo complexes." J Biol Chem **277**(20): 18161-72.

Gilchrist, D. and M. Rexach (2003). "Molecular basis for the rapid dissociation of nuclear localization signals from karyopherin alpha in the nucleoplasm." J Biol Chem **278**(51): 51937-49.

Goldfarb, D., J. Gariepy, et al. (1986). "Synthetic peptides as nuclear localization signals." Nature **322**: 641-44.

Gorlich, D., N. Pante, et al. (1996). "Identification of different roles for RanGDP and RanGTP in nuclear protein import." Embo J **15**(20): 5584-94.

Gorlich, D., S. Prehn, et al. (1994). "Isolation of a Protein That is Essential for the First Step of Nuclear Protein Import." Cell **79**: 767-78.

Gorlich, D., F. Vogel, et al. (1995). "Distinct functions for the two importin subunits in nuclear protein import." Nature **377**: 246-48.

Grandi, P., S. Emig, et al. (1995). "A novel nuclear pore protein Nup82p which specifically binds to a fraction of Nsp1p." J Cell Biol **130**(6): 1263-73.

Grandi, P., N. Schlaich, et al. (1995). "Functional interaction of Nic96p with a core nucleoporin complex consisting of Nsp1p, Nup49p and a novel protein Nup57p." Embo J **14**(1): 76-87.

Griffis, E. R., S. Xu, et al. (2003). "Nup98 localizes to both nuclear and cytoplasmic sides of the nuclear pore and binds to two distinct nucleoporin subcomplexes." Mol Biol Cell **14**(2): 600-10.

Harel, A., R. C. Chan, et al. (2003). "Importin beta negatively regulates nuclear membrane fusion and nuclear pore complex assembly." Mol Biol Cell **14**(11): 4387-96.

Harlow, E. and D. Lane (1988). Antibodies: A Laboratory Manual. Cold Spring Harbor, NY, Cold Spring Harbor Laboratory.

Hatayama, M., T. Tomizawa, et al. (2008). "Functional and structural basis of the nuclear localization signal in the ZIC3 zinc finger domain." Hum Mol Genet **17**(22): 3459-73.

Heck, A. J. (2008). "Native mass spectrometry: a bridge between interactomics and structural biology." Nat Methods **5**(11): 927-33.

Hellmuth, K., D. M. Lau, et al. (1998). "Yeast Los1p has properties of an exportin-like nucleocytoplasmic transport factor for tRNA." Mol Cell Biol **18**(11): 6374-86.

Hinshaw, J. E., Carragher, B.O., Milligan, R.A. (1992). "Architecture and design of the nuclear pore complex." Cell **69**: 1133-1141.

Ho, A. K., T. X. Shen, et al. (2000). "Assembly and preferential localization of Nup116p on the cytoplasmic face of the nuclear pore complex by interaction with Nup82p." Mol Cell Biol **20**(15): 5736-48.

Hodel, A. E., M. T. Harreman, et al. (2006). "Nuclear localization signal receptor affinity correlates with in vivo localization in Saccharomyces cerevisiae." J Biol Chem **281**(33): 23545-56.

Hodel, M. R., A. H. Corbett, et al. (2001). "Dissection of a nuclear localization signal." J Biol Chem **276**(2): 1317-25.

Hsia, K. C., P. Stavropoulos, et al. (2007). "Architecture of a coat for the nuclear pore membrane." Cell **131**(7): 1313-26.

Hurwitz, M. E., C. Strambio-de-Castillia, et al. (1998). "Two yeast nuclear pore complex proteins involved in mRNA export form a cytoplasmically oriented subcomplex." Proc Natl Acad Sci U S A **95**(19): 11241-5.

Isgro, T. A. and K. Schulten (2005). "Binding dynamics of isolated nucleoporin repeat regions to importin-beta." Structure **13**(12): 1869-79.

Isgro, T. A. and K. Schulten (2007). "Association of nuclear pore FG-repeat domains to NTF2 import and export complexes." J Mol Biol **366**(1): 330-45.

Isgro, T. A. and K. Schulten (2007). "Cse1p-binding dynamics reveal a binding pattern for FG-repeat nucleoporins on transport receptors." Structure **15**(8): 977-91.

Isoyama, T., A. Murayama, et al. (2001). "Nuclear import of the yeast AP-1-like transcription factor Yap1p is mediated by transport receptor Pse1p, and this import step is not affected by oxidative stress." J Biol Chem **276**(24): 21863-9.

Izaurralde, E., U. Kutay, et al. (1997). "The asymmetric distribution of the constituents of the Ran system is essential for transport into and out of the nucleus." Embo J **16**(21): 6535-47.

Jovanovic-Talisman, T., J. Tetenbaum-Novatt, et al. (2009). "Artificial nanopores that mimic the transport selectivity of the nuclear pore complex." Nature **457**(7232): 1023-7.

Kaffman, A., N. M. Rank, et al. (1998). "Phosphorylation regulates association of the transcription factor Pho4 with its import receptor Pse1/Kap121." Genes Dev **12**(17): 2673-83.

Kapon, R., A. Topchik, et al. (2008). "A possible mechanism for self-coordination of bidirectional traffic across nuclear pores." Phys Biol **5**(3): 36001.

Karlsson, R., L. Jendeberg, et al. (1995). "Direct and competitive kinetic analysis of the interaction between human IgG1 and a one domain analogue of protein A." J Immunol Methods **183**(1): 43-9.

Kau, T. R., J. C. Way, et al. (2004). "Nuclear transport and cancer: from mechanism to intervention." Nat Rev Cancer **4**(2): 106-17.

Kiseleva, E., Allen, TD, Rutherford, S, Bucci, M, Wente, SR, Goldberg, MW (2003). "Yeast nuclear pore complexes have a cytoplasmic ring and internal filaments." Journal of Structural Biology **145**(3): 272-88.

Klebe, C., H. Prinz, et al. (1995). "The kinetic mechanism of Ran--nucleotide exchange catalyzed by RCC1." Biochemistry **34**(39): 12543-52.

Kose, S., N. Imamoto, et al. (1997). "Ran-unassisted nuclear migration of a 97-kD component of nuclear pore-targeting complex." J Cell Biol **139**(4): 841-9.

Kosugi, S., M. Hasebe, et al. (2008). "Nuclear Export Signal Consensus Sequences Defined Using a Localization-Based Yeast Selection System." Traffic.

Krishnan, V., E. Lau, et al. (2007). "Intramolecular Cohesion of Coils Mediated by Phenylalanine-Glycine Motifs in the Natively Unfolded Domain of a Nucleoporin." PLoS Comput Biol **4**(8).

Kriwacki, R., Hengst, L., Tennant, L., Reed, S.I., & Wright, P.E. (1996). "Structural studies of p21^(Waf1/Cip1/Sdi1) in the free and Cdk2-bound state: conformational disorder mediates binding diversity." Proc Natl Acad Sci U S A **93**: 11504-09.

Krull, S., J. Thyberg, et al. (2004). "Nucleoporins as components of the nuclear pore complex core structure and Tpr as the architectural element of the nuclear basket." Mol Biol Cell **15**(9): 4261-77.

Kubitscheck, U., D. Grunwald, et al. (2005). "Nuclear transport of single molecules: dwell times at the nuclear pore complex." J Cell Biol **168**(2): 233-43.

Kutay, U., G. Lipowsky, et al. (1998). "Identification of a tRNA-specific nuclear export receptor." Mol Cell **1**(3): 359-69.

Lane, C. M., I. Cushman, et al. (2000). "Selective disruption of nuclear import by a functional mutant nuclear transport carrier." J Cell Biol **151**(2): 321-32.

Lange, A., R. E. Mills, et al. (2008). "A PY-NLS nuclear targeting signal is required for nuclear localization and function of the Saccharomyces cerevisiae mRNA-binding protein Hrp1." J Biol Chem **283**(19): 12926-34.

Lange, A., R. E. Mills, et al. (2007). "Classical nuclear localization signals: definition, function, and interaction with importin alpha." J Biol Chem **282**(8): 5101-5.

Lee, B. J., A. E. Cansizoglu, et al. (2006). "Rules for nuclear localization sequence recognition by karyopherin beta 2." Cell **126**(3): 543-58.

Lee, D. C. and J. D. Aitchison (1999). "Kap104p-mediated nuclear import. Nuclear localization signals in mRNA-binding proteins and the role of Ran and Rna." J Biol Chem **274**(41): 29031-7.

Lee, S. J., Y. Matsuura, et al. (2005). "Structural basis for nuclear import complex dissociation by RanGTP." Nature **435**(7042): 693-6.

Leslie, D. M., B. Grill, et al. (2002). "Kap121p-mediated nuclear import is required for mating and cellular differentiation in yeast." Mol Cell Biol **22**(8): 2544-55.

Leslie, D. M., W. Zhang, et al. (2004). "Characterization of karyopherin cargoes reveals unique mechanisms of Kap121p-mediated nuclear import." Mol Cell Biol **24**(19): 8487-503.

Lim, R., N. Huang, et al. (2006). "Flexible phenylalanine-glycine nucleoporins as entropic barriers to nucleocytoplasmic transport." Proc Natl Acad Sci U S A **103**(25): 9512-7.

Lim, R. Y., B. Fahrenkrog, et al. (2007). "Nanomechanical basis of selective gating by the nuclear pore complex." Science **318**(5850): 640-3.

Liu, S. M. and M. Stewart (2005). "Structural basis for the high-affinity binding of nucleoporin Nup1p to the Saccharomyces cerevisiae importin-beta homologue, Kap95p." J Mol Biol **349**(3): 515-25.

Lund, E. and J. E. Dahlberg (1998). "Proofreading and aminoacylation of tRNAs before export from the nucleus." Science **282**(5396): 2082-5.

Macara, I. G. (2001). "Transport into and out of the nucleus." Microbiol Mol Biol Rev **65**(4): 570-94, table of contents.

Makkerh, J. P., C. Dingwall, et al. (1996). "Comparative mutagenesis of nuclear localization signals reveals the importance of neutral and acidic amino acids." Curr Biol **6**(8): 1025-7.

Marelli, M., J. D. Aitchison, et al. (1998). "Specific binding of the karyopherin Kap121p to a subunit of the nuclear pore complex containing Nup53p, Nup59p, and Nup170p." J Cell Biol **143**(7): 1813-30.

Marelli, M., J. J. Smith, et al. (2004). "Quantitative mass spectrometry reveals a role for the GTPase Rho1p in actin organization on the peroxisome membrane." J Cell Biol **167**(6): 1099-112.

Marfatia, K. A., E. B. Crafton, et al. (2003). "Domain analysis of the Saccharomyces cerevisiae heterogeneous nuclear ribonucleoprotein, Nab2p. Dissecting the requirements for Nab2p-facilitated poly(A) RNA export." J Biol Chem **278**(9): 6731-40.

McLane, L. M., K. F. Pulliam, et al. (2008). "The Ty1 integrase protein can exploit the classical nuclear protein import machinery for entry into the nucleus." Nucleic Acids Res **36**(13): 4317-26.

Melcak, I., A. Hoelz, et al. (2007). "Structure of Nup58/45 suggests flexible nuclear pore diameter by intermolecular sliding." Science **315**(5819): 1729-32.

Miao, L. and K. Schulten (2009). "Transport-Related Structures and Processes of the Nuclear Pore Complex Studied through Molecular Dynamics." Structure **17**(3): 449-59.

Michaud, N. and D. Goldfarb (1992). "Microinjected U snRNAs are imported to oocyte nuclei via the nuclear pore complex by three distinguishable targeting pathways." J Cell Biol **116**(4): 851-61.

Michaud, N. and D. S. Goldfarb (1991). "Multiple pathways in nuclear transport: the import of U2 snRNP occurs by a novel kinetic pathway." J Cell Biol **112**(2): 215-23.

Middeler, G., K. Zerf, et al. (1997). "The tumor suppressor p53 is subject to both nuclear import and export, and both are fast, energy-dependent and lectin-inhibited." Oncogene **14**(12): 1407-17.

Minton, A. P. (2006). "How can biochemical reactions within cells differ from those in test tubes?" J Cell Sci **119**(Pt 14): 2863-9.

Minton, A. P. (2006). "Macromolecular crowding." Curr Biol **16**(8): R269-71.

Mittag, T., S. Orlicky, et al. (2008). "Dynamic equilibrium engagement of a polyvalent ligand with a single-site receptor." Proc Natl Acad Sci U S A **105**(46): 17772-7.

Moore, M. S. and G. Blobel (1992). "The two steps of nuclear import, targeting to the nuclear envelope and translocation through the nuclear pore, require different cytosolic factors." Cell **69**(6): 939-50.

Moore, M. S. and G. Blobel (1994). "Purification of a Ran-interacting protein that is required for protein import into the nucleus." Proc Natl Acad Sci U S A **91**(21): 10212-6.

Moroianu, J., G. Blobel, et al. (1996). "Nuclear protein import: Ran-GTP dissociates the karyopherin alphabeta heterodimer by displacing alpha from an overlapping binding site on beta." Proc Natl Acad Sci U S A **93**(14): 7059-62.

Moroianu, J., Blobel, G, and Radu, A (1995). "Previously identified protein of uncertain function is karyopherin alpha and together with karyopherin beta docks import substrate at nuclear pore complexes." Proc Natl Acad Sci U S A **92**: 2008-11.

Moroianu, J., Hijikata, M, Blobel, G, and Radu, A (1995). "Mammalian karyopherin a1B and a2B heterodimers: a1 or a2 subunit binds nuclear localization signal and B subunit interacts with peptide repeat-containing nucleoporins." Proc Natl Acad Sci U S A **92**: 6532-36.

Morrison, J., J. C. Yang, et al. (2003). "Solution NMR study of the interaction between NTF2 and nucleoporin FxFG repeats." J Mol Biol **333**(3): 587-603.

Mosammaparast, N. and L. F. Pemberton (2004). "Karyopherins: from nuclear-transport mediators to nuclear-function regulators." Trends Cell Biol **14**(10): 547-56.

Nachury, M. V. and K. Weis (1999). "The direction of transport through the nuclear pore can be inverted." Proc Natl Acad Sci U S A **96**(17): 9622-7.

Nakielny, S. and G. Dreyfuss (1998). "Import and export of the nuclear protein import receptor transportin by a mechanism independent of GTP hydrolysis." Curr Biol **8**(2): 89-95.

Nigg, E. A. (1997). "Nucleocytoplasmic transport: signals, mechanisms and regulation." Nature **386**(6627): 779-87.

O'Neill, E. M., A. Kaffman, et al. (1996). "Regulation of PHO4 nuclear localization by the PHO80-PHO85 cyclin-CDK complex." Science **271**(5246): 209-12.

Oeffinger, M., K. E. Wei, et al. (2007). "Comprehensive analysis of diverse ribonucleoprotein complexes." Nat Methods **4**(11): 951-6.

Ohtsubo, M., H. Okazaki, et al. (1989). "The RCC1 protein, a regulator for the onset of chromosome condensation locates in the nucleus and binds to DNA." J Cell Biol **109**(4 Pt 1): 1389-97.

Ossareh-Nazari, B., F. Bachelerie, et al. (1997). "Evidence for a role of CRM1 in signal-mediated nuclear protein export." Science **278**(5335): 141-4.

Palmeri, D. and M. H. Malim (1999). "Importin beta can mediate the nuclear import of an arginine-rich nuclear localization signal in the absence of importin alpha." Mol Cell Biol **19**(2): 1218-25.

Pante, N. and M. Kann (2002). "Nuclear pore complex is able to transport macromolecules with diameters of about 39 nm." Mol Biol Cell **13**(2): 425-34.

Paschal, B. M., C. Delphin, et al. (1996). "Nucleotide-specific interaction of Ran/TC4 with nuclear transport factors NTF2 and p97." Proc Natl Acad Sci U S A **93**(15): 7679-83.

Paschal, B. M. and L. Gerace (1995). "Identification of NTF2, a cytosolic factor for nuclear import that interacts with nuclear pore complex protein p62." J Cell Biol **129**(4): 925-37.

Patel, S. S., B. J. Belmont, et al. (2007). "Natively unfolded nucleoporins gate protein diffusion across the nuclear pore complex." Cell **129**(1): 83-96.

Patel, S. S. and M. F. Rexach (2008). "Discovering novel interactions at the nuclear pore complex using bead halo: a rapid method for detecting molecular interactions of high and low affinity at equilibrium." Mol Cell Proteomics **7**(1): 121-31.

Pemberton, L. F. and B. M. Paschal (2005). "Mechanisms of receptor-mediated nuclear import and nuclear export." Traffic **6**(3): 187-98.

Pennisi, E. (1998). "The nucleus's revolving door." Science **279**(5354): 1129-31.

Peters, R. (2003). "Optical single transporter recording: transport kinetics in microarrays of membrane patches." Annu Rev Biophys Biomol Struct **32**: 47-67.

Peters, R. (2005). "Translocation through the nuclear pore complex: selectivity and speed by reduction-of-dimensionality." Traffic **6**(5): 421-7.

Peters, R. (2006). "Use of Xenopus laevis oocyte nuclei and nuclear envelopes in nucleocytoplasmic transport studies." Methods Mol Biol **322**: 259-72.

Pyhtila, B. and M. Rexach (2003). "A gradient of affinity for the karyopherin Kap95p along the yeast nuclear pore complex." J Biol Chem **278**(43): 42699-709.

Radu, A., G. Blobel, et al. (1995). "Identification of a protein complex that is required for nuclear-protein import and mediates docking of import substrate to distinct nucleoporins." Proc Natl Acad Sci USA **92**: 1769-1773.

Radu, A., M. Moore, et al. (1995). "The peptide repeat domain of nucleoporin Nup98 functions as a docking site in transport across the nuclear-pore complex." Cell **81**: 215-22.

Reid, D. G., L. K. MacLachlan, et al. (1997). "Introduction to the NMR of proteins." Methods Mol Biol **60**: 1-28.

Rexach, M. and G. Blobel (1995). "Protein import into nuclei: association and dissociation reactions involving transport substrate, transport factors, and nucleoporins." Cell **83**(5): 683-92.

Ribbeck, K. and D. Gorlich (2001). "Kinetic analysis of translocation through nuclear pore complexes." The EMBO Journal **20**: 1320-1330.

Ribbeck, K. and D. Gorlich (2002). "The permeability barrier of nuclear pore complexes appears to operate via hydrophobic exclusion." Embo J **21**(11): 2664-71.

Ribbeck, K., G. Lipowsky, et al. (1998). "NTF2 mediates nuclear import of Ran." Embo J **17**(22): 6587-98.

Richards, S. A., K. M. Lounsbury, et al. (1996). "A nuclear export signal is essential for the cytosolic localization of the Ran binding protein, RanBP1." J Cell Biol **134**(5): 1157-68.

Richardson, W. D., A. D. Mills, et al. (1988). "Nuclear protein migration involves two steps: rapid binding at the nuclear envelope followed by slower translocation through nuclear pores." Cell **52**(5): 655-64.

Riddick, G. and I. G. Macara (2005). "A systems analysis of importin-{alpha}-{beta} mediated nuclear protein import." J Cell Biol **168**(7): 1027-38.

Riddick, G. and I. G. Macara (2007). "The adapter importin-alpha provides flexible control of nuclear import at the expense of efficiency." Mol Syst Biol **3**: 118.

Rout, M. P. and J. D. Aitchison (2000). "Pore relations: nuclear pore complexes and nucleocytoplasmic exchange." Essays Biochem **36**: 75-88.

Rout, M. P. and J. D. Aitchison (2001). "The nuclear pore complex as a transport machine." J Biol Chem **276**(20): 16593-6.

Rout, M. P., J. D. Aitchison, et al. (2003). "Virtual gating and nuclear transport: the hole picture." Trends Cell Biol **13**(12): 622-8.

Rout, M. P., J. D. Aitchison, et al. (2000). "The yeast nuclear pore complex: composition, architecture, and transport mechanism." J Cell Biol **148**(4): 635-51.

Rout, M. P., G. Blobel, et al. (1997). "A distinct nuclear import pathway used by ribosomal proteins." Cell **89**(5): 715-25.

Rout, M. P. and S. R. Wente (1994). "Pores for thought: nuclear pore complex proteins." Trends Cell Biol **4**(10): 357-65.

Sarkar, S. and A. K. Hopper (1998). "tRNA nuclear export in saccharomyces cerevisiae: in situ hybridization analysis." Mol Biol Cell **9**(11): 3041-55.

Scheifele, L. Z., E. P. Ryan, et al. (2005). "Detailed mapping of the nuclear export signal in the Rous sarcoma virus Gag protein." J Virol **79**(14): 8732-41.

Schlenstedt, G., E. Smirnova, et al. (1997). "Yrb4p, a yeast ran-GTP-binding protein involved in import of ribosomal protein L25 into the nucleus." Embo J **16**(20): 6237-49.

Schrader, N., P. Stelter, et al. (2008). "Structural basis of the nic96 subcomplex organization in the nuclear pore channel." Mol Cell **29**(1): 46-55.

Scott, R. J., L. V. Cairo, et al. (2009). "The nuclear export factor Xpo1p targets Mad1p to kinetochores in yeast." J Cell Biol **184**(1): 21-9.

Seedorf, M. S., PA (1997). "Importin/karyopherin protein family members required for mRNA export from the nucleus." Proc Natl Acad Sci U S A **94**(16): 8590-5.

Sharon, M. and C. V. Robinson (2007). "The role of mass spectrometry in structure elucidation of dynamic protein complexes." Annu Rev Biochem **76**: 167-93.

Shulga, N. and D. S. Goldfarb (2003). "Binding dynamics of structural nucleoporins govern nuclear pore complex permeability and may mediate channel gating." Mol Cell Biol **23**(2): 534-42.

Shulga, N., N. Mosammaparast, et al. (2000). "Yeast Nucleoporins Involved in Passive Nuclear Envelope Permeability." J Cell Biol **149**: 1027-1038.

Shulga, N., P. Roberts, et al. (1996). "In vivo nuclear transport kinetics in Saccharomyces cerevisiae: a role for heat shock protein 70 during targeting and translocation." J Cell Biol **135**(2): 329-39.

Silver, P., Sadler, I., and Osborne, M.A. (1989). J Cell Biol **109**: 983-9.

Smith, A., A. Brownawell, et al. (1998). "Nuclear import of Ran is mediated by the transport factor NTF2." Curr Biol **8**(25): 1403-6.

Solsbacher, J., P. Maurer, et al. (2000). "Nup2p, a yeast nucleoporin, functions in bidirectional transport of importin alpha." Mol Cell Biol **20**(22): 8468-79.

Stoffler, D., Fega, B, Fahrenkrog, B, Walz, J, Typke, D, Aebi, U (2003). "Cryo-electron tomography provides novel insights into nuclear pore architecture: implications for nucleocytoplasmic transport." J Mol Biol **328**(1): 119-30.

Strahm, Y., B. Fahrenkrog, et al. (1999). "The RNA export factor Gle1p is located on the cytoplasmic fibrils of the NPC and physically interacts with the FG-nucleoporin Rip1p, the DEAD-box protein Rat8p/Dbp5p and a new protein Ymr 255p." Embo J **18**(20): 5761-77.

Strambio-de-Castillia, C., J. Tetenbaum-Novatt, et al. (2005). "A method for the rapid and efficient elution of native affinity-purified protein A tagged complexes." J Proteome Res **4**(6): 2250-6.

Strawn, L., T. Shen, et al. (2004). "Minimal nuclear pore complexes define FG repeat domains essential for transport." Nature Cell Biology **6**(3): 197-206.

Strawn, L. A., T. Shen, et al. (2001). "The GLFG regions of Nup116p and Nup100p serve as binding sites for both Kap95p and Mex67p at the nuclear pore complex." J Biol Chem **276**(9): 6445-52.

Suel, K. E., H. Gu, et al. (2008). "Modular organization and combinatorial energetics of proline-tyrosine nuclear localization signals." PLoS Biol **6**(6): e137.

Suntharalingam, M., A. R. Alcazar-Roman, et al. (2004). "Nuclear export of the yeast mRNA-binding protein Nab2 is linked to a direct interaction with Gfd1 and to Gle1 function." J Biol Chem **279**(34): 35384-91.

Suntharalingam, M. and S. R. Wente (2003). "Peering through the pore: nuclear pore complex structure, assembly, and function." Dev Cell **4**(6): 775-89.

Tackett, A. J., J. A. DeGrasse, et al. (2005). "I-DIRT, a general method for distinguishing between specific and nonspecific protein interactions." J Proteome Res **4**(5): 1752-6.

Terry, L. and S. Wente (2007). "Nuclear mRNA export requires specific FG nucleoporins for translocation through the nuclear pore complex." J Cell Biol **178**(7): 1121-32.

Timney, B. L., J. Tetenbaum-Novatt, et al. (2006). "Simple kinetic relationships and nonspecific competition govern nuclear import rates in vivo." J Cell Biol **175**(4): 579-93.

Tran, E. J. and S. R. Wente (2006). "Dynamic nuclear pore complexes: life on the edge." Cell **125**(6): 1041-53.

Tschodrich-Rotter, M. and R. Peters (1998). "An optical method for recording the activity of single transporters in membrane patches." J Microsc **192**(Pt 2): 114-25.

Uversky, V. N., J. R. Gillespie, et al. (2000). "Why are "natively unfolded" proteins unstructured under physiologic conditions?" Proteins **41**(3): 415-27.

Walther, T. C., P. Askjaer, et al. (2003). "RanGTP mediates nuclear pore complex assembly." Nature **424**(6949): 689-94.

Wang, W., L. Wei, et al. (2003). "Multistep purification of an antifreeze protein from Ammopiptanthus mongolicus by chromatographic and electrophoretic methods." J Chromatogr Sci **41**(9): 489-93.

Weis, K. (2002). "Nucleocytoplasmic transport: cargo trafficking across the border." Curr Opin Cell Biol **14**(3): 328-35.

Wen, W., A. T. Harootunian, et al. (1994). "Heat-stable inhibitors of cAMP-dependent protein kinase carry a nuclear export signal." J Biol Chem **269**(51): 32214-20.

White, E. M., Allis, C.D., Goldfarb, D.S., Srivastva, A., Weir, J., and Gorovsky, M.A. (1989). J Cell Biol **109**: 1983-92.

Winey, M., D. Yarar, et al. (1997). "Nuclear pore complex number and distribution throughout the Saccharomyces cerevisiae cell cycle by three-dimensional reconstruction from electron micrographs of nuclear envelopes." Mol Biol Cell **8**(11): 2119-32.

Wozniak, R. W., M. P. Rout, et al. (1998). "Karyopherins and kissing cousins." Trends Cell Biol **8**(5): 184-8.

Wright, P. E. and H. J. Dyson (1999). "Intrinsically unstructured proteins: re-assessing the protein structure-function paradigm." J Mol Biol **293**(2): 321-31.

Wuthrich, K. (1990). "Protein structure determination in solution by NMR spectroscopy." J Biol Chem **265**(36): 22059-62.

Yang, Q., M. P. Rout, et al. (1998). "Three-dimensional architecture of the isolated yeast nuclear pore complex: functional and evolutionary implications." Mol Cell **1**(2): 223-34.

Yang, W., J. Gelles, et al. (2004). "Imaging of single-molecule translocation through nuclear pore complexes." Proc Natl Acad Sci U S A **101**(35): 12887-92.

Yaseen, N. R. and G. Blobel (1997). "Cloning and characterization of human karyopherin beta3." Proc Natl Acad Sci U S A **94**(9): 4451-6.

Zeitler, B. and K. Weis (2004). "The Ft-repeat asymmetry of the nuclear pore complex is dispensable for bulk nucleocytoplasmic transport in vivo." J Cell Biol **167**: 583-90.

Zilman, A., S. Di Talia, et al. (2007). "Efficiency, selectivity, and robustness of nucleocytoplasmic transport." PLoS Comput Biol **3**(7): e125.

Zimmerman, S. B. and A. P. Minton (1993). "Macromolecular crowding: biochemical, biophysical, and physiological consequences." Annu Rev Biophys Biomol Struct **22**: 27-65.

Zimmerman, S. B. and S. O. Trach (1991). "Estimation of macromolecule concentrations and excluded volume effects for the cytoplasm of Escherichia coli." J Mol Biol **222**(3): 599-620.